Earth-Science Reviews xxx (xxxx) xxx–xxx

Contents lists available at ScienceDirect

Earth-Science Reviews

journal homepage: www.elsevier.com/locate/earscirev

A review of the Famatinian Ordovician magmatism in southern South America: evidence of lithosphere reworking and continental subduction in the early proto-Andean margin of Gondwana

Carlos W. Rapela[a,*], Robert J. Pankhurst[b], César Casquet[c], Juán A. Dahlquist[d], C. Mark Fanning[e], Edgardo G. Baldo[d], Carmen Galindo[c], Pablo H. Alasino[f], Carlos D. Ramacciotti[d], Sebastián O. Verdecchia[d], Juán A. Murra[d], Miguel A.S. Basei[g]

[a] Centro de Investigaciones Geológicas (CIG), CONICET, Universidad Nacional de la Plata, Diagonal 113 N° 275, La Plata 1900, Argentina
[b] Visiting Research Associate, British Geological Survey, Nottingham NG125GG, UK
[c] Departamento de Mineralogía y Petrología (Universidad Complutense), Instituto de Geociencias (CSIC-UCM), Madrid 28040, Spain
[d] Centro de Investigaciones en Ciencias de la Tierra (CICTERRA), CONICET, Universidad Nacional de Córdoba, Av.Véle Sarsfield 1611, Pab.Geol, Córdoba X5016CGA, Argentina
[e] Research School of Earth Sciences, The Australian National University, Canberra ACT0200, Australia
[f] Centro Regional de Investigaciones Científicas y Transferencia Tecnológica de La Rioja (CRILAR), Consejo Nacional de Investigaciones Científicas y Técnicas (CONICET), Entre Ríos y Mendoza, 5301, Anillaco, La Rioja, Argentina
[g] Instituto de Geociências, Universidade de São Paulo, São Paulo, Brazil

ARTICLE INFO

Keywords:
Famatinian magmatism
U–Pb geochronology
Hf isotopes
O isotopes
Continental growth
Tectonics

ABSTRACT

Along the proto-Pacific margin of Gondwana, from Venezuela to northeastern Patagonia, the Early–Middle Ordovician Famatinian orogeny was the first orogenic event following assembly of the supercontinent. Previous isotope studies of the igneous and (meta-)sedimentary rocks of southwestern Gondwana yield ambiguous implications for the role of juvenile mantle addition during the early crustal growth at the supercontinental margin. To interpret the geological and tectonic evolution of the orogen and the magma sources in different episodes we look at evidence from a large area of southern South America, including the 700 × 600 km type sector of the orogen in the Sierras Pampeanas (27°–33°S), the Precordillera, and northeastern Patagonia. Previous geological, geochemical and geochronological results are reviewed together with new U—Pb SHRIMP crystallization ages, $^{177}Hf/^{176}Hf$ and $^{18}O/^{16}O$ data for dated zircon, and whole-rock Sr and Nd isotope compositions.

Four geological domains are recognized in the Sierras Pampeanas (Western, Central, Eastern and Foreland Famatinian domains). Magmatism is mostly restricted to the interval 463 ± 4 to 486 ± 7 Ma, with the most intense period of emplacement between 468 and 472 Ma constituting a magmatic flare-up. Granitoid emplacement in both northeastern Patagonia and the Cordon de Lila (Puna Altiplano, Chile) was effectively synchronous with that in the Sierras Pampeanas, defining a continuous belt. Combined geochemical and isotopic data (whole-rock Sr, Nd; Hf, O in zircon) indicate that the source of calcic metaluminous suites is the subcontinental lithosphere – both mantle and mafic lower crust – with variable contamination by the Early Paleozoic metasedimentary country rocks. The lithospheric mantle involved is assumed to underlie the outcropping 1330–1030 Ma age basement of the Western Domain, which exhibits tectonic characteristics of active continental margin in the north and oceanic arc-back arc in the south. The latter sector is the potential source of some minor Famatinian igneous rocks with less evolved isotopic compositions, although a restricted asthenospheric addition cannot be discarded in this case. Minor peraluminous granites are spatially associated with the metaluminous sequence, but major highly-peraluminous batholiths occur on the eastern flank of the Central Domain. Field relations and geochemical/isotopic evidence indicate that the most obvious source of these crustal melts was the very thick post-early Cambrian metasedimentary sequence comprising the host country rocks.

Episodic tectono-magmatic evolution of the Famatinian magmatic belt in two overlapping stages is invoked to explain different characteristics in the four recognized domains in the type sector:

- ca. 474–486? Ma, roll-back stage. This is a mainly extensional interval involving asthenospheric upwelling and thinning of the subcontinental mantle; full development of the marine ensialic basins and early

* Corresponding author.
E-mail address: crapela@cig.museo.unlp.edu.ar (C.W. Rapela).

https://doi.org/10.1016/j.earscirev.2018.10.006
Received 28 March 2018; Received in revised form 3 October 2018; Accepted 8 October 2018

emplacement of both metaluminous granites and highly-peraluminous batholiths in the Central and Eastern Famatinian domains. Trondhjemite plutons with an adakitic signature were emplaced in the Foreland Domain

- ca. 468–482 Ma, slab break-off stage. Steepening of the oceanic slab and arc migration to the southwest ended with slab break-off due to subduction of continental crust during continental collision with the Precordillera terrane. This stage produced voluminous metaluminous magmatism at the western edge of the Central Domain (the flare-up episode), K-bentonites in the Precordillera, leucogranites in the Western Domain and scattered metaluminous and peraluminous plutons in all Famatinian domains.

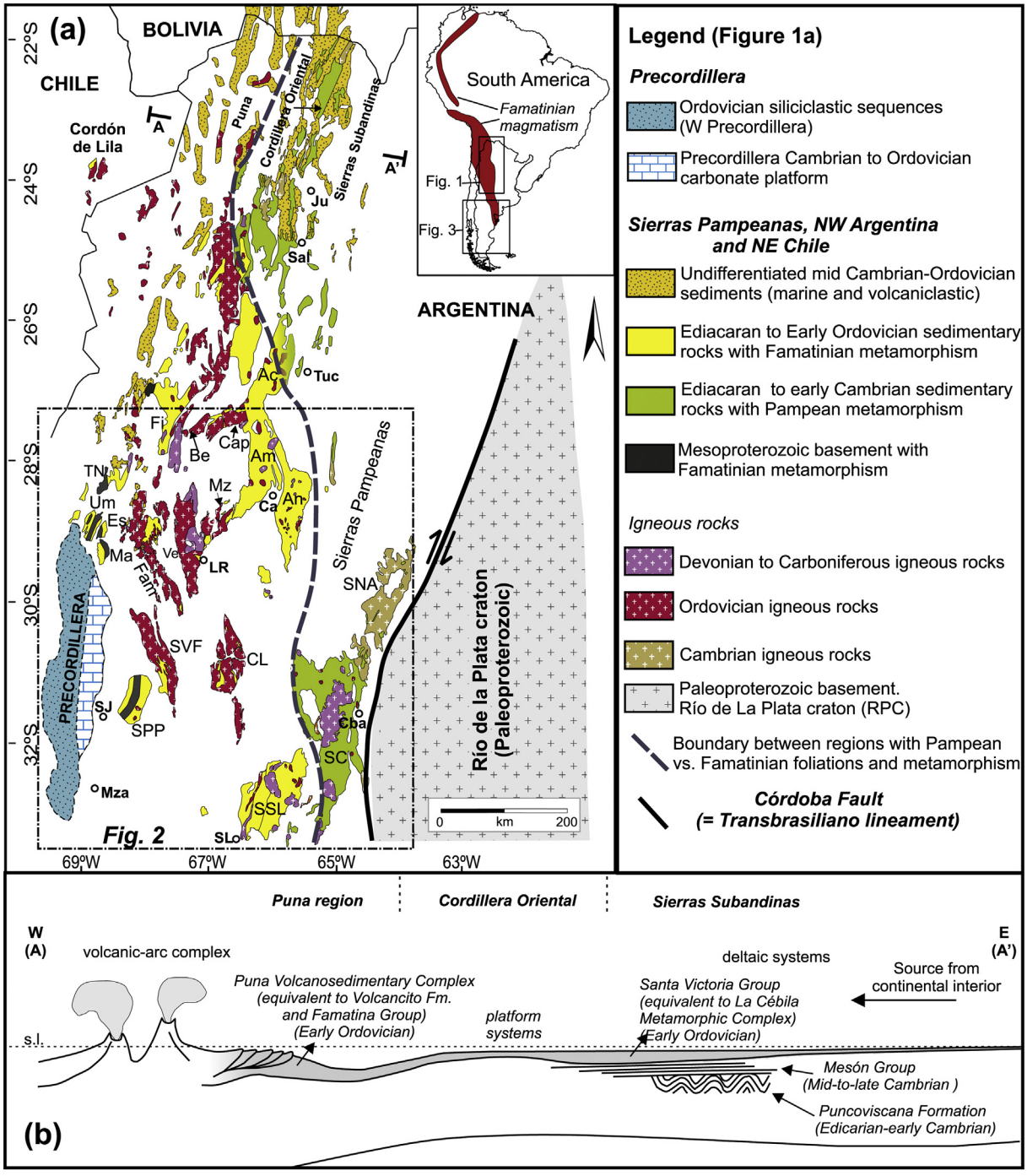

Fig. 1. (a). Early Paleozoic geology of the Sierras Pampeanas, Precordillera, Puna, Cordillera Oriental and Sierras Subandinas. Main ranges in the studied sector in the Sierras Pampeanas are indicated: Sierra de Aconquja (Ac), Sierra de Ambato (Am), Sierra de Ancasti (An), Sierra de Belén (Be), Sierra de Capillitas (Cap), Sierra del Espinal (Es), Sierra de Famatina (Fam), Sierra de Fiambalá (Fi), Sierras de Chepes-Los Llanos (CL), Sierra de Maz (Ma), Sierra de Mazán (Mz), Sierra de Córdoba (SC), Sierra Norte-Ambargasta (SNA), Sierra de Pie de Palo (SPP), Sierra de San Luis (SSL). Sierra del Toro Negro (TN), Sierra de Valle Fertil (SVF), Sierra de Velasco (Ve), Sierra de Umango (Um). Town localities: Jujuy (Ju), Salta (Sal), Tuc (Tucumán), Catamarca (Ca), La Rioja (LR), San Juan (SJ), Córdoba (Cba), Mendoza (Mza), San Luis (Slo). Modified from Rapela et al., (2016). (b) A-Á: cross section of Early Paleozoic units in Northwestern Argentina (From Astini, (2003). Inset shows the distribution of Famatinian magmatism in South America and the study areas of Figs. 2 and 3.

Both slab roll-back and break-off stages developed during a high-T regime typical of hot orogens.

Although asthenospheric mantle was a necessary heat source for lithospheric melting, its material contribution to the growth of Early Paleozoic crust was apparently very minor. Recycling of Mesoproterozoic lithosphere, including the subcontinental mantle, coupled with crustal melting of Early Paleozoic metasedimentary sequences, accounts for most Famatinian magmatism. Comparable results from the Central Andes and East Antarctica confirm that the early stages of the Terra Australis orogen in SW Gondwana were dominated by lithospheric reworking processes.

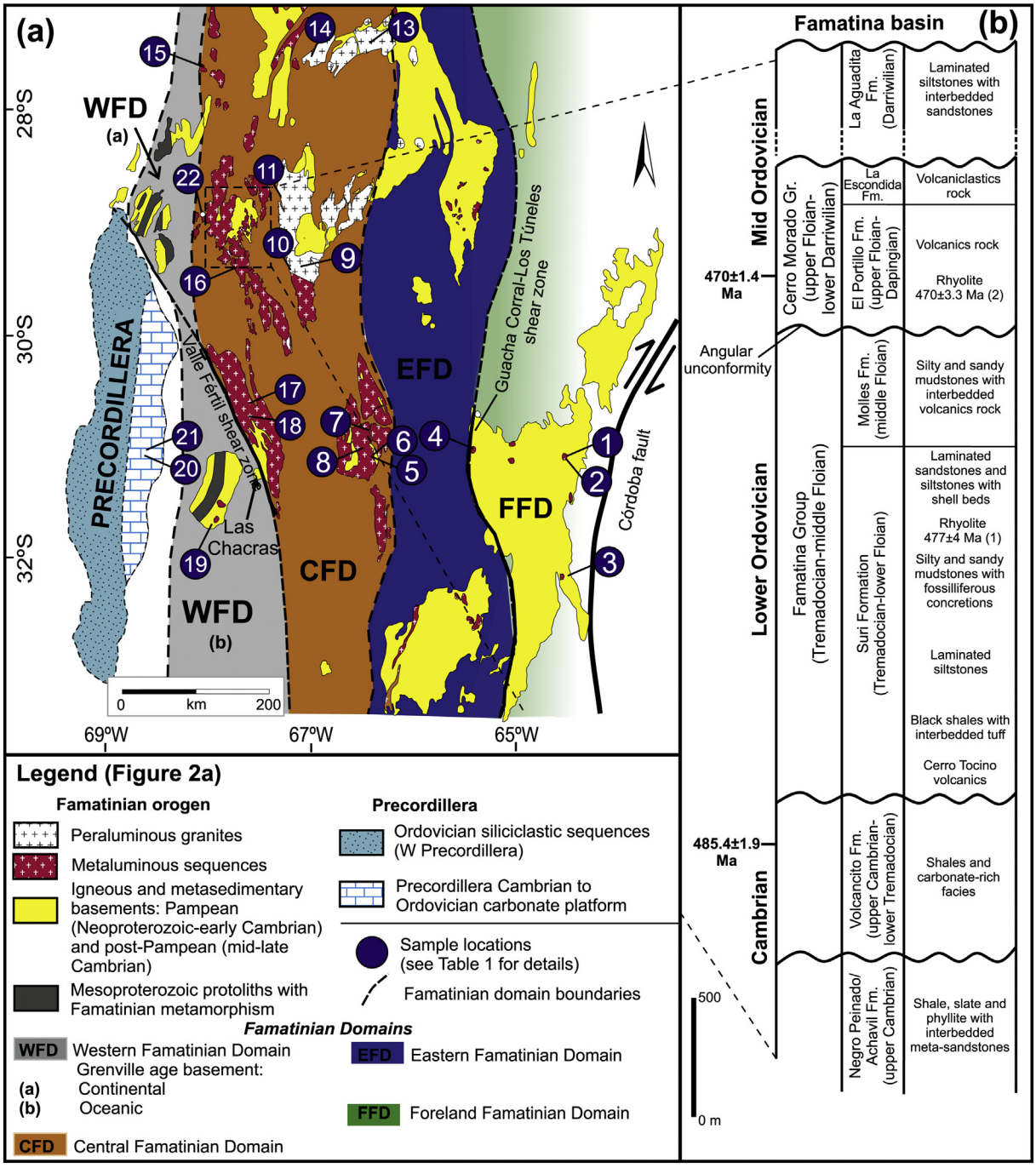

Fig. 2. (a) Proposed domains and sample localities in the type sector of the Famatinian orogen. FFD: Foreland Famatinian Domain; EFD: Eastern Famatinian Domain; CFD: Central Famatinian Domain and WFD: Western Famatinian Domain. Location of the studied samples are indicated with numbers in blue circles, and the GPS location, lithology and U—Pb age are given in Table 1. (b) Restored columnar section for the Ordovician units in the Sierra de Famatina basin (adapted from Astini, 2003). Numerical ages for the recognized Ordovician stages in the Famatina basin are from the IUGS International Chronostratigraphic Chart, v. 2018/v08 (Cohen et al., 2013, updated). (For interpretation of the references to colour in this figure legend, the reader is referred to the web version of this article.)

1. Introduction

Perhaps one of the most intractable issues in geological science is the mechanism and timing of continental crust formation during the ~ 4.6 Ga life of the planet (e.g., Kemp and Hawkesworth, 2014 and references therein). Gondwana–Pangea assembly and disintegration is the last and best-known of the evolutionary stages of the continental crust, where geochemical and isotopic evidence can be placed in a relatively well-constrained paleogeographic context.

Following the early Cambrian Pampean orogeny, which marks the final assembly of SW Gondwana (552–520 Ma, Casquet et al., 2018), the next important episode along the proto-Andean margin was major Early Ordovician magmatism, extending from Venezuela to northeast Patagonia (Pankhurst et al., 2006; Chew et al., 2007; Alasino et al., 2016; Van der Lelij et al., 2016; García-Ramírez et al., 2017; see Fig. 1 inset). The term Famatinian Cycle was coined by Aceñolaza and Toselli (1976) after the 6000 m high Sierra de Famatina in northwest Argentina, which mainly consists of Early Ordovician granites and metasedimentary rocks (Fig. 1a). In many places along the magmatic belt there is evidence of strong Ordovician deformation, metamorphism and shearing, so that the term Famatinian orogeny has often been invoked, although this paper concentrates on the magmatism.

In the northern and central Andes the Famatinian outcrop areas are narrow and essentially sub-parallel to the modern Andean chain, along the western edge of the Amazon craton and in the Arequipa block. However, south of 22°S there is a very wide sector (ca. 600 km) between the Río de la Plata craton and the westernmost inliers in the Andean belt. Farther west at 25–33°30′S, later magmatic arcs young oceanwards through Late Paleozoic and Mesozoic (Andean) events (Rapela et al., 2007). The orogenic arrangement in this wide sector generally resembles that of the Tasmanide accretionary orogen of eastern Australia (e.g., Collins, 2002; Cawood, 2005).

While the Andean orogeny has been the focus of study using almost all the geological disciplines, the problem of Famatinian crustal growth is still unresolved. Some isotope studies in the Central Andes and East Antarctica have led to the interpretation that magmatism was dominated by crustal recycling (e.g., Bahlburg et al., 2009; Dahlquist et al., 2013; Yakymchuk et al., 2015), while others suggest that juvenile mantle addition might be significant (e.g., Otamendi et al., 2017 and references therein).

In places the Famatinian belt is largely covered by younger sedimentary units (e.g., in Peru and Ecuador, Chew et al., 2007) or is represented by small remnants (e.g., in northeastern Patagonia, Pankhurst et al., 2006). The main exception is in the Sierras Pampeanas, particularly behind the modern flat-slab segment of the Nazca plate, where Tertiary uplift resulted in well-exposed blocks up to 600 km from the coast. Conspicuous Famatinian plutonic and volcanic rocks of varying characteristics occur over a 500 km wide transect at 27°–33°S that includes Sierra de Famatina (Figs. 1, 2) (Pankhurst et al., 2000; Dahlquist et al., 2013, and references therein). At about 28°S Famatinian rocks show a marked change in exposed paleo-depth, with the deepest plutonic levels being exposed to the south (Sierras Pampeanas), while volcanic complexes and coeval ensialic basins dominate the Puna plateau to the north (Otamendi et al., 2012 and references therein).

The country rocks of this type sector of the Famatinian belt vary significantly along the transect. Ediacaran–early Cambrian metasedimentary rocks previously affected by the early Cambrian Pampean orogeny occur in the east (Sierras de Córdoba), mid Cambrian–Early Ordovician metasedimentary rocks in the central part of the belt, and a Mesoproterozoic (Stenian) basement in the Western Sierras Pampeanas and the Precordillera (Rapela et al., 2016 and references therein) (see Figs. 1, 2). The Precordillera is an enigmatic tectonic block formed by thick early Cambrian to Middle Ordovician carbonate and siliciclastic platform that allegedly originated south of the Appalachian platform during Early Cambrian times, travelled as an isolated block and amalgamated with Gondwana in Middle to Late Ordovician times (e.g., Astini et al., 1995; Thomas and Astini, 1996). The classic tectonic hypothesis treats the Western Sierras Pampeanas as part of the Cuyania microcontinent, an enlarged version of the Precordillera terrane (Ramos, 2004; van Staal et al., 2011 and references therein). A more recent hypothesis considers the Western Sierras Pampeanas as part of a large Proterozoic continental block (MARA) that drifted away from Laurentia and collided with Gondwana during the early Cambrian (Casquet et al., 2012a). In both models, Famatinian magmatism developed across contrasting crustal domains, and we might expect that lithospheric variation could be reflected in the genesis of Famatinian magmas propose subdivision of the Famatinian belt into domains based on position within the belt, sedimentary record, and metamorphic P/T type, as well as the composition and volume of igneous rocks. Famatinian igneous chronology within the different domains is revisited in the light of new U—Pb data. Hypotheses for magma genesis are reviewed within the framework of new O and Hf isotope analyses of igneous zircon and a large assembled dataset of whole-rock Sr and Nd isotope determinations. Samples are representative of a large area that includes the type section of the belt in the Sierras Pampeanas, the Precordillera and northeastern Patagonia. This review leads us to propose a model of tectonomagmatic evolution to explain the variation of characteristics in the recognized geological domains.

2. Regional geology and Early Ordovician magmatism

2.1. Precordillera to Sierras Pampeanas Transect

In the modern flat-slab segment of the Nazca plate (26°–33°30′S) the westernmost evidence of Early Ordovician magmatism appears in the Precordillera, west of the Sierras Pampeanas (Fig. 1a). K-bentonite horizons interpreted as altered volcanic infall are interbedded with Ordovician limestones and have been taken as evidence of felsic volcanism contemporaneous with carbonate sedimentation (Huff et al., 1998; Fanning et al., 2004).

Ordovician rocks of the Famatinian belt are superbly exposed in SE Bolivia, NE Chile and particularly NW Argentina from 22° to 33°30′S (Fig. 1a). The northern sector including the Puna, Cordillera Oriental and Sierras Subandinas (22°–27° S) is dominated by plutonic igneous rocks and low-grade metasedimentary/metavolcanic sequences up to > 5000 m thick, which allegedly formed in a continuous Ordovician basin (Fig. 1b) (Astini, 2003, 2008; Niemeyer et al., 2014; Pankhurst et al., 2016 and references therein).

The large geological province of Sierras Pampeanas to the east is mostly composed of magmatic, metamorphic and sedimentary rocks of Ordovician age. Caminos (1973) first recognized two lithologically contrasting sectors here. A western sector adjacent to the Precordillera is characterized by abundant ultramafic and mafic polymetamorphic complexes, metamorphosed carbonate sequences, and an absence of major batholiths. Subsequent U—Pb geochronological studies demonstrate a dominant Late Mesoproterozoic basement affected by protracted Neoproterozoic–Early Paleozoic tectonism, sedimentation and magmatism (see below). From here to the Sierras de Córdoba in the east the Sierras Pampeanas are characterized by abundant granitic bodies, ranging from small plutons to large batholiths of early Cambrian to Carboniferous age (Rapela et al., 1990; Dahlquist et al., 2013) and a late Cambrian to Middle Ordovician marine basin (Astini, 2003) (Fig. 1). While the early Cambrian and Ordovician magmatism is associated with deformation and orogenic episodes, A-type Devonian and Carboniferous granites in the Eastern Sierras Pampeanas have been interpreted as the products of intracontinental magmatism (Dahlquist et al., 2016 and references therein): the Carboniferous granites commonly intruded Ordovician granite bodies. The country rocks are low- to high-grade siliciclastic rocks (metapelite to metagreywacke) and subordinate carbonate sequences.

Existing geological, petrological, and geochronological studies of

the Early Paleozoic rocks of the Sierras Pampeanas generally indicate two partially overlapping belts, corresponding to the Pampean and Famatinian orogens (Fig. 1). In NW Argentina the Pampean orogen (on the eastern side) is composed of an Ediacaran to early Cambrian metasedimentary sequence, the Puncoviscana Formation, with an age constrained by trace fossils and U—Pb ages of *syn*-sedimentary tuffs and detrital zircon coeval with arc volcanic rocks and granitic rocks that intrude the sequence (Durand and Aceñolaza, 1990; Escayola et al., 2011; Casquet et al., 2018 and references therein). In the southern part of the orogen, at the latitude of the modern flat-slab segment, early Cambrian high-grade metamorphic and magmatic rocks have been considered to be mid-crustal equivalents of the northern sector rocks, as they show coeval deformation, magmatism and the same detrital zircon pattern as the metasedimentary rocks (Rapela et al., 1998, 2016; von Gosen and Prozzi, 2010; Iannizzotto et al., 2013).

In the Sierras Pampeanas recognition of stratigraphic units and unconformities is only possible in the Famatina basin SSW prolongation of the Puna basin (Figs. 1, 2b). Sedimentary successions cropping out here exceed 3000 m in thickness and include fossiliferous late Cambrian to Middle Ordovician carbonates and siliciclastic rocks, and volcano-sedimentary deposits (Astini, 2003 and references therein). South of 27°S the lithology is dominated by granitic rocks intruded into the high- to low-grade metasedimentary sequences.

Sedimentary evidence seems to indicate that initiation of the Ordovician basins was approximately coeval in NW Argentina and the Sierra de Famatina. In the Cordillera Oriental and Sierras Subandinas, platform sedimentation of the Santa Victoria Group started in the latest Cambrian and unconformably overlies sandstones/conglomerates of the mid-Cambrian Mesón Group. The latter in turn unconformably overlies the Ediacaran–early Cambrian Puncoviscana Formation, which was folded during the early Cambrian Pampean orogeny (Fig. 1b) (Astini, 2003, 2008 and references therein). In the Sierra de Famatina, the earliest sedimentation is preserved in the southern sector of the Puna-Famatina basin, where the shales and carbonate-rich facies of the Volcancito Formation nonconformably overlie the metamorphic and foliated post-Pampean Achavil Formation (Collo et al., 2009, Fig. 2b). High-resolution conodont dating has placed the Cambrian/Ordovician boundary approximately 80 m above the base of the carbonate-rich Lower Member of the Volcancito Formation (Fig. 2b) (Albanesi et al., 2000). Early Tremadocian black shales dated by graptolite biostratigraphy were intruded by granite at 485 ± 7 Ma in northern Sierra de Famatina (U—Pb, Rubiolo et al., 2002) so that volcanism must have started here in late Tremadocian time.

Although the stratigraphic successions are discontinuous and strongly disrupted by Andean faulting, at least three Early Ordovician unconformities are recognized in the Puna and the Famatina basin (Fig. 2b). An angular unconformity between late Tremadocian and early Floian in the Puna (Hongn and Vaccari, 2008 among others) is also recorded as a stratigraphic gap at about 480 Ma within the Famatina Group (Astini, 2003). There is a very important late Early Ordovician angular unconformity (about 470 Ma) between the fold-thrust Famatina Group and the volcanic Middle Ordovician Cerro Morado Group (Astini and Dávila, 2004; Fig. 2b). The third unconformity is represented by a stratigraphic gap between the top of the Cerro Morado and the overlying Carboniferous strata. The Aguadita Formation records Late Ordovician syntectonic deposition younger than 460 Ma (Astini, 2003; Collo et al., 2009 and references therein).

2.1.1. Famatinian Domains in the Sierras Pampeanas

In order to describe the varied Ordovician rocks in this large area, we propose a division of the Famatinian belt into four domains (Fig. 2a). This is based on criteria such as the relative position within the belt, the type and exposed area of magmatism, age and metamorphic P/T type of the basement and the sedimentary record. The boundaries between domains are in most cases major faults and shear zones that generally obscure original relationships. Shear zones within these Famatinian domains have been reported as late Ordovician to Silurian in age, overprinting Famatinian granites and basement rocks (e.g., Mulcahy et al., 2011; Cristofolini et al., 2014; Semenov and Weimberg, 2017; Demartis et al., 2017 and references therein). The age of initial shearing may have been masked by later reactivation episodes, particularly in the major shear zones as shown by Demartis et al. (2017), that reported ~474 Ma U-Pb ages for tabular-to-lensoid leucogranites coeval with the main deformational event of the Guascha Corral-Los Túneles shear zone (Fig. 2). This fault is considered one of the most significant thrusts in the western Gondwana margin (Semenov and Weimberg, 2017).

The *Western Famatinian Domain* (**WFD**) is a thrust-stack of nappes formed under low- to middle-grade metamorphism and intermediate P/T conditions during Ordovician westward-directed thrusting (Casquet et al., 2001; Vujovich et al., 2004; Mulcahy et al., 2011; van Staal et al., 2011 and references therein). Thrusting affected: (a) complex 1330–1030 Ma Late Mesoproterozoic (Stenian) basement (Casquet et al., 2006) intruded by Neoproterozoic A-type granites and carbonatites (Rapela et al., 2010 and references therein), (b) lower Ediacaran to early Cambrian (pre-Pampean) sedimentary cover (the Difunta Correa Metasedimentary Sequence, Ramacciotti et al., 2015 and references therein), and (c) mid-Cambrian (post-Pampean) sedimentary cover (the Nikizanga Group, Ramacciotti et al., 2013). Basement evolution was dominated by a mature continental arc with late anorthositic massifs in the northern sector and a juvenile oceanic arc and back-arc system in the south (Fig. 2) (Rapela et al., 2010). Juvenile (meta-)trondhjemite-adakite-tonalite and metagabbro are abundant in the Las Matras block and the San Rafael massif, located between the Sierras Pampeanas and northern Patagonia (Sato et al., 2000; Cingolani et al., 2017; Galindo et al., 2017).

The Late Mesoproterozoic basement of the **WFD** was first considered part of the Laurentian Precordillera/Cuyania terrane that is thought to have collided against SW Gondwana in the early Ordovician (i.e., the lower plate during Famatinian subduction, e.g., Astini et al., 1995; Ramos, 2004 and references therein). However, $^{40}Ar/^{39}Ar$ metamorphic ages in hornblende mylonites from the Sierra de Pié Palo provide evidence for locating this block in the outer forearc (upper plate) of the Gondwana margin by Cambrian time (Mulcahy et al., 2007). This conclusion was reiterated in more recent studies based on structural, magmatic and detrital zircon ages (Mulcahy et al., 2011; Ramacciotti et al., 2013).

Evidence of Famatinian magmatism in the **WFD,** first reported by Pankhurst and Rapela (1998), consists of sills of leuco-monzogranite injected into the upper part of the nappe stack in the Sierra de Pie de Palo, largely coeval with thrusting (Mulcahy et al., 2011; Baldo et al., 2012). They have also been described in the Sierra de Umango, where Famatinian magmatism is associated with nappe and klippe structures (Varela et al., 2011). At Las Chacras, on the southwestern edge of Sierra de Valle Fértil (Fig. 2a), a small block of high-grade metasedimentary migmatite and Famatinian juvenile garnet amphibolite equivalent to the Villarcán Gneiss of Mulcahy et al. (2014) is preserved along the Valle Fértil shear zone (Casquet et al., 2012b sample SVF-709, 31° 17′17′′S; 67° 32′ 00′′W),.

The 100–200 km wide *Central Famatinian Domain* (**CFD**) is largely dominated by Famatinian igneous rocks that extend northwards into the Faja Eruptiva de la Puna Occidental and Cordón de Lila in Chile (Fig. 1). This domain also includes the Famatina sedimentary basin. The western limit of the **CFD** is the major Valle Fértil shear zone, which appears on a regional scale as numerous discontinuous belts over 25 km wide (Cristofolini et al., 2014)(Fig. 2a).

Each range of the **CFD** has its own lithological characteristics. The sierras of Famatina, Valle Fértil and Chepes–Ulapes–Los Llanos (Figs. 1, 2) are dominated by metaluminous lithology, ranging from predominantly layered mafic–ultramafic bodies at depth to metaluminous tonalite–granodiorite plutons (the most abundant lithology) and restricted bodies of leucogranite (Pankhurst et al., 1998, 2000; Dahlquist

et al., 2008, 2013; Otamendi et al., 2012; Alasino et al., 2014, 2016; Ducea et al., 2017 and references therein).

Minor peraluminous bodies, usually spatially related to high-grade metasedimentary septa, occur at shallow levels in the metaluminous sequence (e.g., Pankhurst et al., 1998; Dahlquist et al., 2005). On the other hand, the northeastern sector of the **CFD** (the sierras of Velasco, Mazán and Capillitas; Figs. 1, 2) contains large bodies of peraluminous granodiorite and monzogranite with biotite, muscovite ± sillimanite ± andalusite ± garnet ± cordierite (Pankhurst et al., 2000; Toselli et al., 2005, 2007, 2014; Bellos et al., 2015). They commonly exhibit a porphyritic facies with K-feldspar megacrysts. Basic rocks are rare or absent here, but weakly peraluminous porphyritic biotite monzogranite with microgranular enclaves is common. Major shear zones affecting the granites are common in Sierra de Velasco (e.g., Höckenreiner et al., 2003; Grosse et al., 2011; Larrovere et al., 2016 and references therein) and in its southern sector a wide transitional zone with conspicuous shear zones separates peraluminous and metaluminous suites (Bellos et al., 2015).

A very rare example of Early Ordovician fossil brachiopods is preserved in medium-grade meta-sandstones of the La Cébila complex, Sierra de Ambato (**EFD**, Fig. 2a) (Verdecchia et al., 2007), suggesting that the Famatina basin was wide. However in most cases the age of the metasedimentary country rocks has been inferred from the age patterns of detrital zircon compared to those of the Pampean orogen and the **WFD** (Rapela et al., 2016). The lower-to-mid Cambrian slates of the Negro Peinado Formation, which form the basement of the Famatina basin, show provenance from mixed sources in the **WFD** and the Pampean orogen to the east (Collo et al., 2009). Conspicuous early Cambrian detrital zircon in metasedimentary host rocks in the **CFD** show that these are mainly post-Pampean (Verdecchia et al., 2011; Cristofolini et al., 2012; Ducea et al., 2010; Rapela et al., 2016).

The *Eastern Famatinian Domain* (**EFD**) is loosely defined as the area between the **CFD** and the Famatinian foreland (Fig. 2a). This domain shows very low- to high-grade Famatinian regional metamorphism (resulting in slates and migmatites) with development of at least one penetrative foliation overprinting Cambrian (Pampean) structures (Willner, 1983). The **EFD** extends northwards into the Cordillera Oriental of NW Argentina (Fig. 1). Coeval, small to medium-size Early Ordovician peraluminous and metaluminous plutons are scattered throughout (Reissinger, 1983; Dahlquist et al., 2012; Larrovere et al., 2015). Emplacement was at relatively shallow levels in all cases. Early Ordovician shallow mafic–ultramafic complexes such as that of Las Aguilas–Virorco in Sierra de San Luis allegedly formed in a back-arc basin, host concentrations of platinum group elements (Sims et al., 1998; Ferracutti et al., 2013 and references therein). The metasedimentary country rocks are in part similar to those in the Pampean orogen (see below), but with a strong Famatinian overprint (penetrative foliation, shearing and metamorphism) that hinders recognition of original tectonic features. Subordinate post-Pampean metasedimentary rocks are also found (e.g., the Pringles complex of Sierra de San Luis: Drobe et al., 2011 and references therein).

The limit between the **EFD** and the *Famatinian Foreland Domain* (**FFD**) is located along the western edge of the Sierras de Córdoba, coinciding with the wide Guacha Corral–Los Túneles shear zone (Martino et al., 2003; Simpson et al., 2003; Semenov and Weimberg, 2017; Demartis et al., 2017 (Fig. 2a). To the east the Famatinian foreland abuts the Córdoba fault (albeit not in outcrop, Booker et al., 2004), an important tectonic boundary separating the Pampean belt from the Paleoproterozoic Rio de la Plata craton (Fig. 1a). This fault, correlated with the Transbrasiliano Lineament of southern and central Brazil, sustained right-lateral displacement of the craton relative to the orogenic belt at the end of the Pampean orogeny (Rapela et al., 2007) (Fig. 1a). The early Cambrian igneous and metamorphic rocks of the Sierras de Córdoba underwent brittle deformation during the Famatinian orogeny, with low-grade hydrothermal alteration focused along active faults and ductile shear zones (Baldo et al., 2014 and references therein).

Famatinian magmatism in the **FFD** is characterized by a TTG suite of small to medium-size plutons dominated by trondhjemite, leucotonalite and granodiorite (Rapela et al., 1998; Pankhurst et al., 2000). Thermal softening and local ductile deformation was apparently promoted by the emplacement of hot trondhjemitic magmas along a large-scale boudinage zone (D'Eramo et al., 2013).

The host metamorphic rocks of the Famatinian plutons in the **FFD** belong for the most part to the pre-Pampean Puncoviscana Formation and Ancaján Series. Based on comparison of detrital zircon age patterns, the Ediacaran to early Cambrian Ancaján Series has been considered the lateral equivalent of the Difunta Correa Metasedimentary Series of the **WFD** (Ramacciotti et al., 2015, 2013; Rapela et al., 2016; Murra et al., 2016). These authors considered the Puncoviscana and Ancaján formations of the **FFD** were imbricated during the collisional Pampean orogeny, implying a similar Late Mesoproterozoic basement below both the EFD and CFD. This is the view point adopted in this paper.

2.1.2. The Precordillera terrane

The Paleozoic stratigraphy of the Precordillera terrane, immediately west of the Sierras Pampeanas at 28°–32°S, contrasts with that of the Famatinian domains further east. It is well known because the lowest exposed rocks are mid-Cambrian to Middle Ordovician platform limestones (e.g., Astini et al., 1995) with fossil faunas described as showing a time progression from Laurentian to Gondwanan types (e.g., Benedetto, 2004; Benedetto et al., 2009). In addition, evidence for a hidden Late Mesoproterozoic metamorphic basement comes from the dating of amphibolite xenoliths in Miocene intrusive rocks (Abruzzi et al., 1993; Rapela et al., 2010). Galindo et al. (2004) and Mulcahy et al. (2007) among others considered that the ca. 515 Ma Pirquitas thrust fault along the western side of Sierra de Pie de Palo separates the Precordillera terrane from the Late Mesoproterozoic rocks of the **WFD**. In a recent reinterpretation of detrital zircon ages from the Cambrian Caucete Group in Sierra de Pie de Palo, Ramacciotti et al. (2013) include the whole range within the **WFD**, placing the inferred limit with the Precordillera terrane further west.

Since Famatinian magmatism is the central issue of this paper, O and Hf zircon isotope data of the Precordillera Ordovician K-bentonites are also considered here. However, the discussion of the origin and tectonic history of the Precordillera terrane is beyond the scope of this paper. As a general framework, this topic is only very briefly summarized here referring to key contributions. The Paleozoic strata and the inferred Late Mesoproterozoic basement have together been taken to represent an allochthonous terrane derived from Laurentia during the Cambrian and accreted to Gondwana in the Early Ordovician (e.g., Astini et al., 1995; Thomas and Astini, 1996). Alternative para-autochthonous strike-slip models for the Precordillera terrane have also been proposed (e.g., Aceñolaza and Toselli, 2000; Finney, 2007 and references therein). A modification of the allochthonous hypothesis is that the Precordillera rifted from eastern Laurentia as part of a larger block, the MARA continent, that collided with Gondwana earlier – during the Early Cambrian (Pampean collision, Rapela et al., 2016). According to this, the Precordillera may have subsequently migrated along the margin of Gondwana by transcurrent fault movements or remained as a continental ribbon or terrane separated from the supercontinent by a seaway of oceanic crust – the seaway would have closed during the Famatinian event, culminating in accretion of the Precordillera to the continental margin as proposed in this paper (see Section 6.4).

As noted in Section 2.1, K-bentonite horizons interpreted as altered volcanic ejecta are interbedded with Ordovician limestones of the Precordillera, and have been taken as evidence of felsic volcanism contemporaneous with carbonate sedimentation (Fig. 2a). Huff et al. (1997) presented U—Pb multi-grain zircon data indicating a Mid Ordovician age of 464 ± 2 Ma for one of these K-bentonite horizons. Subsequently, two K-bentonite layers yielded indistinguishable SHRIMP

U—Pb zircon dates of 470 ± 3 Ma (Fanning et al., 2004).

2.2. Northeastern Patagonia

To the south of the flat-slab sector, from ca. 33°30′S to northern Patagonia, the area is mostly covered by modern sediments but there are scattered and isolated outcrops of Famatinian granites (Chernicoff et al., 2010; Pankhurst et al., 2014). The apparent paucity of Early Paleozoic magmatism in this region may simply reflect greater exposure in the Sierras Pampeanas due to Tertiary block uplift.

Northeastern Patagonia is extensively covered by younger sedimentary sequences, Jurassic rhyolites and Cenozoic plateau basalts. Exposure of metamorphic basement and 467–476 Ma Early Ordovician granites is restricted to erosional windows such as Sierra Grande, and the Yaminué–Tardugno–Valcheta and Río Colorado areas (Fig. 3) (Pankhurst et al., 2006, 2014 and references therein). Early Cambrian granites of 522–529 Ma, whose host rocks are undefined, have been also reported in the Valcheta area, and are considered equivalents to those in Pampean orogen (Rapalini et al., 2013; Pankhurst et al., 2014).

The host rocks of the Ordovician granites in northeastern Patagonia are the fine-grained meta-sandstones of the El Jagüelito and Nahuel Niyeu formations. González et al. (2011) argue for Cambrian deposition of the former on the basis of its relationship to the granites and trace fossil content. Detrital zircon in both formations was studied by Pankhurst et al. (2006), those of the El Jagüelito having a minimum-age peak at ~ 535 Ma while that of the Nahuel Niyeu formation was slightly younger at ~515 Ma. These detrital patterns are similar to those of the post-Pampean metasedimentary rocks in the **CFD** and **EFD** in the Sierras Pampeanas (Rapela et al., 2016).

3. Geochemistry and Sr—Nd isotopic signature of Famatinian magmatism

A compilation of geochemistry and whole-rock Sr and Nd isotope data for Famatinian magmatism in the Sierras Pampeanas domains and northeastern Patagonia is shown in Figs. 4 and 5. The main characteristics have been described in detail in previous papers (Rapela et al., 1998; Pankhurst et al., 2000, 2014; Otamendi et al., 2012; Dahlquist et al., 2008, 2013; Grosse et al., 2011; Ducea et al., 2017; Alasino et al., 2016 and references therein), and therefore only those features that are relevant to the purpose of the present paper are reviewed below. However, as there is also available a comprehensive geochemical and isotopic data set for the country rocks in the different Famatinian domains, it is possible to place some constraints on sources for the Early Ordovician magmatism. For this purpose we have also assembled Sr and Nd isotopic data for the Neoproterozoic–Cambrian metasedimentary rocks and Late Mesoproterozoic basement rocks recalculated to a common 'initial' age of 475 Ma: the full database including unpublished or partially published results is presented as Supplementary Data File S1, with the respective sample locations.

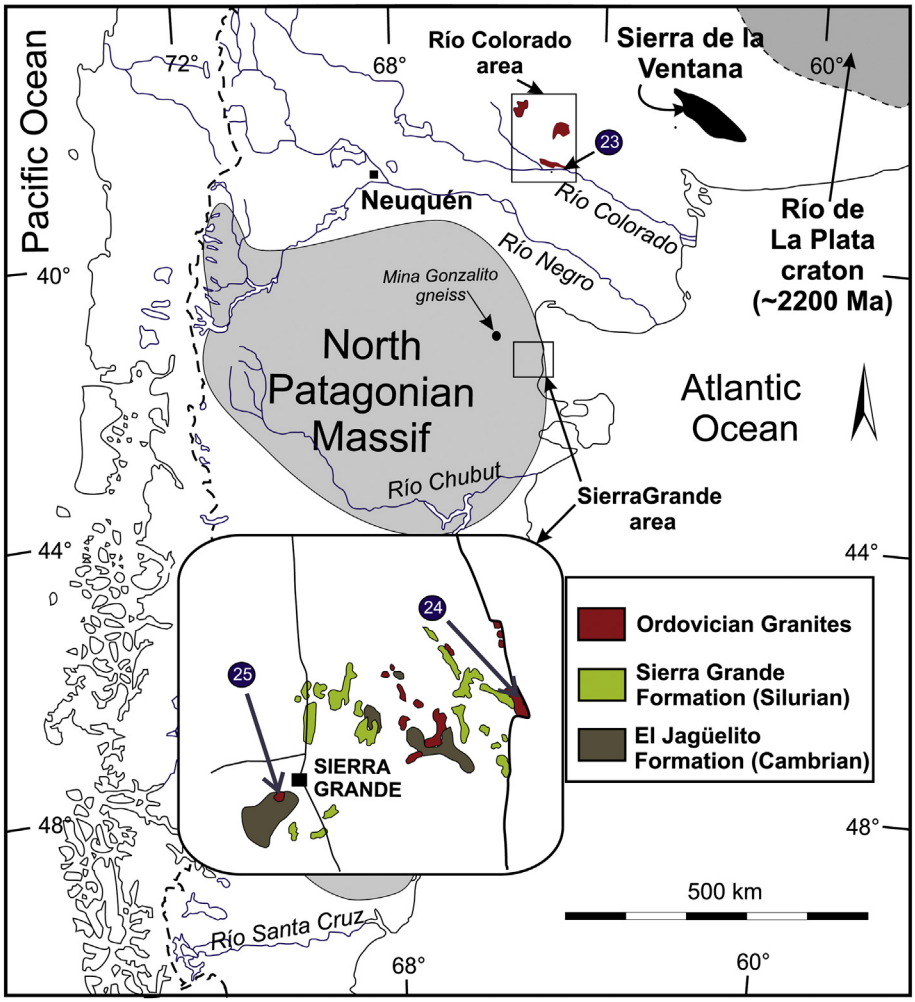

Fig. 3. Sketch map of northeastern Patagonia showing the Early Paleozoic units in the Río Colorado and Sierra Grande areas, and the location of samples analysed for Hf and O isotopes in zircon (Table 2).

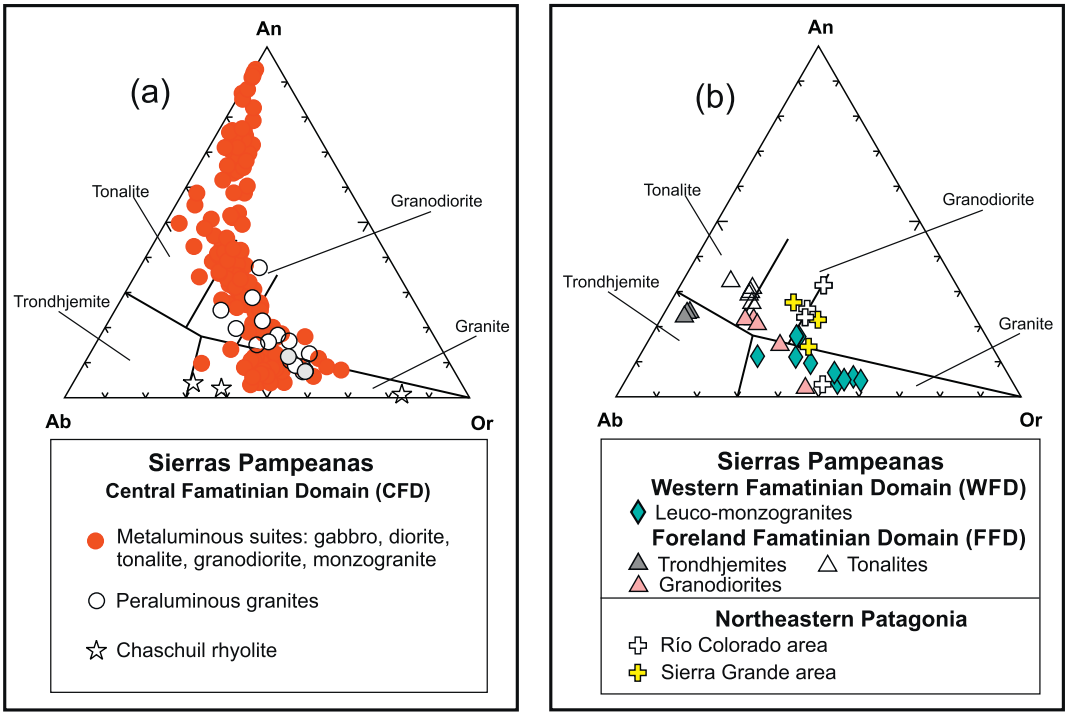

Fig. 4. Normative Ab-An-Or diagram for: (a) the Central Famatinian Domain of the Sierras Pampeanas and (b) the Western and Foreland Famatinian domains of the Sierras Pampeanas and northeastern Patagonia. Data for the Sierras Pampeanas are from Rapela et al. (1998), Pankhurst et al. (1998, 2000), Dahlquist et al. (2007, 2012) and Rapela (unpublished). Data for northeastern Patagonia are from Pankhurst et al. (2014) and Rapela (unpublished).

3.1. Sierras Pampeanas

The **CFD** is dominated by metaluminous suites, ranging from gabbro to monzogranite (Fig. 4) with a wide range of SiO_2 (40–79%, with an apparent gap at 55–57%) and ASI (Alumina Saturation Index) rarely above 1.1 (Fig. 5a, b). The granodiorite and tonalite units have K_2O contents of 1–5%, and are generally representative of cordilleran batholiths formed at continental margins, with a Peacock Index of 63 corresponding to the calcic series (Pankhurst et al., 1998) (Fig. 5a). In Sierra de Valle Fértil a tilted arc section exposes shallower paleo-depths towards the east, with a transition in lithology from mafic (gabbro/diorite) to intermediate (tonalite/diorite) via transitional (tonalite/granodiorite) and silicic (granodiorite/ monzogranite) (Otamendi et al., 2012; Ducea et al., 2017). Less abundant leucogranitic bodies have the most extreme composition with 75–78% SiO_2 and conspicuous negative Eu anomalies (Eu/Eu* = 0.25–0.8). Small bodies of peraluminous granite, often cordierite-bearing, are frequently associated with high-grade metasedimentary screens and rafts in the metaluminous suites of the sierras of Chepes–Los Llanos and Valle Fértil (e.g., Pankhurst et al., 1998; Dahlquist et al., 2005; Otamendi et al., 2012).

A notable feature of the **CFD** metaluminous suites is that the abundant amphibole-bearing meta-noritic or troctolitic gabbros with < 50% SiO_2 have the same elevated initial $^{87}Sr/^{86}Sr$ ratios and low εNd_t as the intermediate and acidic I-type rocks (Pankhurst et al., 1998, 2000; Dahlquist et al., 2013) (Fig. 6). This is also apparent in more recent studies (e.g., Otamendi et al., 2012; Ducea et al., 2010). In contrast, high-silica rhyolites at the westernmost edge of the **CFD** in the Chaschuil and Famatina areas (Fanning et al., 2004; Dahlquist et al., 2008) have distinctive low-CaO contents (Fig. 4a) and less evolved Sr and Nd isotopic compositions (Fig. 6).

For the metaluminous suite εNd_t values overlap the field of Neoproterozoic–Cambrian metasedimentary rocks, whereas $(^{87}Sr/^{86}Sr)_i$ falls below the equivalent field, although not for samples with over 55% SiO_2. The Late Mesoproterozoic basement of the **WFD** shows a wide range of Sr and Nd isotope compositions at 475 Ma, and the continental sector of this age shows very low, negative, εNd_t at high silica content, which precludes these rocks from being considered as sources of the metaluminous suites. On the other hand, the juvenile Late Mesoproterozoic oceanic basement sector of the **WFD** shows Sr and Nd isotope compositions at 475 Ma that are comparable to those of the less evolved rocks of the Sierras Pampeanas, such as the Las Chacras amphibolites and Chaschuil rhyolite of the **CFD**, and trondhjemite/ granodiorite in the **FFD** (Fig. 6).

Granite in the sierras of Capillitas, Velasco and Mazán in the northeastern sector of the **CFD** (Fig. 1) shows a different dominant lithology to the metaluminous suites (Grosse et al., 2011). The silica range is 64–76% and most samples have ASI values of 1.2–1.7 and high initial $^{87}Sr/^{86}Sr$ ratios that are mainly similar to those of the country rock Neoproterozoic–Cambrian metasedimentary rocks at 475 Ma (Figs. 5b, 6). Similarly their εNd_t values mainly overlap the metasedimentary field (Fig. 6c, d). Granites of this sector are calc-alkalic, a composition inherited from the crustal source or through significant crustal contamination of the metaluminous suites at the same silica range (Fig. 5a). Cordierite, andalusite, sillimanite and two-mica facies are common. Compared to metaluminous suites in the same silica interval they are poor in CaO and Sr and rich in P_2O_5, Rb and K_2O, with large negative Eu-anomalies (Pankhurst et al., 2000).

Granites of the *Eastern Famatinian Domain* (**EFD**), mostly exposed in the sierras of Ancasti and San Luis (Fig. 1), are far less abundant than those of the **CFD** (Fig. 2). Deformed small to medium-size plutons of both metaluminous and peraluminous granite have been reported here (Reissinger, 1983; Steenken et al., 2006; Morosini et al., 2009; Dahlquist et al., 2012 and references therein). Although we present no analyses for these granites, the above-mentioned studies indicate that their geochemistry and Nd isotope data overlap compositional fields for the **CFD** in Figs. 5 and 6.

A belt of layered mafic–ultramafic rock 3–5 km wide and extending over 100 km from NE to SW in Sierra de San Luis is perhaps the most remarkable feature of the **EFD** (Ferracutti et al., 2013 and references therein). Igneous rocks of this complex have been dated at 478 ± 6 Ma

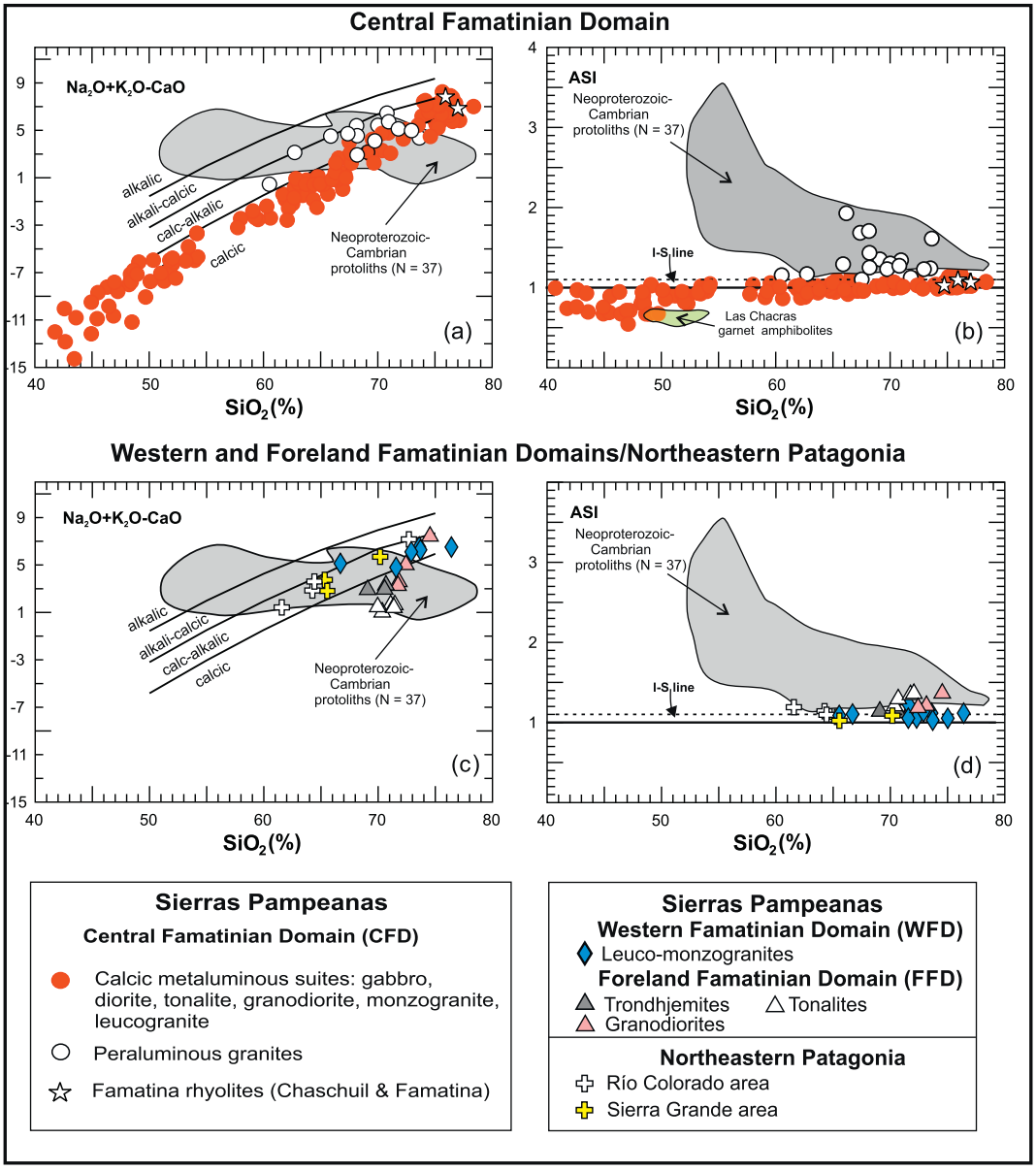

Fig. 5. Major element geochemical trends in the Famatinian domains of the Sierras Pampeanas and northeastern Patagonia. Variation of the modified alkali–lime diagram (Frost et al., 2001) and the Alumina Saturation Index (ASI, Zen, 1986) vs. SiO_2 in the Central Famatinian Domain (a,b) and in the Western and Foreland domains/northeastern Patagonia (c,d). (b).The I-type/S-type granite boundary is from Chappell and White (1974). Data sources as in Fig. 4.

and 484 ± 7 Ma (a felsic segregation in pyroxenites and a related felsic intrusion, respectively; Sims et al., 1998). They bear sulphide mineralization and platinum group minerals, are contemporaneous with peraluminous Famatinian granites, and have been associated with backarc extension (Delakowitz et al., 1991; Ferracutti et al., 2013).

Even less abundant than this, magmatism of the **FFD** has been described as a TTG association by Rapela et al. (1998), Pankhurst et al. (2000) and D'Eramo et al. (2013, 2014). The igneous rocks are relatively enriched in Na_2O compared with metaluminous sequences of the **CFD** (Fig. 4). Their geographical distribution indicates that tonalite and granodiorite to monzogranite dominate the northern part of the domain, while trondhjemite bodies are characteristic of the southeastern sector.

The southern trondhjemites are enriched in Na_2O (6.5–3.2%), CaO (3.4–2.6%) and Sr (800–400 ppm), and highly depleted in K_2O (0.65–2.02%), FeO_t (0.70–1.20%), Cs (0.2–2.3 ppm), Y (1–23 ppm) and U (0.2–1.5 ppm). These rocks have very low Rb/Sr ratios (0.015–0.12), high Sr/Y ratios (35–800), positive or absent Eu anomalies (Eu/Eu* = 0.9–2.4), [La/Yb]n ratios between 20 and 55, relatively low $(^{87}Sr/^{86}Sr)_i$ ratios (0.704–0.707) and εNd_t between +1.5 and − 4.9 (Fig. 6; D'Eramo et al., 2014 and references therein). Compared to granites in the other Famatinian domains, the high Na_2O (Fig. 4) and Sr/Y ratios (not shown) are distinctive geochemical features that plot in the high-Al adakite field in the Y vs. Sr/Y and (Yb)N vs. (La/Yb)N diagrams (Rapela et al., 1998; D'Eramo et al., 2014). The southern adakitic trondhjemites of the San Agustín, Calmayo and El Hongo bodies are enriched in Na_2O and Sr and depleted in K_2O, Rb, Ba and La compared to the tonalites and granodiorites of the northern sector of the **FFD** (D'Eramo et al., 2014) (Figs. 4, 5, 6, 8, 9 and 12).

The geochemistry and Sr—Nd isotope compositions of two bodies of weakly peraluminous (ASI = 1.0–1.1) garnet-biotite-muscovite leucomonzogranite in the **WFD** (Sierra de Pie de Palo) are shown in Figs. 4–6. They have 66 and 76% SiO_2, $(^{87}Sr/^{86}Sr)_i$ of 0.7062 and 0.7072, and εNd_t of −5.1 and − 1.6, similar to the **CFD** leucogranites (Fig. 6b, d). Very small bodies of metagabbro or amphibolite and dykes intrude the Ediacaran and early Cambrian metasedimentary sequences in the

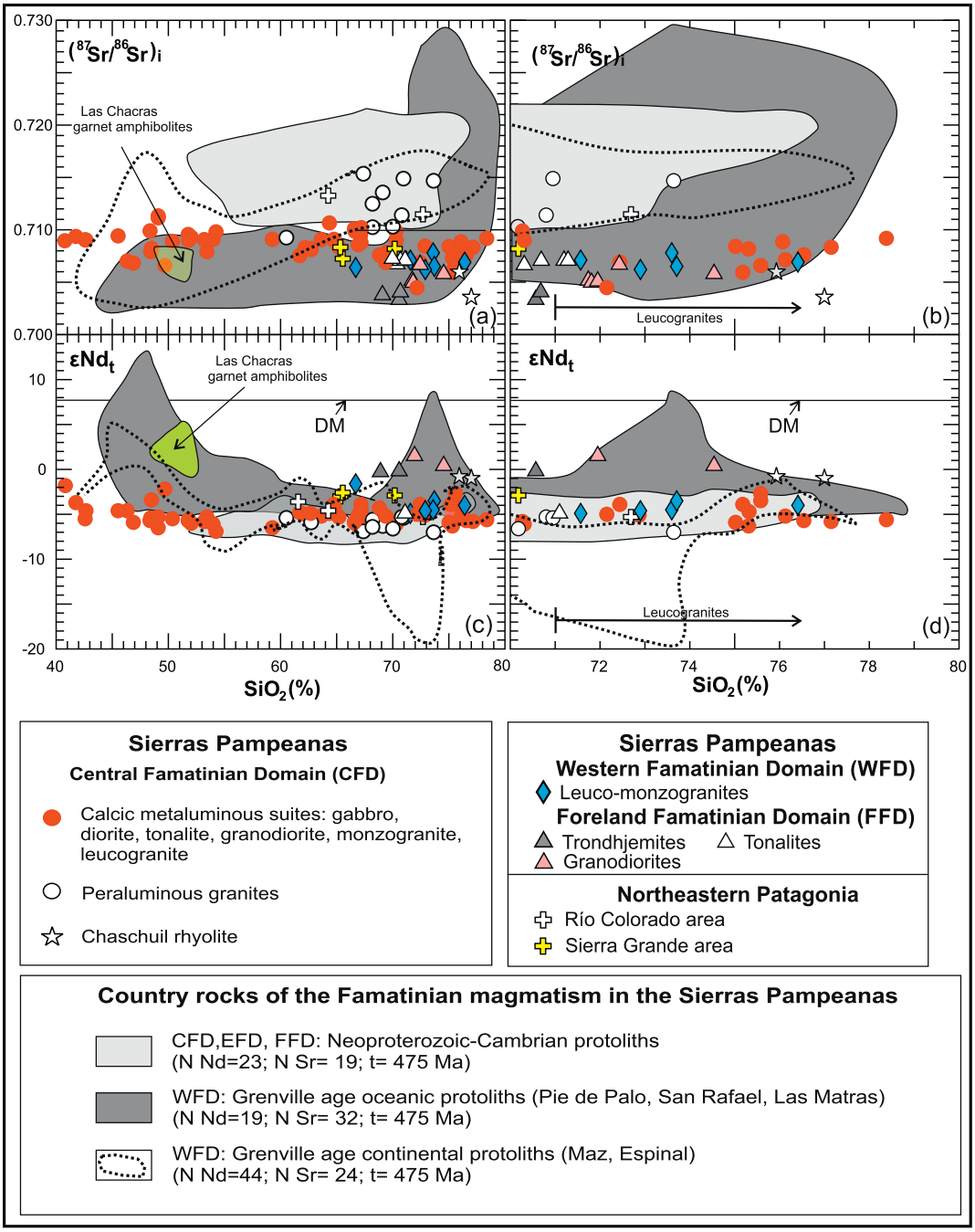

Fig. 6. Variation of $(^{87}Sr/^{86}Sr)_i$ (a, b) and εNd_t (c, d) vs. SiO_2 in the Famatinian domains of the Sierras Pampeanas and northeastern Patagonia. Nd T_{DM}* is according to DePaolo et al. (1991). 6b and 6d are expanded from the higher SiO_2 section of 6a and 6c, respectively. Data sources for the magmatic rocks as in Fig. 4 and Casquet et al. (2012b). The field of Grenville-age oceanic country rocks of the WFD is from Sato et al. (2000), Rapela et al. (2010) and Cingolani et al. (2017), while the field of Grenville-age continental country rocks in the WFD is from Rapela et al. (2010).

southeastern sector of the **WFD**. The Las Chacras garnet amphibolites (Fig. 2a), a former small mafic intrusion in a forearc position, underwent metamorphism at 12 kbar resulting from underplating of the magmatic arc: they have juvenile (positive) εNd_t values but more evolved $(^{87}Sr/^{86}Sr)_i$ ratios (Fig. 6a, c) (Casquet et al., 2012b; Mulcahy et al., 2014).

3.2. Northeastern Patagonia

The geochemistry and Nd—Sr isotope composition of the Ordovician granites in northeastern Patagonia were re-considered by Pankhurst et al. (2014). Representative compositions of granite in the Sierra Grande and Río Colorado areas (Fig. 3) are shown in Figs. 4–6. In the small sierra of Pichi Mahuida (Río Colorado) peraluminous biotite granodiorite and two-mica monzogranite have 62–73% SiO_2, $(^{87}Sr/^{86}Sr)_i$ of 0.7115 and 0.7133, and εNd_t of −4.7 and − 5.3, similar compositions to those of the peraluminous granites of the **CFD** of the Sierras Pampeanas (Fig. 5). In contrast, in the Sierra Grande area biotite- and biotite-hornblende metaluminous to low peraluminous granodiorite with 65–70% SiO_2 have $(^{87}Sr/^{86}Sr)_i$ of 0.7072–0.7083 similar to the metaluminous suite of the **CFD** (Fig. 6a) but less evolved εNd_t (−2.6 to −3.0, Fig. 6c).

4. Geochronology

4.1. Previous studies

Syn-sedimentary Ordovician volcanism was recognized in northwest Argentina > 50 years ago (e.g., Turner, 1964) but dating of the widespread granitoid rocks of this part of the Gondwana margin was for a long time confused by the failure to distinguish Famatinian rocks within the long sequence of Cambrian to Carboniferous magmatism and concomitant resetting of K—Ar and Rb—Sr systems. Modern reliable dating of Ordovician magmatism in South America may be said to have started with precise U—Pb monazite ages of 467–476 Ma for granitic rocks in the Puna of NW Argentina (Lork and Bahlburg, 1993). The first comprehensive study of Famatinian granitoids in the Sierras Pampeanas (petrology, setting, major and trace elements geochemistry, and Rb—Sr and U—Pb geochronology) was centred on the Los Llanos–Ulapes batholith (Pankhurst et al., 1998), yielding a range of Early–Mid Ordovician ages of 450–490 Ma. The age span of the major episode was refined to ca. 470–490 by U–Pb SHRIMP zircon dating over a much wider area by Pankhurst et al. (2000) and Dahlquist et al. (2008). Niemeyer et al. (2014) and Pankhurst et al. (2016) used U—Pb SHRIMP to date Ordovician granites in northern Chile, obtaining ages of 461–484 Ma and suggesting continuation of the Famatinian magmatic belt through Cordón de Lila at 24°S. Some recent studies have concentrated on porphyritic granites in Sierra de Velasco: de los Hoyos et al. (2011) reported a conventional TIMS (thermal ionisation mass-spectrometry) U—Pb monazite age of 476 ± 2 Ma and Bellos et al. (2015) reported eight U—Pb SHRIMP zircon ages, six in the range 464–474 Ma and two younger ages of 456 ± 7 and 442 ± 5 Ma which they claim show continued magmatism over at least 40 Ma. Laser analysis using inductively-coupled plasma mass-spectrometry (LA-ICP-MS) has been applied to the Famatinian igneous complex of Sierra de Valle Fértil by Ducea et al. (2010). In an important development Ducea et al. (2017) have followed this up with high-precision U—Pb dating

Table 1
Summary of SHRIMP U—Pb zircon ages.

Sample N°	Sample	Lat. (S)	Long. (W)	Locality/Unit/Rock type	Age (Ma)
Figs. 2, 3		deg min	deg min		
Famatinian Foreland Domain					
1	LCA142 (1)	30 56.680	64 25.660	Sierras de Córdoba, Güiraldes tonalite	470 ± 3[a]
2	LCA143 (1)	30 56.680	64 25.660	Sierras de Córdoba, Güiraldes tonalite	474 ± 3
3	SCS184 (1)	30 59.010	65 23.440	Sierras de Córdoba, San Agustín trondhjemite	482 ± 4
4	LPL150 (3)	31 58.380	64 23.770	Sierras de Córdoba, La Playa granodiorite (Bt + Mu)	469 ± 4[a]
Eastern Famatinian Domain					
	ANC10017 (7)	28 57.317	65 22.805	Sierra de Ancasti, Las Cañadas monzogranite	470 ± 5[c]
Central Famatinian Domain					
	Peraluminous				
5	TUA1029 (3)	31 08.010	66 32.848	Sierra de Chepes, Tuaní cordierite monzogranite	486 ± 7[a]
9	VEL1026 (3)	29 20.818	67 15.137	Sierra de Velasco, La Puerta Bt monzogranite	482 ± 3[a]
10	VEL3000 (1)	29 15.567	67 15.900	Sierra de Velasco, cordierite monzogranite	481 ± 3
11	ANT8 (2)	28 49.440	67 18.647	Sierra de Antinaco, monzogranite	475 ± 3[c]
12	VMA1018 (3)	28 46.018	66 35.372	Sierra de Mazan, peraluminous monzogranite	480 ± 3[a]
13	CAP1021 (3)	27 27.055	66 23.505	Sierra de Capillitas, cordierite monzogranite	474 ± 3[a]
14	BEL7 (2)	27 36.765	67 01.077	Sierra de Capillitas, Belén, monzogranite	472 ± 3[c]
22	FAM7086 (6)	29 11.187	68 27.415	Sierra de Famatina, Cerro Toro tonalite	481 ± 4
Metaluminous					
6	TUA1028 (3)	31 08.010	66 32.848	Sierra de Chepes, Tuaní leucomonzogranite	482 ± 3[a]
7	NAC256 (3)	30 49.420	66 25.000	Sierra de Chepes, Nacate granodiorite (Hb + Bt)	474 ± 3[a]
8	RLC236 (1)	30 58.250	66 39.400	Sierra de Chepes, Río de las Cañas granodiorite	469 ± 4[a]
	OLT279 (3)	30 37.960	66 19.630	Sierra de Chepes, Olta monzogranite	473 ± 4[a]
	FAM7081 (6)	29 09.375	68 29.410	Sierra de Famatina, Potrero Grande rhyolite	477 ± 4
15	CHA3008 (4)	27 47.735	68 03.167	Sierra de Las Planchadas, Chaschuil, rhyolite	468 ± 3
16	MIR1014 (3)	29 20.498	67 46.458	Sierra de Famatina, Ñuñorco granodiorite (Bt + Hb)	478 ± 4[a]
	FAM7083 (6)	29 09.375	68 29.410	Sierra de Famatina, Ñuñorco monzogranite	463 ± 4
	VCA1007 (3)	28 58.830	68 13.127	Sierra de Famatina, Cerro Toro diorite	467 ± 3[a]
17	SVF577 (3)	30 39.280	67 36.170	Sierra de Valle Fértil, hornblende gabbro	472 ± 5[a]
18	SVF508 (1)	30 46.410	67 34.380	Sierra de Valle Fértil, tonalite (Hb + Bt)	474 ± 3
	SVF593 (3)	30 40.210	67 30.300	Sierra de Valle Fértil, granodiorite	466 ± 4[a]
Western Famatinian Domain					
19	SPP6093 (1)	31 43.967	67 58.575	Sierra de Pie de Palo, leucomonzogranite	469 ± 9[b]
Precordillera (K-bentonites)					
20	TAL6071 (4)	31 00.572	68 46.268	Talacasto K-bentonite	470 ± 3
21	TAL6073 (4)	31 01.583	68 45.077	Talacasto K-bentonite	470 ± 3
Patagonia					
23	PIM113 (5)	38 48.360	64 59.787	Río Colorado, Pichi Mahuida granodiorite	474 ± 6
	PIM115 (5)	38 47.798	65 00.683	Río Colorado, Pichi Mahuida granite	475 ± 5
	SGR16 (5)	41 34.268	65 06.783	Sierra Grande area, Arroyo Salado monzogranite	475 ± 6
24	SGR019 (5)	41 32.817	65 00.083	Sierra Grande area, Playas Doradas granodiorite	476 ± 4
25	SGR035 (5)	41 40.247	65 22.612	Sierra Grande area, Sierra Grande monzogranite	476 ± 6

Age errors quoted are 2 s.
(1) this paper, ANU SHRIMP data; (2) this paper, Sao Paolo SHRIMP data; (3) Pankhurst et al. (2000), (4) Fanning et al. (2004); (5) Pankhurst et al. (2006); (6) Dahlquist et al. (2008); (7) Dahlquist et al. (2012)
[a] Age recalculated from original data or reanalysis (see text).
[b] Upper intercept age.
[c] LA-ICP-MS analysis: all others SHRIMP.

using chemical abrasion and thermal ionisation mass-spectrometry (CA-TIMS) yielding six ages ranging from 467.38 ± 0.15 to 471.64 ± 0.002 Ma, which they claim dates emplacement of the entire gabbro-to-granite sequence of Sierra de Valle Fértil within the interval 472–468 Ma.

4.2. Methodology and new results

For the present work some of our earliest SHRIMP data (analyses carried out in 1997–98) have been reprocessed using SQUID software (Ludwig, 2009), as indicated in Table 1. Most of these ages have only changed within a 3σ bandwidth (i.e., by < 2%) due to this reprocessing. However, two samples (RLC-236 and LCA-142) were originally on a mount with a poor-quality zircon standard: these have been completely reanalysed using Temora (Black et al., 2003) and the determined ages thereby reduced by almost 30 Ma, so that Famatinian magmatism older than 490 Ma is no longer considered a credible interpretation. Seven further samples have been analysed for the first time, five of them at the Research School of Earth Sciences at the Australian National University using the same methodology as in Pankhurst et al. (2016) (Table 1, Fig. 7). Except where stated otherwise, common Pb correction of $^{206}Pb/^{238}U$ was based on the ^{207}Pb measurement so that no test for concordance was possible. Calculated ages are reported with 2-sigma (or 95% confidence limit) uncertainties, including reproducibility of the U/Pb calibration standard (generally 0.3–0.5%). U—Pb crystallization ages of zircon from the other two samples (ANT8 and BEL7) were determined at the Geochronological Research Center, Sao Paulo University, Brazil, using a193-nm excimer laser (Photon Machines) coupled to a Neptune multicollector, double-focusing, magnetic sector ICP-MS. Operating procedures and parameters were as discussed by Sato et al. (2010) and Basei et al. (2013).

The results for the analysed samples are described below; initial numbers in parentheses (from Table 1) refer to localities in Fig. 2. Full analytical data are given in Supplementary Data File S2.

4.3. Foreland Famatinian Domain

(1) LCA142. This sample is from a tonalite pluton at Güiraldes on

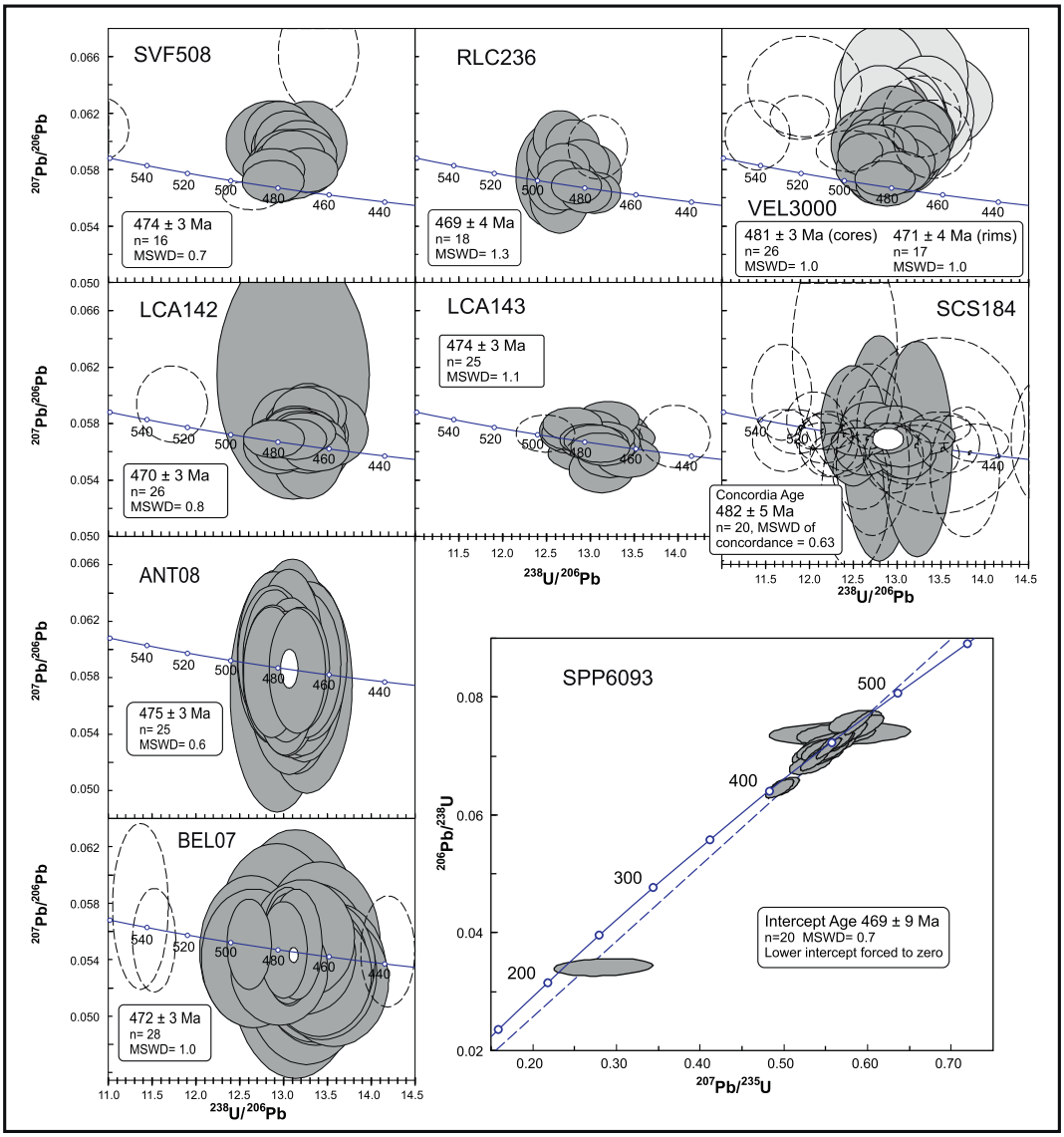

Fig. 7. Partial Tera-Wasserburg plots for new SHRIMP U—Pb zircon dating as listed in Table 1; some inherited zircon data are not shown. Error ellipses are plotted at 2σ and the dotted outlines show data not used in the age calculation. For samples SVF508, RLC236, VEL3000, LCA142 and LCA143 the data are uncorrected for common Pb; for the remainder they are corrected using the measured ^{204}Pb. Age uncertainties are 2σ or 95% confidence level allowing for calibration uncertainties as shown in Supplementary Data File S2.

the northeastern side of Sierra Chica de Córdoba. Rapela et al. (1998) reported a SHRIMP U—Pb zircon age of 499 ± 5 Ma for this but, as noted above, the standard grains on the mount were considered unsatisfactory. *Re*-analysis against the current Temora standard yields a much younger age of 470 ± 3 Ma. The new result is confirmed by simultaneous analysis of zircon from an equivalent sample nearby (2, LCA143) which gives 474 ± 3 Ma. Cathodoluminescence images of both samples show euhedral grains with oscillatory outer zones on complex (sometimes multi-stage) cores.

(3) SCS184 from San Agustín, in the southeastern part of Sierra Chica de Córdoba, is a sodium-rich trondhjemite. Relatively high U contents in zircon (typically around 400 ppm) enabled meaningful common-Pb correction using the measured ^{204}Pb. With very few exceptions the U—Pb data are spread along Concordia between 450 Ma and 530 Ma, probably reflecting both inheritance and Pb-loss (one spot gave a Paleoproterozoic age), but with a relative concentration at ca. 480 Ma. A Concordia age of 482 ± 5 Ma was obtained but only after filtering out the youngest and oldest within this range as well as some discordant points. Conventional (multi-grain) U—Pb zircon ages of 506 ± 5 Ma and 512 ± 3 Ma for two nearby trondhjemite plutons (D'Eramo et al., 2013) were based on mostly discordant data, uncorrected for common-Pb. All these ages for trondhjemite plutons, including sample SCS184 of this study, should be considered with caution, although they could indicate a relatively early stage of Famatinian magmatism.

4.4. Central Famatinian Domain

(8) RLC236, granodiorite, Río de la Cañas, Sierra de Chepes. Previous U—Pb zircon ages for this sample (Pankhurst et al., 1998) were 486 ± 4 Ma (TIMS analysis, Concordia upper intercept) and 497 ± 6 Ma (SHRIMP). Re-analysis of the original SHRIMP mount with Temora gives consistent data with a weighted mean ^{238}U/^{206}Pb age of 469 ± 4 Ma, within the range of most ages for the **CFD** granitoids.

(10) VEL3000. This is a cordierite granite with a blastomylonitic fabric from Sierra de Velasco. Zircon is present mostly as whole grains with concentric oscillatory zoning on small luminescent cores but with well-developed low-luminescence overgrowths up to 100 μm thick and with Th/U ratios typically < 0.1 that are ascribed to in situ metamorphism. Preliminary results for this sample were summarized by Rapela et al. (2001) and are confirmed by the reprocessed data which yield ages of 481 ± 3 Ma for the igneous cores and 471 ± 4 Ma for the overgrowths. Development of the rims is thought to have occurred immediately after emplacement at the climax of local Famatinian metamorphism. Rapela et al. (2001) and Casquet et al. (2012b) reported consistent ages of 466 ± 4 Ma, 467 ± 8 Ma and 468 ± 2 Ma for similar metamorphic zircon rims in samples of migmatite from Sierra de Valle Fértil.

(11) ANT8 and (14) BEL7 are two very similar samples of garnet and cordierite monzogranite from Sierra de Velasco and Sierra de Capillitas respectively. Zircon was separated and analysed by LA-MC-ICP-MS at Instituto de Geociências, University of São Paulo, Brazil. The grains are mostly whole, elongated and euhedral with prismatic terminations; concentric oscillatory zoning is developed on structureless or complex cores. ANT08 zircon has high U contents (mostly > 1000 ppm) and after correction using the measured ^{204}Pb yield a well-constrained Concordia age of 475 ± 3 Ma (disregarding a single anomalously young point). For BEL7, with more moderate U contents, the U—Pb data are more scattered, showing a range of inherited zircon (ca. 500–550 Ma and ca. 1400–2000 Ma) in addition to Early Ordovician

Table 2
Summary of Hf and O isotope results.

Locality	Sample No.	Lithology	εHf(t)	TDM (Ga)[a,b]	δO‰	
(Figs. 2, 3)			Range[c]		Range[a]	Mean
Sierras Pampeanas-Foreland Famatinian Domain						
1	LCA142		(−14.5) −8.1 to −1.8	1.5–1.9 (2.3)	+6.1 to +8.7 (+11.4)	+7.8
2	LCA143		−5.4 to −1.8	1.5–1.7	+6.3 to +8.2	+7.5
3	SCS184		−4.6 to +10.3	0.7–1.7	+4.3 to +11.7	+6.5
4	LPL150		+0.9 to +8.4	0.8–1.3	+3.6 to +5.7	+5.1
Sierras Pampeanas-Central Famatinian Domain						
	Peraluminous granites					
5	TUA1029		−6.7 to −2.8	1.6–1.8	+8.3 to +10.5	+9.4
9	VEL1026		−6.2 to −2.0	1.5–1.7	+8.8 to +11.2	+10.1
10	VEL3000		(−23.4) −6.8 to −3.3	1.6–1.8 (2.8)	+7.5 to +14.1	+10.2
11	ANT8		0.0 to −9.3	1.4–2.0		
13	CAP1021		(−11.9) −8.7 to +0.6	1.3–1.9 (2.1)	+7.2 to +11.6	+10.3
14	BEL-7		−26.1 to −17.8	2.5–3.0		
Metaluminous suites						
6	TUA1028		−6.5 to −1.5	1.5–1.8	+6.8 to +11.3 (+13.5)	+8.7
7	NAC256		−8.3 to −1.5	1.5–1.9	+7.2 to +9.2	+8.2
8	RLC236		−8.1 to −3.9	1.6–1.9	+7.2 to +8.4	+7.8
15	CHA3008		+2.7 to +5.2	1.0–1.2	+4.0 to +5.5	+4.9
16	MIR1014		−4.5 to –0.7	1.4–1.6	+5.2 to +7.3	+6.3
17	SVF577		−5.3 to −2.5	1.5–1.7	+6.5 to +8.1	+7.4
18	SVF508		−5.8 to −1.3	1.5–1.7	+6.7 to +9.5	+7.8
Sierras Pampeanas-Western Famatinian Domain						
19	SPP6093		−5.1 to +3.2	1.2–1.7	+5.3 to +6.7	+5.9
Precordillera (K-bentonites)						
20	TAL6071		−3.5 to −1.7 (+1.9)	1.2–1.6	+4.6 to +6.5	+5.5
21	TAL6073		−5.5 to +1.6	1.4–1.8	+3.7 to +7.6	+5.6
Northeastern Patagonia						
23	PIM113		−6.1 to −4.1	1.6–1.7	+9.5 to +10.4	+9.9
24	SGR19		−2.3 to +1.0	1.3–1.5	+6.8 to +9.1	+8.2
25	SGR35		−3.3 to +1.5	1.3–1.6	+8.5 to +9.8	+8.9

[a] Model age for separation from depleted mantle.
[b] Obvious outliers in paratheses.

grains. In the $^{207}Pb/^{235}U$ vs $^{206}Pb/^{238}U$ plot (not shown) there is clear scatter between the Ordovician age of concordant zircons and a Proterozoic age of about 2000 Ma, suggesting partial inheritance. In view of the unusual Hf-isotope composition (see below) additional cores were analysed, but many appear to have equilibrated U—Pb systems in which cores and rims yield indistinguishable Ordovician ages; the overall Concordia age is 472 ± 3 Ma.

(18) SVF508. Tonalite, Quebrada de Las Juntas, Sierra de Valle Fértil. Zircon forms mostly large (100 μm) single grains with fine oscillatory zoning, some on unzoned cores, and with a luminescent outer rim too thin to analyse. The U—Pb data are consistent except for a single late Neoproterozoic inheritance age and yield a weighted mean $^{238}U/^{206}Pb$ age of 474 ± 3 Ma.

4.5. Western Famatinian Domain

(19) SPP6093. This leuco-monzogranite cuts the Neoproterozoic Difunta Correa Metasedimentary Series in Sierra Pie de Palo (Baldo

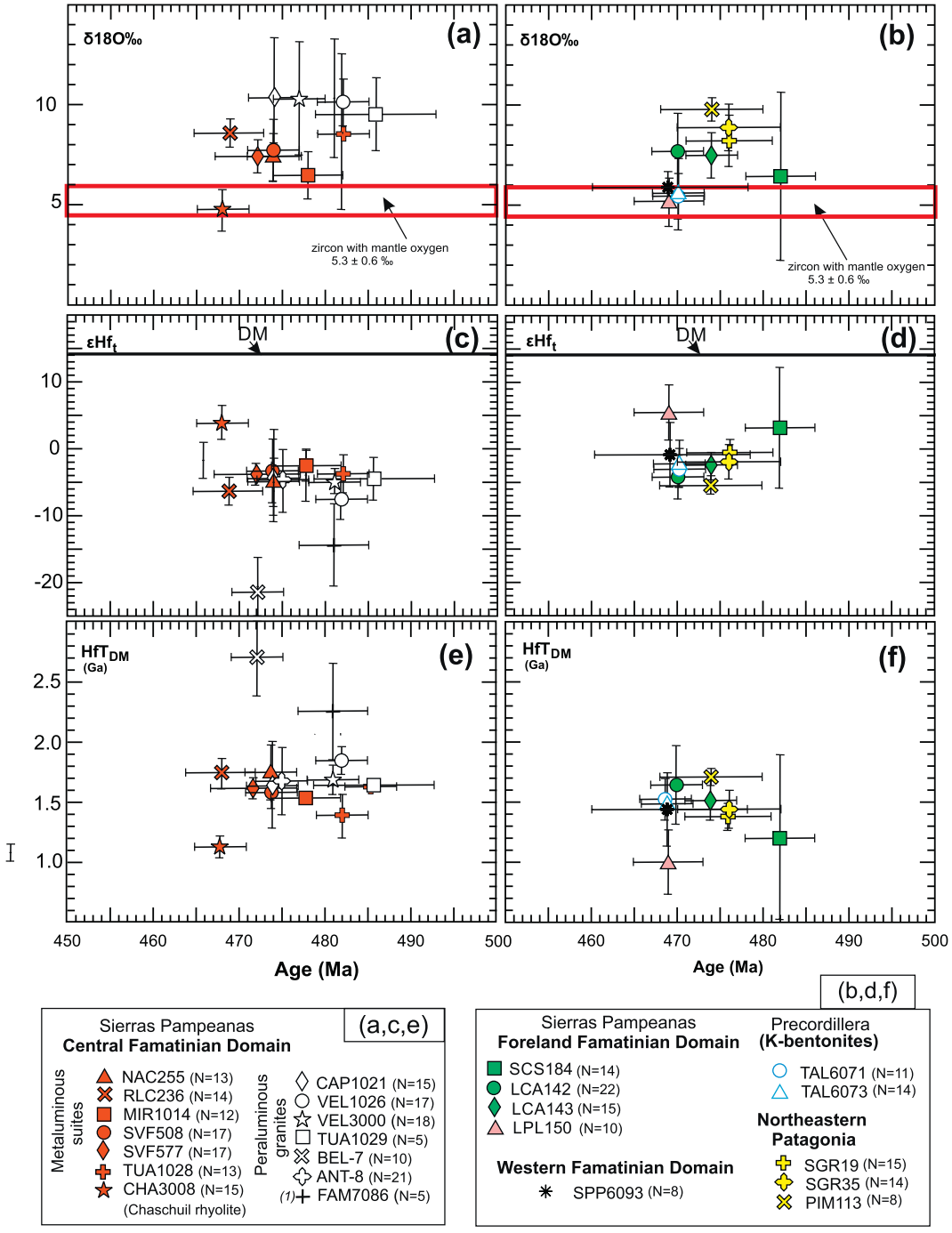

Fig. 8. U—Pb zircon ages ($^{206}Pb/^{238}U$) vs. $\delta^{18}O‰$, εHf_t and HfT_{DM} (Depleted Mantle model age) values for zircons analysed in this study for samples from the Central Famatinian Domain (a,c,e) and the Foreland and Western Famatinian domains, the K-bentonites of the Precordillera and northeastern Patagonia (b,d,f). The range of error in crystallization ages of individual samples are shown by horizontal bars from Table 1. Two standard deviation error vertical bars show the isotopic variability of $\delta^{18}O‰$, εHf_t and HfT_{DM} within samples. Numbers of analysed zircon grains per sample are shown between brackets. The value for zircon with mantle $\delta^{18}O$ is from Valley et al. (2005) while Hf TDM ages are for crystallization from a crust-type source with $^{176}Lu/^{177}Hf = 0.150$ (Goodge and Vervoort, 2006) assuming original depleted mantle values from Vervoort and Blichert-Toft (1999). Sample data in Supplementary Data File S3. *(1)* From Dahlquist et al. (2013).

et al., 1998, 2012; Galindo et al., 2004) and is the sole representative from the **WFD** analysed here. Elongated zircon grains show outer zoned areas on various types of core. The U—Pb data are rather discordant and best interpreted in the Wetherill diagram after common Pb correction using ^{204}Pb; this yields a reasonable upper intercept age of 469 ± 9 Ma.

5. O and Hf isotope analysis in zircon

Hf and O isotope analyses of zircon at RSES were made after removing the ion-probe pits made during U—Pb dating by light polishing. In some cases the samples were transferred into megamounts and O-isotope compositions were measured using SHRIMP II following procedures similar to those described by Ickert et al. (2008). The O-isotope ratios and calculated $\delta^{18}O_{VSMOW}$ values were normalized relative to the weighted mean for reference zircon FC1 in the respective analytical session. Hf isotope compositions were then obtained in the same dated spot using a Neptune multicollector inductively-coupled plasma mass spectrometer (ICP-MS) together with a HelEx 193 nm ArF Excimer laser ablation system (Eggins et al., 2005). The initial ^{176}Hf/^{177}Hf ratios were calculated using the U—Pb crystallization age of each grain or area. Hf isotope compositions for samples BEL7 and ANT8 were determined at University of Sao Paulo also using a Thermo-Finnigan Neptune multicollector ICP-MS with nine Faraday collectors on the same zircon areas that were previously dated: procedures were as described by Sato et al. (2010) and Basei et al. (2013).

Full O and Hf isotope data in zircon are provided in Supplementary Data File S3, with results summarized in Table 2. The isotopic

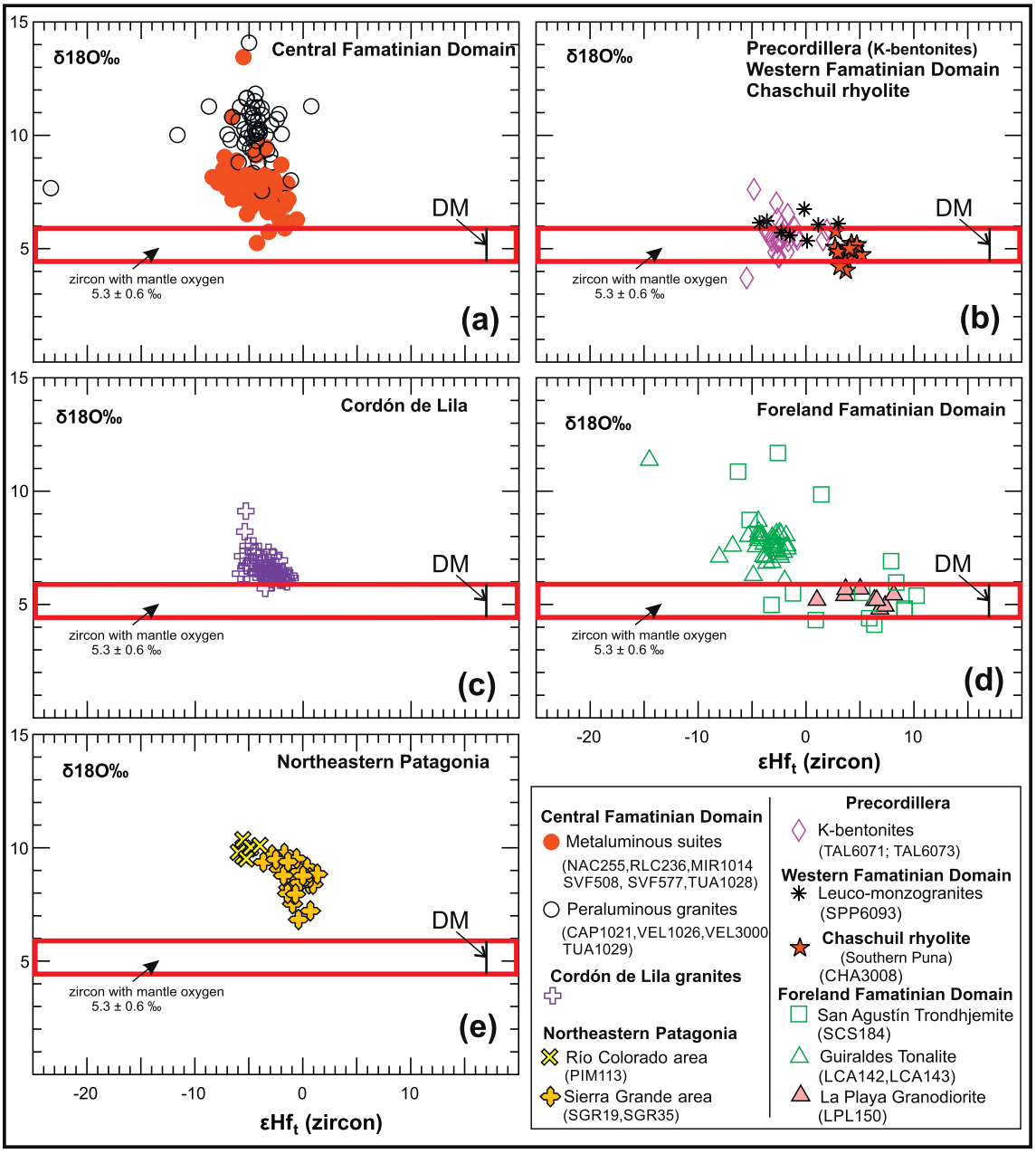

Fig. 9. Plots showing εHf$_t$ vs. δ^{18}O‰ values in zircon from the Central Famatinian Domain (a), the Western Famatinian Domain, the Precordillera K-bentonites and the Chaschuil rhyolite (b), the Cordón de Lila, Chile (c), the Foreland Famatinian Domain (d) and northeastern Patagonia (e). The value for zircon with mantle δ^{18}O is from Valley et al. (2005) while εHft for DM at 475 Ma is calculated assuming original depleted mantle values from Vervoort and Blichert-Toft (1999). Sample data in Supplementary Data File S3 and Pankhurst et al. (2016) for Cordón de Lila.

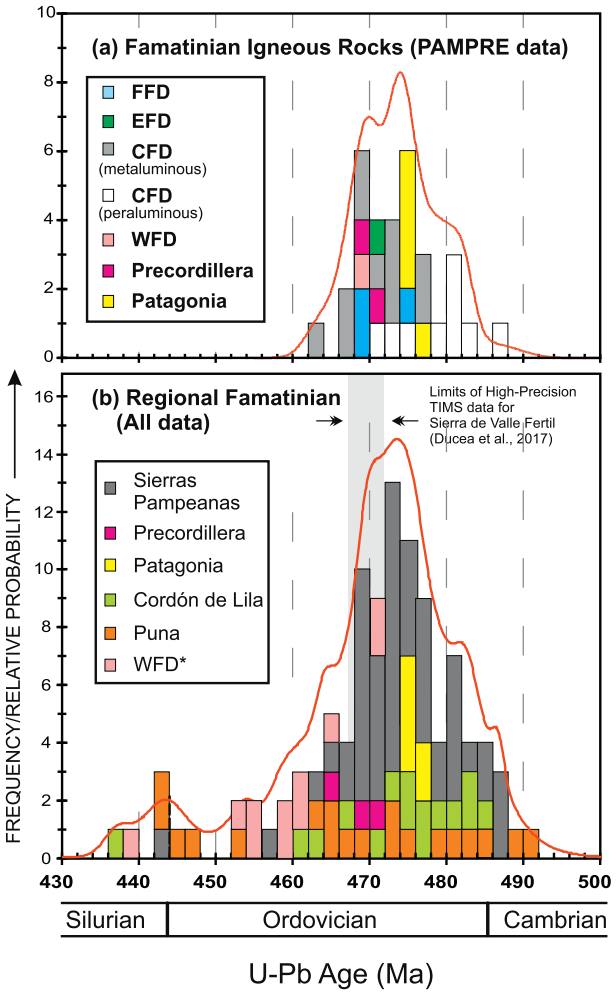

Fig. 10. Distribution of U—Pb zircon ages for Famatinian igneous rocks: (a) dated by our research group (PAMPRE, Table 1), (b) with the addition of further U—Pb zircon ages from the Sierras Pampeanas (Sims et al., 1998; Varela et al., 2011; Rubiolo et al., 2002; Ducea et al., 2010; Bellos et al., 2015), the Puna (Viramonte et al., 2007; Hauser et al., 2011; Insel et al., 2012), northern Chile (Niemeyer et al., 2014; Pankhurst et al., 2016), the Precordillera (Huff et al., 1997) and Patagonia (Varela et al., 1998). The range of high-precision TIMS U—Pb zircon ages of Ducea et al. (2017) for Sierra de Valle Fértil is also shown. See text for discussion of data of Bahlburg et al. (2016).

variability within sample vs. age is shown in Fig. 8 using 2 standard deviation error bars of the given isotopic parameter, arranged according to the domains distinguished in the Sierras Pampeanas, the Precordillera and northeastern Patagonia. Fig. 9 show all the collected O and Hf individual isotopic data from samples of the different domains and regions.

Oxygen data for the Sierras Pampeanas **CFD** clearly distinguish the metaluminous suites from the highly peraluminous granites with ASI > 1.1, the latter having high $\delta^{18}O$, with averages > 9.5‰ (Fig. 8a), indicating crustal reworking of metasedimentary source rocks. On the other hand, εHf_t shows a similar restricted range of negative values, mostly between −2 and −7, for both (Fig. 8c), with Meso- to Paleoproterozoic depleted mantle model ages of 1.4–1.9 Ga (Fig. 8e). Occasional grains of the peraluminous granites VEL3000 and CAP1021 have highly negative εHf_t values, but this is true for all analysed grains of peraluminous granites BEL7 and FAM7086 (Fig. 8c)

The Chaschuil rhyolite CHA3008, located at the northwestern border of the **CFD** (Fig. 2), has more juvenile $\delta^{18}O$ (+4.0 to +5.9‰) and εHf_t (+2.07 to +7.0), and younger Mesoproterozoic Hf TDM ages, than the majority of the metaluminous suites and peraluminous granites (Fig. 8a, c, e). The very similar U—Pb ages of sample CHA3008 (468 ± 3 Ma) and the K-bentonites of the Precordillera (both gave 470 ± 3 Ma, Table 1) have been taken as an evidence of the proximity of the Precordillera to the Famatinian arc at ca. 470 Ma (Fanning et al., 2004). However the K-bentonites have more evolved εHf_t (Fig. 8c, d), slightly higher $\delta^{18}O$ (+3.7 to +7.6‰) (Fig. 9b) and Paleoproterozoic TDM ages similar to the range observed in the **CFD** (Fig. 8e, f), precluding direct derivation from ashes produced during the eruption of Famatinian rhyolites such as those at Chaschuil.

TTG plutons of the **FFD** emplaced at different times from ca. 482 to 469 Ma show contrasting O and Hf zircon isotope signatures. The oldest body (San Agustín trondhjemite, 482 ± 4 Ma, sample SCS184, Fig. 2) has zircon with variable $\delta^{18}O$ values, many of them within the presumed mantle range (Table 2) and rather variable εHf_t values, with more than half of them positive (+0.5 to +10.3) (Fig. 9d). Sample LPL150, located within the Guascha Corral–Los Túneles shear zone that separates the **FFD** from the **EFD** in northwestern Córdoba (Fig. 2, 469 ± 4 Ma), also has juvenile $\delta^{18}O$ and εHf_t as well as late Mesoproterozoic Hf T_{DM} ages (Fig. 8b, d, f). On the other hand, the two samples of the Güiraldes leucotonalite from the northeastern sector of the Sierras de Córdoba (samples LCA142 and LCA143, 470 ± 3 Ma; 473 ± 4 Ma, Table 1), have more evolved $\delta^{18}O$, similar to the metaluminous suites of the **CFD**, and εHf_t values and T_{DM} ages that cannot be distinguished from those of either the metaluminous suites or the peraluminous granites of the **CFD** (Fig. 8b, d, f).

The sample of leuco-monzogranite from the **WFD** (SPP6093) shows a high degree of scatter in the Ordovician crystallization ages, probably associated with Pb-loss during penetrative Ordovician ductile deformation of the granite and the country rocks (Fig. 7). Although it has similar εHf_t and T_{DM} ages to the bulk of **CFD** (Fig. 8d, f) and also similar $(^{87}Sr/^{86}Sr)_i$ and εNd_t (Fig. 6b, d), the O isotope composition is within or very close the range of mantle zircon (Figs. 8b, 9b). These characteristics are similar to those of the Precordillera K-bentonites (Fig. 9b), suggesting a Proterozoic source that remained isolated in the deep crust, retaining its original oxygen mantle signature.

Zircon from granites of the two studied areas in northeastern Patagonia does not show consistent Hf and O isotope signatures (Fig. 8b, d, f and Fig. 9e). That for the peraluminous granite from the Río Colorado area (Fig. 3, sample PIM113, 474 ± 6 Ma) has positive $\delta^{18}O$ values and negative εHf_t values indistinguishable from those in the peraluminous granites of the **CFD** (Fig. 9e,a). Granodiorites in the Sierra Grande area to the south (Fig. 3, samples SRG19 and SRG35, 476 ± 4 Ma, 476 ± 6 Ma) have positive $\delta^{18}O$ values of +7.5 to +9.8‰ and εHf_t values of −3.0 to +1.2 (Fig. 9e). Those values are also within the bulk range of the granites of the **CFD** (compare Fig. 9a, e), although the εHf_t ratios of Northeast Patagonia are slightly less evolved than those of the bulk of the metaluminous suites of the **CFD** (Table 2, Fig. 8d, and Fig. 9a,e).

6. Timing and areal extent of Famatinian magmatism (27°-42°S)

Twenty-six Famatinian igneous rocks from the Sierras Pampeanas have been dated in this and previous publications by our research group (Table 1), twenty-three of these using SHRIMP at ANU and three using LA-MC-ICP-MS at USP. Our SHRIMP results for two K-bentonites from the Precordillera and five granites from NE Patagonia are also listed. The total age range, allowing for reprocessing and re-analysis as described above, is 463 ± 4 to 486 ± 7 Ma (of which 90% fall between 468 and 482 Ma). When fitted to a relative probability curve (Fig. 10a), the age distribution shows a clear bimodal maximum apparently representing episodes at ca. 469 Ma and ca. 474 Ma, together with a significant older peak at ca. 480 Ma that is closely associated with some peraluminous granites of the **CFD**. Magmatism in the **FFD** seems to have occurred throughout the Early and the Middle Ordovician, whereas the single dated sample from the **WFD** (the Difunta Correa granite, 469 ± 9 Ma, Table 1) falls within the youngest peak.

All available U—Pb zircon ages for Famatinian magmatic rocks from the Puna of NW Argentina, Sierras Pampeanas, Cordón de Lila in Chile and the North Patagonian Massif are plotted in Fig. 10b (91 ages, see caption for data sources). The K-bentonite ages and the Chaschuil rhyolite reinforce the 472–468 Ma peak (Table 1), dating a "magmatic flare-up" for the type section of the magmatic belt, as so termed by Ducea et al. (2010, 2017). Further possible peaks within the maximum are noted at ca. 473 Ma and ca. 476 Ma but the difficulty of making precise comparisons in view of differences in sampling and analytical conditions and treatment mean that these cannot confidently be ascribed to individual magmatic pulses as opposed to merely blurring those identified in Fig. 10a, b. Whether magmatism was semi-continuous throughout the Famatinian belt or locally occurred in discrete short-lived events, such as the ca. 4 Ma interval demonstrated by Ducea et al. (2017) for the gabbro–granite crustal section in Sierra de Valle Fértil, cannot be resolved with the lower-precision data based on SIMS methodology. The most intense period of emplacement is defined by the fact that 53 ages (58%) fall between 468 and 478 Ma, Floian and Dapingian in stratigraphical terms (IUGS IC Chart, Cohen et al., 2013).

The large high-peraluminous batholith of Capillitas at the northeastern edge of the CFD was intruded during the main episode, ca. 472–474 Ma (samples CAP1021 and BEL7, Table 1). Tonalite and granodiorite plutons were also emplaced in the **FFD** during this flare-up episode (samples LCA142, LCA143 and LPL150, Table 1). Granitoid emplacement in both northern Patagonia and the Córdon de Lila were effectively synchronous with this event in the Sierras Pampeanas.

Regarding the spread of determined ages outside the main episode, seventeen are older than 478 Ma, mostly by > 2σ errors and with a peak at ca. 480 Ma. This group includes peraluminous (S-type) granites of Sierra de Velasco, Sierra de Chepes and Sierra de Famatina metaluminous granites, as well as the less precise age for the trondhjemite of San Agustín in Sierras de Córdoba (**FFD**). Volcanism of the Famatina basin started in the Late Tremadocian (see section 2.1.1), consistent with the age inferred for this first intrusive episode.

In the case of sample VEL3000, as noted above, there is internal evidence (core–rim data, see Fig. 7) of crystallization of the peraluminous granite up to ca. 10 Ma before metamorphism coeval with the main phase Famatinian magmatism. The ca. 480 Ma episode has not

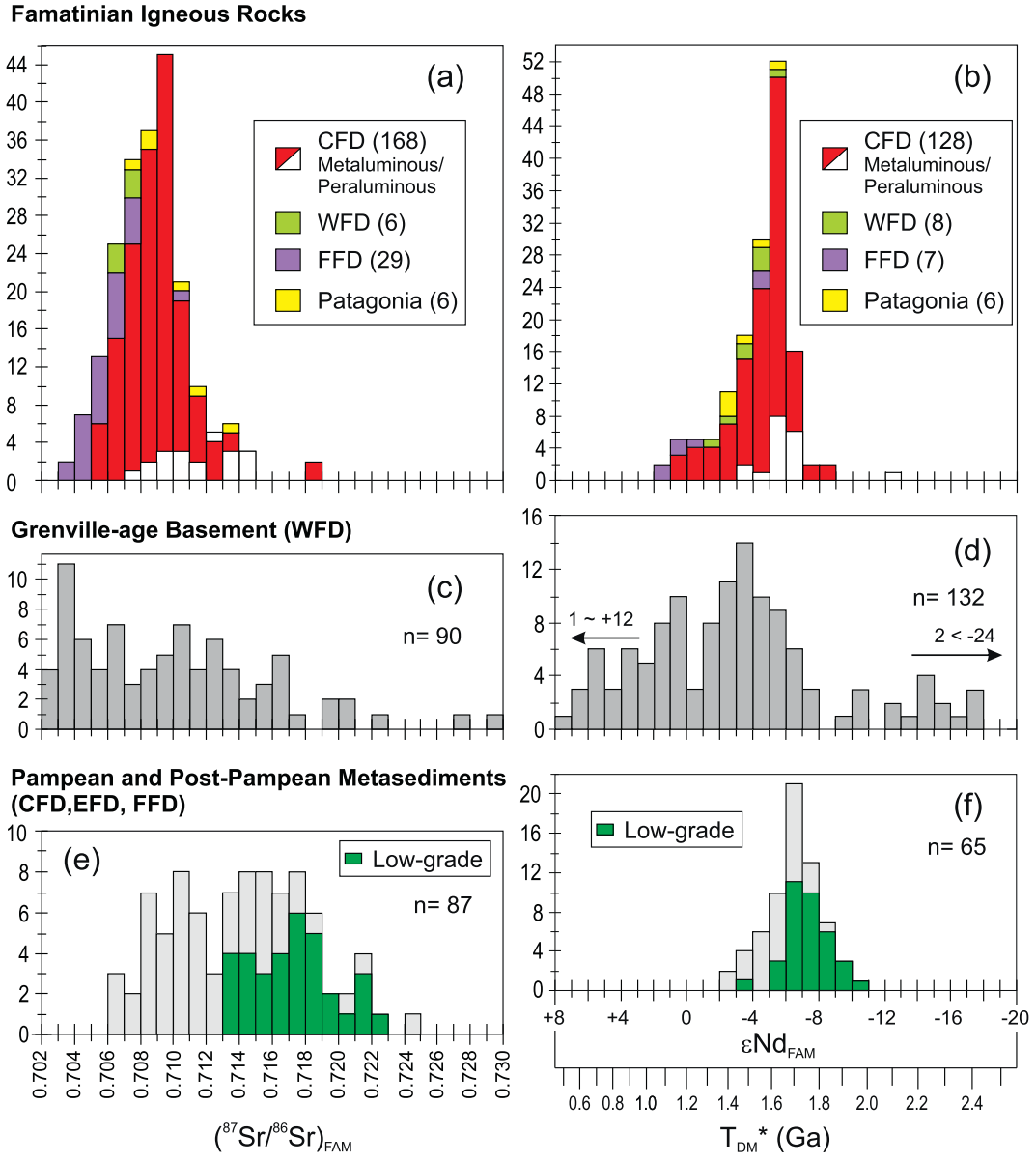

Fig. 11. Histograms of $(^{87}Sr/^{86}Sr)_i$ and εNd_t for the igneous (a,b) and different basement rocks of the Famatinian orogen recalculated at 475 Ma (c,d,e,f). NdT_{DM} ages corresponding to εNd_t values are shown in (f). Sample data and source references are given in Supplementary Data File S1.

yet been identified in the **WFD** and we suggest that the first stage of magmatism was restricted to the central and eastern part of the **CFD** where it involved large-scale melting of upper crustal metasedimentary rocks (see Section 6.3). The subsequent peak of post-480 Ma flare-up in the **CFD** suggests migration of the arc to the SW, with the youngest (ca. 470 Ma) phase of gabbroic–granitic intrusions along the general strike of Sierra de Valle Fértil (Fig. 1).

Isolated ages at the younger end of the spectrum, such as those of 442 ± 5 and 456 ± 7 Ma for metaluminous granites from southern Sierra de Velasco (Bellos et al., 2015), are difficult to interpret. Bahlburg et al. (2016) reported consistent U—Pb zircon ages (LA-ICP-MS data) in the range 444–453 Ma for peraluminous granites from the Faja Eruptiva de la Puna Oriental in NW Argentina, which would represent the youngest magmatism associated with the Famatinian event. However, this belt lies well to the east of the Cordón de Lila in Chile, where the majority of determined granite emplacement ages conform to the main Early–Middle Ordovician magmatic climax. Bahlburg et al. (2016) ascribe the late stage magmatism in the Puna to crustal melting during sinistral deformation associated with the Late Ordovician Ocloyic orogeny. In another study Bahlburg et al. (2009) presented U—Pb LA-ICP-MS dating of detrital zircon in metasedimentary rocks from the Late Paleozoic accretionary complex of northern Chile. They plotted a histogram of all ages 'between 513 and 416 Ma' which showed a broad distribution centred on maxima at 464 and 479 Ma which they interpreted as showing derivation from, and the time frame of, Famatinian magmatic rocks. A similar age spread in detrital zircon of the Famatina basin was also reported by Dahlquist et al. (2008). This is confirmed, but more precisely defined, by the crystallization ages presented here.

In addition to the geochronological data, the new Hf and O isotope in zircon show that Ordovician igneous rocks from the Cordón de Lila in Chile and as far south as northeastern Patagonia, display similar isotopic signatures (Fig. 9a, c, e). This is consistent with results based on geochemistry and S—Nd isotopes, strongly suggesting that the Famatinian rocks formed in a continuous belt throughout this vast sector. Moreover, a high-grade metasedimentary garnet gneiss from the North Patagonian Massif has zircon with metamorphic rims dated at 472 ± 5 Ma (Mina Gonzalito gneiss, Pankhurst et al., 2006), which is consistent with similar evidence for late-magmatic Famatinian metamorphism in the **CFD** (e.g., Velasco, Las Chacras – see above). Pre-metamorphic zircon cores in the Mina Gonzalito gneiss have an age pattern indistinguishable from the post-Pampean metasedimentary basement of the **CFD** (Pankhurst et al., 2006; Rapela et al., 2016).

The 468 Ma Las Cañadas granitic complex in the **EFD** (Sierra de Ancasti, Figs. 1, 2) also shows geochemical and Nd-isotope signatures (εNd_t = −3.3 to −5.5; T_{DM} = 1.5–1.6 Ga) suggesting their inheritance from old continental crust (Dahlquist et al., 2012), as in the case of the granitic rocks of the **CFD**. Altogether, the above convergent evidence of sedimentary, magmatic and metamorphic evolution indicates a continuity of at least the **CFD** and the **EFD** into northeastern Patagonia.

7. Discussion

7.1. Magma source of the metaluminous sequences

The isotopically evolved signature (Sr, Nd, Hf, O) of the basic and ultrabasic rocks is a remarkable attribute of the Famatinian arc. In contrast, the typical Mesozoic Cordilleran granites all along the Pacific rim of the America generally show evidence of a variable but obvious juvenile component, usually ascribed to an asthenospheric mantle wedge (e.g., Sendek, 2016; Shaw et al., 2014; Hervé et al., 2007, among many others). There are some, however, such as the granites of the Salinian arc in coastal California, in which even the mafic and ultramafic intrusions yield evolved Sr and Nd isotope ratios ($(^{87}Sr/^{86}Sr)_i$ is 0.7061 to 0.7092 and εNd_t + 1.4 to −5.9); in that case the source was ascribed instead to a 'enriched' lithospheric upper mantle (Chapman et al., 2014).

The Famatinian calcic metaluminous suite exhibits an extended range in silica content, from 42% (gabbro, metagabbro, ultramafic cumulates) to 77% SiO_2 (weakly peraluminous leuco-monzogranite) (Fig. 5a, b). A gap at 55–57% SiO_2 in our data set might be a sampling artefact or might reflect a significant break in the otherwise continuous trend which could then be divided into low silica (42–55% SiO_2,) and high-silica (57–77% SiO_2) subsets.

A fundamental geochemical characteristic is that throughout the wide range of lithological types 90% of the $(^{87}Sr/^{86}Sr)_i$ ratios remain within a limited range of 0.706–0.711, and εNd_t likewise stays within the range − 3 to −7 (Fig. 6). Detailed studies of mafic and ultramafic cumulates in western Sierra de Famatina and Sierra de Valle Fértil show that most εNd_t values lie in the range − 5.1 to −0.2, with only one gabbro from Sierra de Valle Fértil and two amphibolites from western Famatina having slightly positive values (+0.1 to +0.3) (Otamendi et al., 2012; Alasino et al., 2016). Importantly, the metaluminous sequence of the **CFD** shows no correlation between isotope compositions and SiO_2 content (Fig. 6, n = 57). The complete dataset of 133 Sr and 127 Nd isotope analyses (Supplementary Data File S1), including many for which SiO_2 has not been determined, emphasizes these restricted isotopic compositions (Fig. 11a, b). The limited isotope compositions contrast with those of the Late Mesoproterozoic exposed country rocks of the **WFD** recalculated at 475 Ma, mainly due to the long crustal residence time of the latter (Fig. 6, Fig. 11c, d). The metasedimentary basement of the **CFD**, **EFD** and **FFD** (including high-grade gneiss in the Sierras de Cordoba and the low-grade Puncoviscana Formation and equivalents) have consistently higher $(^{87}Sr/^{86}Sr)_i$ ratios than the metaluminous sequence, even in rocks of > 70% SiO_2 (Fig. 6b, although there is a partial overlap when considering the enlarged data set (Fig. 11e). The differences are less obvious in the case of Nd isotopes, which show slightly more negative εNd_t values in the basement rocks, but overlap at intermediate and high silica content (Fig. 6 c, d, Fig.11b, f). Felsic granites from the **WFD** and Patagonia show the same limited range of isotope compositions as the metaluminous sequence of the **CFD** (e.g., εNd_t of −1.6 to −5.3, Fig. 11a). We conclude that the exposed basement throughout the Sierras Pampeanas is unsuitable as a direct source of the Famatinian metaluminous suite magmas, despite the largely positive $\delta^{18}O$ in zircon which suggests a reworked crustal source. Whether or not the exposed crust nevertheless participated in any contamination process is considered below.

A rather restricted and evolved range in Hf isotope compositions in zircon is also characteristic of the different plutonic rocks of the metaluminous sequences (εHf_t of −1.0 to −8.0; Fig. 8c). This is comparable to the range of εHf_t in Early Paleozoic detrital zircon derived from Famatinian arc rocks according to Bahlburg et al. (2009). Thus, radiogenic isotopes are unable to distinguish gabbro and diorite of the low-silica subset from the associated tonalite, granodiorite and leucogranite of the high-silica subset. This is also commonly the case when O isotopes are considered (Table 2): a gabbro with 42.6% SiO_2 (SVF577; $\delta^{18}O$ + 6.5 to +8.1‰) exhibits essentially the same positive $\delta^{18}O$ range as the dominant Ho + Bi tonalites and granodiorites with 64.3–67.1% SiO_2 (SVF508, RLC236, NAC256; +6.7 to +9.5‰) and a leucogranite with 76.1% SiO_2 (TUA1028; +6.8 to +11.3‰). The sample with the lowest $\delta^{18}O$ values is the 75.2% SiO_2 monzogranite from Cuesta de Miranda (MIR1014; +5.2 to +7.3‰.

Several hypotheses have been proposed to explain the origin of the Famatinian magmas, which are briefly summarized.

(1) Melting of a whole lithospheric section including an old 'lithophile-enriched' mantle to explain the mafic and ultrabasic rocks (Pankhurst et al., 1998, 2000). Dahlquist et al. (2008, 2013) also proposed that generation of Ordovician magmas was dominated by crustal reworking rather than addition of new juvenile material.
(2) The dioritic and tonalitic rocks are hybrids formed by either (i) bulk assimilation of metasedimentary materials into primitive mantle

magmas, or (ii) multi-stage and complex interactions between gabbroic rocks and metasedimentary-derived leucogranitic melts. Primitive gabbroic rocks, metaluminous intermediate magmas and anatectic leucogranitic melts mixed to produce the silicic calc-alkaline granodiorites and monzogranites (Otamendi et al., 2009, 2012; Ducea et al., 2010; Ducea et al., 2017 and references therein).

(3) The granitoid magmas, specifically those of Sierra de Valle Fértil (Fig. 1a) resulted from prolonged, punctuated MASH (melting, assimilation, storage, homogenization) processes in the lower crust, in which case isotopes may be the only residual evidence of assimilation within the mafic zone (Walker Jr. et al., 2015).

(4) Alasino et al. (2016), based on whole-rock chemical composition and isotope analyses (Sr, Nd, O), suggested that the mafic igneous rocks of the west-central edge of Sierra de Famatina, **CFD** (Fig. 1a) were formed by progressive mixing of two different isotopic reservoirs. Pyroxenite (± garnet) from a metasomatized sub-arc lithospheric mantle (± lower crust) with ^{18}O-enriched signature was the probable source of older gabbroic magmas. This was followed by more primitive melts resulting from upwelling of the asthenospheric mantle wedge peridotite after lithospheric foundering.

In order to explain the relatively evolved Sr—Nd (whole rock) and Hf—O (zircon) signature of the basic/ultrabasic rocks and their limited variation over the full SiO_2 range, we propose melting of old underlying lithophile-enriched subcontinental mantle (probably together with mafic lower crust) as the main magma source of the metaluminous sequences (Hypothesis 1). Pankhurst et al. (1998, 2000) and Dahlquist et al. (2008, 2013) proposed early versions of this model, and recently Alasino et al. (2016) also considered metasomatized sub-arc lithospheric mantle (± lower crust) as one of the main sources of these rocks (Hypothesis 4). Field, geochemical and isotopic evidence indicate that these melts underwent fractional crystallization and contamination with the metasedimentary envelope at middle and upper levels of the crust. Further considerations and constraints on this hypothesis are considered below at the light of our new data.

The evolved and rather consistent isotopic signature throughout the bulk compositional range and for widely separated plutonic bodies of the metaluminous sequence appears to rule out simple mixing/and or hybridization between isotopically juvenile asthenospheric mantle melts and evolved crustal end members (Hypothesis 2) as the major factor in the generation of diorites, intermediate rocks and leucogranites. It is difficult to reconcile with direct assimilation because it would require that each batch of juvenile magma had assimilated just the right amount of extremely heterogeneous crustal material to acquire the same restricted range of Nd, Sr, Hf and O isotopic composition. Hybridisation cannot easily explain how the entire compositional spectrum of Sierra de Valle Fértil, including the metaluminous sequence, formed from mantle-derived magmas and crustal melts from the Pampean and post-Pampean metasedimentary envelope. As shown above, even the basic rocks have relatively evolved isotope compositions and the associated granodiorite–leucogranite bodies, allegedly representing the 'most crustal' product, show essentially the same composition as local basic rocks – in particular their $^{87}Sr/^{86}Sr$ initial ratios generally fall well below the fields for the metasedimentary country rocks (in Ordovician times) and the highly peraluminous Famatinian bodies (Figs. 6, 11). At the mafic end of the spectrum there is no substantial record of juvenile isotope signatures that could represent an un-hybridized mantle end-member. It is also worth pointing out that "crustal leucogranites" in this model are described as showing in situ relationships within the metasedimentary migmatites, and appear as veins or dykes in the intermediate and silicic units (Otamendi et al., 2012) and SiO_2 > 71%; FeOt + Mg < 2.7% (Ducea et al., 2010). On the other hand, leucogranites at the silica-rich end of the metaluminous sequences in this paper (Fig. 6b, d) are tabular bodies of up to 11 × 0.3 km but usually smaller (Sierra de Chepes-Los Llanos and upper section of the Sierra de Valle Fértil): they intrude the dominant intermediate granodiorites and tonalites, from which they are considered to have been derived by fractional crystallization (e.g., Dahlquist, 2002; Dahlquist et al., 2012) and have lower initial $^{87}Sr/^{86}Sr$ ratios than peraluminous leucogranites in the same silica range (Fig. 6b).

Contamination/hybridization of mafic/ultramafic magmas by the host metasedimentary rocks was considered as having played a minor role in western Famatina and Sierra de Valle Fértil (geochemical and Sr isotope plots, Alasino et al., 2016; Walker Jr. et al., 2015) (Fig. 6a), while some interaction with high-grade metasedimentary septa has been reported in Sierra de Valle Fértil (Otamendi et al., 2012). Local contamination of the intermediate metaluminous magmas involving partial reaction with high-grade metapelite occurs in roof zones and anatectic peraluminous veins and dykes are evident and widespread; high-grade metamorphic septa are observed in the sierras of Chepes, Valle Fértil and western Famatina (Pankhurst et al., 2000; Dahlquist et al., 2005; Otamendi et al., 2012; Alasino et al., 2014). Furthermore, evidence for local interaction between metaluminous magmas and partially molten country rocks at mid-crustal level has been described in the granites of central sector of Sierra de Velasco and western Famatina (Grosse et al., 2011; Alasino et al., 2014). The shift from the calcic to the calc-alkalic field at 65–73% SiO_2 in these granites is produced by hybridization with crustal melts and is not a primary characteristic of the magmas (Fig. 5a). Forthe reasons given above, we do not think that such hybridization of the intermediate units with crustal melts or contamination with metasediments can explain the observed similar isotope compositions of the basic and silicic units of the calcic metaluminous sequences.

Because a simple contamination Hypothesis 2 cannot adequately describe the mafic rocks of Sierra de Valle Fértil (Walker Jr. et al., 2015) invoked the MASH model of Hypothesis 3. In this, interaction of crustal material and primitive mantle melts occurs in the lower crust, alternating with cumulate removal events, during which the isotopic compositions of Sr and Nd remain nearly constant but are significantly 'enhanced' compared to those of primitive mantle. However, some objections to the simple contamination hypothesis could also apply here. It is hard to see how this mechanism could explain the similar trends of Sr and Nd isotopic composition on a regional scale over 100–200 km (e.g., across the sierras of Valle Fértil, western Famatina and Chepes–Los Llanos at least, possibly much further afield). This would need the metaluminous sequences to have evolved from isotopically similar initial magmas, formed in all cases by interaction between primitive mantle melts and highly variable crustal components. Additionally we have found no evidence of mafic/ultramafic rocks with asthenospheric Sr and Nd isotope signatures that might represent uncontaminated primary magma, although we agree that many of the ultramafic and mafic rocks are cumulates, and fractional crystallization was a common process in the mafic to silicic units.

7.2. Highly peraluminous granites

Highly peraluminous granites, frequently cordierite-bearing, occur as minor bodies within the metaluminous sequences (e.g., TUA1029, Sierra de Chepes) but also form medium to large bodies in the Sierra de Capillitas (CAP1021; BEL7), Sierra de Velasco (ANT8; VEL1026; VEL3000) and Sierra de Mazán (VMA-1018) (Fig. 2a). Despite their different modes of occurrence, these granites cannot be distinguished in terms of chemical and isotopic (Sr, Nd, Hf, O) compositions (Figs. 5, 6, 8). They plot in the Sr and Nd isotope fields of the metasedimentary rocks of the **FFD**, **EFD**, and **CFD**, suggesting large-scale crustal reworking of the country rocks (Figs. 6–8). The obvious local source is the very thick metapelite/metagreywacke-rich post-Pampean sequence, which has detrital zircon age peaks at 525, 630 and 970–1080 Ma (Rapela et al., 2016), although very few inherited zircon ages have been reported from the peraluminous granites (e.g., Pankhurst et al., 2000).

The highly peraluminous bodies show some notable characteristics:

(a) large bodies such as Capillitas and Velasco are located to the east of the young metaluminous sequences in the western margin of the **CFD**, such as Sierra de Valle Fértil and Sierra de Famatina (Fig. 2); (b) some samples such as BEL7 and FAM7086 have anomalous negative εHf_t zircon values (from −22 to −14, Fig. 12a) and very old Archaean HfT_{DM} model (Fig. 8e), which is broadly consistent with evidence of inheritance seen in the U—Pb data (see above). Further LA-ICP-MS analyses of inherited zircon cores in BEL7 were carried out, but no Archaean ages were found, only a few Paleoproterozoic (2), Mesoproterozoic (2), Neoproterozoic (1), and Cambrian (3) ages (M. Basei, unpublished). However the εNd_t and $T_{DM}Nd$ (whole- rock) of these samples are no different from those of other peraluminous granites, so the anomalous Hf isotopic compositions show decoupled Hf—Nd behaviour in Fig. 12a, b. The relatively high crystallization temperature estimated for sample BEL7 ($T = 819\,^{\circ}C \pm 43\,^{\circ}C$, zircon saturation temperature from Miller et al., 2003) might explain the highly negative εHft – Villaros et al. (2012) and Farina et al. (2014) have shown that dissolution of old inherited zircon is transferred to *syn*-magmatic zircon in highly peraluminous magmas, leading to anomalous and/or variable εHft values (and old HfT_{DM} model ages). A few grains in other peraluminous **CFD** granites also have very low εHft ratios (sample VEL3000, Table 2).

The 471 ± 4 Ma age of metamorphic rims in the cordierite granite from Sierra de Velasco (sample No. 9 in Fig. 2, corresponding to VEL3000 in Fig. 7) is similar to that of metamorphic rims in high-grade migmatites located 290 km to the SSW at Las Chacras, Sierra de Valle Fértil (Casquet et al., 2012b) (Fig. 2). Since the entire Sierra de Valle Fértil igneous section is considered to have been formed in the 468–472 Ma interval (Ducea et al., 2017) and emplacement of metaluminous magma and regional metamorphism were largely coeval (Alasino et al., 2014), this suggests that a thermal event of the same age affected the whole **CFD**, even including northeastern Patagonia. Together with the emplacement of large peraluminous batholiths, these are characteristic features of "hot orogen" (Collins, 2002).

7.3. Isotopic constraints on magma sources

For most Famatinian rocks, especially the metaluminous suite, there is a positive correlation between εNd_t (whole rock) and average εHf_t (zircon), similar to the trend shown by oceanic basalts (Fig. 12a). Considering that Nd represents a bulk magma composition whereas the Hf signature represents a highly refractory mineral component, this is a strong argument that both represent the composition of the magmas from which each rock crystallized. Data for the Patagonian granites also fall on or very close to this trend, and those for the TTG suites of the FFD extend it up to $\varepsilon Hf_t = +6$ and εNd_t (wr) = +2.

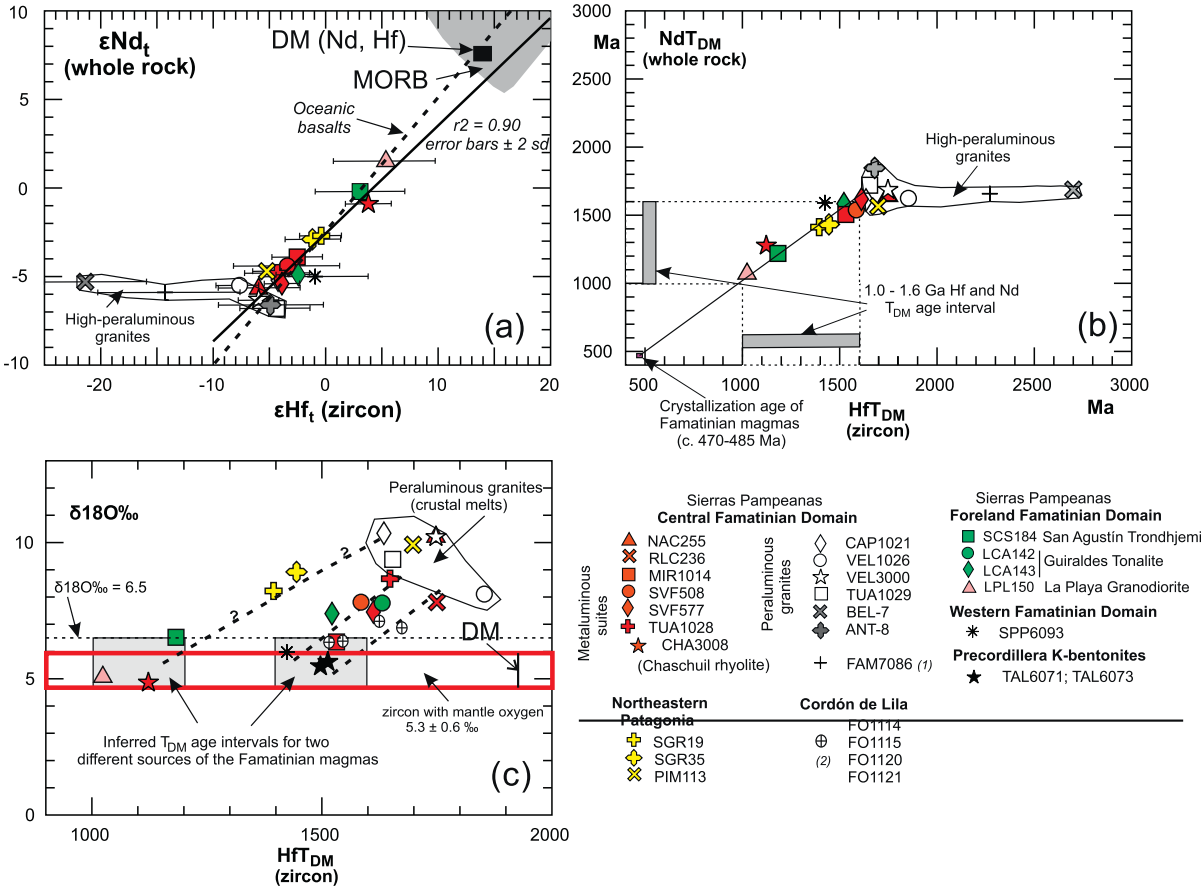

Fig. 12. (a) Sample averages of εHf_t (zircon; 2 sigma errors bars) vs. εNd_t (whole rock) for the Famatinian igneous rocks. Individual sample variation of εHf_t is show in Fig. 8c,d. (b) Average HfT_{DM} (zircon) vs. NdT_{DM} (whole-rock). Individual sample variation of HfT_{DM} is show in Fig. 8e,f. (c) Average HfT_{DM}(zircon) vs. average $\delta^{18}O‰$ in the Famatinian igneous rocks. Mean $\delta^{18}O$ is shown in Table 2 and individual sample variation in Fig. 8a,b. Shaded boxes with $\delta^{18}O‰ < 6.5$ and T_{DM}(Hf) intervals at 1000–1200 Ma and 1400–1600 Ma suggest that inferred main crustal formation episodes for the Famatinian sources occurred during the Mesoproterozoic.NdT_{DM} is according to DePaolo et al. (1991) and Hf $_{DM}$ is for crystallization from a crust-type source with $^{176}Lu/^{177}Hf = 0.150$ (Goodge and Vervoort, 2006) assuming original depleted mantle values from Vervoort and Blichert-Toft (1999). The "Oceanic Basalts" (MORB, OIB, IAB) and the MORB fields are from Vervoort et al. (1999). The value for zircon with mantle $\delta^{18}O$ is from Valley et al. (2005) while the limit of up to 6.5‰ for zircon with minor or negligible contamination is from Cavosie et al. (2005). Data sources for mean Hf T_{DM} and εHf_t of the Famatinian igneous rocks analysed in this study are in Supplementary Data File S3, whereas those of the Cordón de Lila are from Pankhurst et al. (2016). Data for Nd isotopes are in Supplementary Data File S1. *(1)* From Dahlquist et al. (2013); *(2)* From Pankhurst et al. (2016).

When these independent isotope signatures are reformulated as average Hf and Nd model ages, there is real one-to-one correspondence (i.e., each system gives essentially the same Proterozoic model ages within a range from ca. 1.0 Ga to 1.6 Ga (Fig. 12b). As any form of mixing/contamination process is likely to affect model ages (Arndt and Goldstein, 1987), the zircon oxygen isotope compositions have been used to screen them (Fig. 12c). The highly peraluminous granites are taken as defining the field of the upper crustal component as a potential contaminant (HfT_{DM} = 1700–1900 Ma; $\delta^{18}O$ = +8.0 to +10.5‰), whereas rocks with $\delta^{18}O$ < 6.5‰ could represent lithospheric mantle that has effectively never been contaminated with upper crust (Kemp et al., 2006). The HfT_{DM} ages for most of the **CFD** metaluminous suite granites fall between these values with HfT_{DM} at 1600–1750 Ma, which is coincident with a peak of NdT_{DM} ages in metaluminous and peraluminous Famatinian granites (Pankhurst et al., 1998; Dahlquist et al., 2013). Most probably this age range reflects a mixture of pure end-member sources and may overestimate residence ages of the lower lithosphere prior to Ordovician magmatism.

In all Famatinian domains there are igneous rocks with zircon $\delta^{18}O$ < 6.5‰, i.e., within or very close to the range of mantle oxygen. These rocks fall into two groups, according to HfT_{DM} ages (Fig. 12c): (i) an Early Mesoproterozoic (Calymmian) group (1.4–1.6 Ga) and (ii) a Late Mesoproterozoic (Stenian) group (1.0–1.2 Ga).

The older and dominant group includes rocks with 42–76% SiO_2 from the **CFD**, **WFD**, Cordón de Lila and, with the exception of two grains, the K-bentonites of the Precordillera (Fig. 8f). An olivine-pyroxene-metagabbro from western Famatina reported by Alasino et al. (2016) is significantly depleted in whole-rock ^{18}O ($\delta^{18}O$ of 5.3‰), but shows evolved Sr and Nd isotopic signatures (Sri = 0.7082; εNd_t = −2.2) and NdT_{DM} of 1.39 Ga, indicating that this basic rock also belongs to this group. In fact the entire 1.4–1.6 Ga model age group with $\delta^{18}O$ < 6.5‰ has negative zircon εHf_t (Fig. 12a). With the exception of the Chaschuil rhyolite, and regardless of the residence ages, all samples of the **CFD** have negative εHf_t values (Fig. 9a). This agrees with the negative whole-rock εNd_t, and relatively high $(^{87}Sr/^{86}Sr)_i$ ratio of rocks of the **CFD** and **WFD** (Fig. 6a, c). Such isotopic decoupling between O and Sr-Nd-Hf could occur if mantle-derived magma crystallizes and remains in the deep crust without interacting with upper crustal material – the O isotopic composition in zircon will retain the juvenile signature but the radioactive isotopes continue to evolve by radioactive decay (e.g., Castillo et al., 2017). Rocks from these areas with $\delta^{18}O$ > + 8‰ converge to the field of peraluminous granites with HfT_{DM} ages up to ca. 1750 Ma and $\delta^{18}O$ of 8.2–8.9‰ (Fig. 12c). Note that slight crustal contamination represented by $\delta^{18}O$ up to +8‰ does not change the HfT_{DM} age interval inferred for basic and intermediate rocks of the **CFD**.

Mesoproterozoic residence ages for the Famatinian magma sources such as those shown in Fig. 12c can be explained if Mesoproterozoic continental lithosphere similar to that exposed in the **WFD** underlies the **EFD** and **CFD**. This is assumed in the MARA terrane hypothesis, where the whole sector is seen as an extension of the Antofalla-Arequipa region of northern Chile and Peru (Casquet et al., 2008, 2012a, 2018), which was thought to have collided against Gondwana in early Cambrian times (Rapela et al., 2016).

It is therefore unsurprising that there is a younger group of 1.0–1.2 Ga HfT_{DM} ages with low $\delta^{18}O$, defined by a small number of trondhjemite samples from the **FFD** and a rhyolite from northwestern Famatina in the **CFD** (Fig. 12c). Schröter et al. (2004) have shown that high-pressure melting of dioritic gneisses in the lower crust produces trondhjemite melts. All these samples show positive εHft values that fall well below the depleted mantle (DM) value (samples SCS184, CHA3008, LPL150; averages in Fig. 12a). This group may also include the La Chacras amphibolites to the west of Sierra de Valle Fértil, due to their similar NdT_{DM} age and positive εNd_t – higher than gabbros of the **CFD** metaluminous sequence in the same silica range (Fig. 6c). These four samples with consistent differences in Nd and Hf isotope systematics compared to the metaluminous sequence of the **CFD** are considered to have been derived from a different source. They plot in the εNd_t field of the Grenville oceanic basement of the **WFD** recalculated at 475 Ma (Fig. 6c). For this reason, a potential source for these rocks would be the more primitive Mesoproterozoic oceanic arc–backarc igneous lithosphere of the **WFD** (Rapela et al., 2010), as exemplified by Sierra de Pie de Palo rocks considered among the most primitive Mesoproterozoic magmatic rocks known on Earth (Vujovich and Kay, 1998). Galindo et al. (2017) recently reported Late Mesoproterozoic trondhjemite with adakite affinities in the San Rafael Massif, to the south of Sierra de Pie de Palo, with NdT_{DM} ages close to the crystallization age. Some of these samples are closely associated with the Guacha Corral (sample 4 in Fig. 2a) and Valle Fértil major shear zones (Las Chacras block), or to shear zones in the WFD (sample 19). Nevertheless, due to their juvenile geochemical and isotopic signature, subordinate asthenospheric additions coeval with the flare-up Famatinian event cannot be discarded for the samples of this group (Alasino et al., 2016).

Finally, volcanic rocks from both residence-age groups (K-bentonites and the Chaschuil rhyolite), are among those that preserve their juvenile $\delta^{18}O$ signature, suggesting extraction from deep sources and rapid eruption without contamination by the supracrustal metasedimentary rocks.

7.4. Construction of the southwestern Gondwana margin

Most of the geodynamic models so far proposed for Famatinian magmatism are based on studies of the metaluminous sequences in the western edge of the **CFD** (i.e, Sierras de Valle Fértil, western Famatina and Chepes–Los Llanos). However, as described above, the evolution of the magmatic belt is more complex and involved distinct episodes in the four Famatinian domains recognized here.

Although Famatinian magmatism has generally been related to a convergent margin environment, it has been clear from the start of combined geochemical and isotope-geochronological studies that the geodynamic scenario must include TTG suites and peraluminous batholiths developed far inboard of the volcanic front (Rapela et al., 1990; Pankhurst et al., 2000). Mesozoic–Recent Andean granites in Peru, e.g., the Coastal Batholith, are located ca. 60 Km west of the high-Na Cordillera Blanca batholith (Petford and Atherton, 1996), while the distance from the equivalent TTG suites in the FFD to the metaluminous suites of Sierra de Valle Fértil in the CFD is ca. 340 km, an estimate that does not even take into account Andean shortening (Fig. 2a). In this regard, the layout of Famatinian magmatism is more like that of the Tasman orogenic system of eastern Australia (Collins and Richards, 2008). Nevertheless, although the area affected by Famatinian magmatic rocks is very large, the duration of magmatism was relatively short, about 20 Ma in the type sector, whereas the Andean Patagonian batholith, for example, continued to evolve over > 180 Ma.

In the **CFD** and **EFD** Famatinian magmatism was mostly developed in a thick metapelite-rich sequence of post-early Cambrian age. The basement of these sequences is not exposed, but a Late Mesoproterozoic lower crust and the underlying lithospheric mantle may be inferred, as for the MARA continental block (Casquet et al., 2012a; Rapela et al., 2016). Mesoproterozoic basement is well exposed in the **WFD**: it has continental characteristics in the north (Sierras de Maz and Espinal) but mixed oceanic–continental appearance in the south (Sierra de Pie de Palo, and the San Rafael massif further south, Cingolani et al., 2017 and references therein). The range of Late Mesoproterozoic U—Pb ages is similar in both sectors (Rapela et al., 2010). A thin basement lithosphere in the southern part of the magmatic belt might have favoured formation of mid-Cambrian/Ordovician platforms and back-arc basins when proto-Pacific subduction started after Gondwana assembly. The Neoproterozoic platform cover of the Late Mesoproterozoic basement was imbricated with continental crust of the Gondwana margin in the **FFD** during the early Cambrian Pampean orogeny (Murra et al., 2016).

Despite its comparatively short life, the geological history of Famatinian magmatism seems to have been complex, involving several distinct events. Previous information and new data from this study provide important features that should be taken into account for constructing a geodynamic scenario:

(1) U—Pb ages further confirm the duration of Famatinian magmatism in the type section, which is constrained to the 465–486 Ma interval. A 468–472 Ma age peak indicates a "flare-up" episode, after which magmatism faded in the proto-Andean sector, but apparently continued further north in the Puna into Late Ordovician and Early Silurian times.

(2) The oldest magmatic rocks at the type sector (478–486 Ma) are emplaced in the central part of the **CFD** while trondhjemitic plutons with "adakitic" composition intruded the **FFD**, far from the continental margin. Those at the **CFD** show metaluminous and peraluminous evolved geochemical and isotopic compositions, whereas the trondhjemites display less evolved isotopic signatures (Sr, Nd, Hf and O), and high Sr/Y and La/Yb ratios, suggesting high-pressure melting of a garnet-bearing gabbroid source (Pankhurst et al., 2000).

(3) Remnants of extensive Ordovician marine basins lie along the Sierra de Famatina show a volcanism that started in late Tremadocian times and intrusion of granitic plutons that are coeval with the main Famatinian magmatism (Fig. 2b). Stratigraphical data suggest a major extensional event in this region that could have resulted in arc-splitting, crust slivers and isolated ensialic basins during the Early to Mid-Ordovician time (Astini and Dávila, 2004; Astini et al., 2007). Probable Floian/Dapingian marine fossils in metasedimentary rocks in Sierra de Ambato (**EFD**, Figs. 1a, 2a) show that some of these basins were very wide, and the shallow-water marine succession indicates deposition near the outermost Gondwana foreland at that time (Verdecchia et al., 2011). For most of its history the volcanic arc was close to sea level and coeval with sedimentary rocks.

(4) Multiple interlayering of marine sediments with volcanic and volcaniclastic rocks in the Puna-Famatina basins and the apparent absence of high positive topography suggest that coeval extension prevailed during long periods in the type section. However angular unconformities in these basins indicate compression (Fig. 2b), so the long period of lithospheric extension was interrupted by discontinuous contraction episodes, a process described as tectonic switching by Collins (2002).

(5) The dominant metaluminous suites of all Famatinian ages show a distinctive 'evolved' signature compatible with a magmatic source in the sub-continental lithospheric mantle (± mafic lower crust). Asthenospheric additions were minor (see Sections 6.3.1, 6.3.2).

(6) Significant volumes of peraluminous magma were emplaced

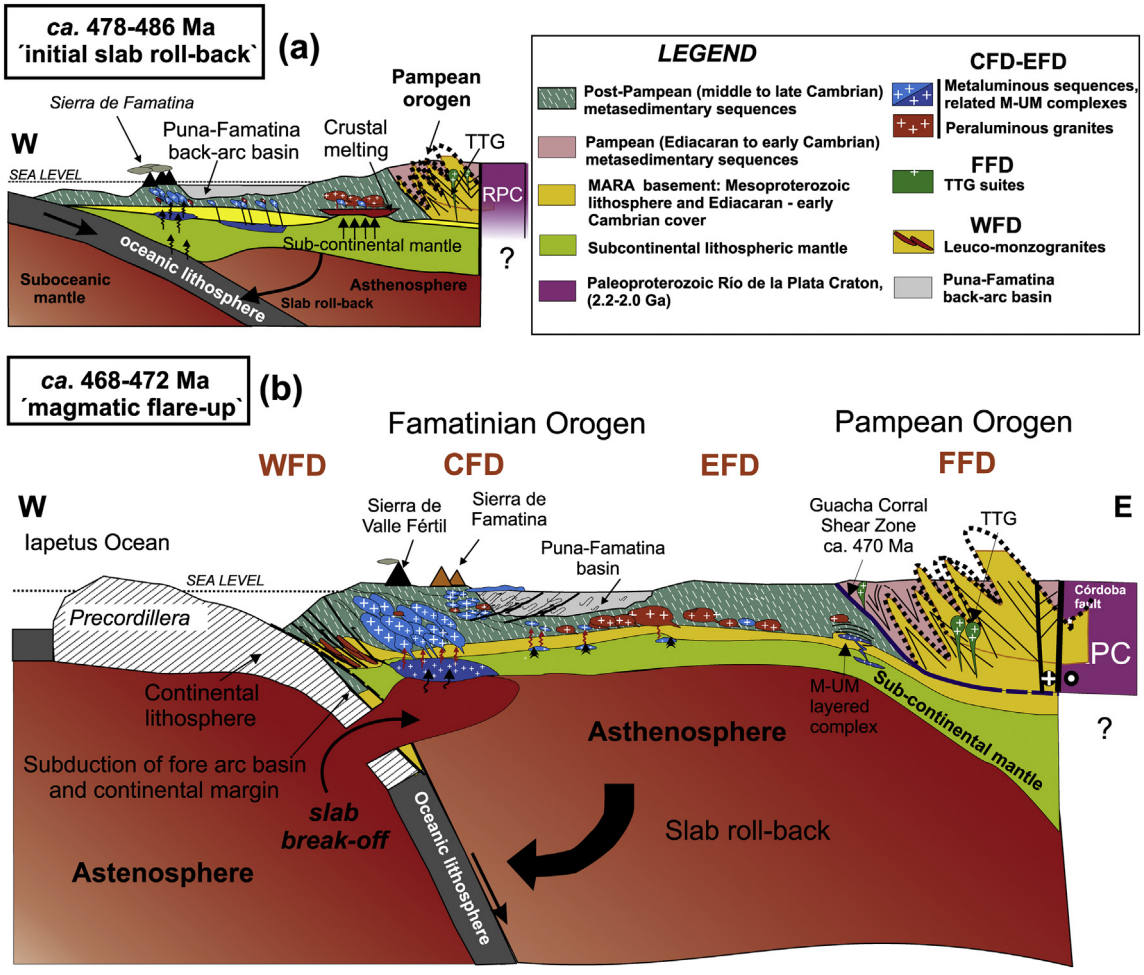

Fig. 13. ca. 468–486 Ma geodynamic model for generation of Famatinian magmatism in the type section of the Sierras Pampeanas (27°–33°S). Not drawn to scale. WFD, CFD, EFD and FFD are Western, Central, Eastern and Foreland Famatinian domains respectively. Compared to an "Andean-type" convergent margin, in which the juvenile asthenospheric component of the mantle wedge is frequently found in Cordilleran granites, the equivalent Famatinian magmatism is dominated by lithospheric sub-continental mantle and crustal recycling components. High heat flow must be involved during in this process, which can be explained by a wide asthenospheric upwelling below a thin stretched lithosphere. The evolution culminates with continental subduction and slab break-off. See text for explanation.

inboard of the ca. 470 Ma voluminous metaluminous suites that dominate the western edge of the **CFD**. Their origin involved large-scale crustal reworking of the thick metapelite/metagreywacke -rich post-Pampean sequence (see Section 6.3.3).

(7) Leuco-monzogranite sills at ca. 470 Ma, largely coeval with thrusting and nappe deformation in the **WFD**, show 'evolved' Sr, Nd and Hf signatures but O isotopes close to mantle values. This may indicate a deep crustal source that had matured over a long time without contamination with upper crustal rocks.

Our model for sequential tectono-magmatic evolution of Famatinian magmatism is illustrated in E–W cross-sections through the type area (Fig. 13). The model accommodates the different characteristics described above (a–g).

*474–486 Ma, slab roll-back (*Fig. 13a*).*

The time of initiation of the Famatinian event remains elusive. D'Eramo et al. (2013) claim that emplacement of 501–512 Ma trondhjemitic plutons with adakite afinitties occurred along large-scale ductile zones during a contracted episode. If correct, this could indicate that the roll-back episode was preceded by a contractional event, with adakites generated far from the trench over a low-angle, "flat-slab", subduction of the oceanic plate. Adakite magmatism has been described associated with Neotethyan "flat-slab" subduction prior to India–Asia collision (Wen et al., 2008; Zhang et al., 2012).

Slab roll-back and coeval asthenospheric upwelling produced the onset of extension and full development of the Ordovician ensialic intra-arc basins (Dahlquist et al., 2013; Augustsson et al., 2015 among others). Ensialic basins started to open during the late Cambrian in the Puna–Sierra de Famatina area (**CFD**), and volcanism started in the Tremadocian (Fig. 2b). At 482–486 Ma, adakitic trondhjemites intruded the FFD and metaluminous sequence and, especially, peraluminous granites intruded the post-Pampean basement basin in the Sierra de Famatina and Sierra de Chepes-Los Llanos (Table 1).

Heat produced by asthenospheric upwelling and thinning of the subcontinental mantle led to a highT/low P regime to the west of the Pampean belt, culminating in anatexis of the fertile, metapelite/metagreywacke-rich, post-Pampean metasediments, and probably the less fertile Late Mesoproterozoic lower crust; thus led to intrusion of peraluminous batholiths in the northeastern edge of the **CFD,** and isolated peraluminous/ metaluminous plutons in the **EFD**. Metaluminous sequences and coeval volcanism were located in eastern Sierra de Famatina, Chepes-Los Llanos and southern Velasco, which might be considered the arc front at this stage.

*468–472 Ma, continental subduction and slab break-off (*Fig. 13b*).*

Steepening roll-back of the subducted oceanic slab continued to widen the Famatinian arc and the ensialic Puna-Famatina basin basins, by now also filled with volcanic and volcaniclastic rocks (Fig. 2b). However, at ca. 470 Ma an important deformation of the Famatina Group is represented by an east-vergent fold-thrust belt involving a major angular unconformity between Early and Middle Ordovician rocks, the latter represented by the volcanic Cerro Morado Group (Figs. 2b, 13c) (Astini and Dávila, 2004). The age distribution of igneous rocks suggests southwestward migration of the main magmatic activity located along the Sierra de Valle Fértil.

Subduction of Early Paleozoic metasediments and sectors of the Late Mesoproterozoic lower crust at the thinned continental margin are inferred from early top-to-the-west deformation along oblique thrusts in the **WFD**, linked to episodes of arc and retro-arc deformation and magmatic flare-up in the arc (Mulcahy et al., 2011). Flare-up episodes in continental arcs have been ascribed to large scale crustal shortening (e.g., Ducea et al., 2017) or recently to slab break-off during continental subduction (Hildebrand and Whalen, 2017). The evolution described above for the Famatinian orogen is more consistent with the slab break-off model, as it involved initial collision with the Precordillera terrane (Fanning et al., 2004) after a protracted period of subduction of oceanic crust dominated by extension in the arc and arc-back-arc region (474–486 Ma slab roll-back stage, see Fig. 13).

Slab break-off occurs when the buoyancy forces resisting the subduction of continental lithosphere are as strong as those pulling oceanic lithosphere downwards (Cloos et al., 2005). Evidence of this is seen in a sector of the Las Chacras block (Fig. 2a) in the major Valle Fértil shear zone, the boundary between the **WFD** and the **CFD** (Fig. 2a). The rocks of this block are dominated by metasedimentary high-pressure upper granulite-amphibolite facies migmatites and garnet amphibolites (Casquet et al., 2012b; Mulcahy et al., 2014). PT conditions of 12 ± 1 kbar and 780 ± 45 °C and a U—Pb age of 468 ± 4 Ma in U/Th zircon metamorphic rims in the migmatites was reported by Casquet et al. (2012b), who considered that this block was part of the continental fore-arc that was rapidly thrust down beneath the lower crust of the arc (Fig. 13b). The age is coincident within error with the age of magmatic flare-up and related high-grade metamorphism in the **CFD** (Ducea et al., 2017). Mulcahy et al. (2014) reported similar high P-T conditions for the equivalent Villarcán gneiss at Las Chacras (~12 Kb and ~868 °C; U—Pb age of titanite: 407 ± 11 Ma), and proposed that Ordovician crustal melts 'remained at temperatures above the solidus for 20–30 Ma after peak granulite facies metamorphism' at 461 Ma. We doubt this, but agree that Late Ordovician–early Silurian shear zones in the **WFD** could be ascribed to compressive deformation associated with collision of the Precordillera terrane (Mulcahy et al., 2011, Fig. 17).

Slab break-off at 468–472 Ma resulted in upwelling of the suboceanic mantle, melting of the lithospheric mantle and magmatic "flare-up" at the continental margin. This produced voluminous metaluminous magmatism at the western edge of the **CFD**, but also metaluminous and peraluminous bodies of the same age sparingly distributed in all Famatinian domains (Table 1).

The coeval rhyolitic volcanism at the continental margin of the Famatinian belt, the K-bentonites deposits in the Precordillera and the intrusion of leuco-monzogranitic sills in the **WFD**, all show low $\delta^{18}O‰$ (Fig. 9b), suggesting Mesoproterozoic crustal sources that have not been contaminated with fluid from the upper crust (Fig. 12b,c). Baldo et al. (2012) interpreted the **WFD** leucogranites of Sierra de Pie de Palo as formed in a continental collision scenario, which is consistent with the structural interpretation of van Staal et al. (2011) and Mulcahy et al. (2011, 2014).

Shallow break-off may result in generation of coeval magmas of a large compositional diversity, formed by partial melting of various sources, including the ascending asthenosphere, the enriched lithospheric mantle and the overlying crust (Wen et al., 2008; Hildebrand and Whalen, 2017 and references therein). In the Famatinian arc, largely coeval flare-up magmatism at this time includes low $\delta^{18}O‰$ volcanism in the Precordillera and Sierra de Famatina, voluminous isotopically 'evolved' metaluminous basic to acid sequences, widespread high-T metamorphism and associated crustal melting at the continental margin. A younger, more juvenile basic magmatic pulse has also been inferred for the same time interval (Alasino et al., 2016). All these different magmas, derived from different sources, are here considered to have been instigated by slab break-off of the oceanic lithosphere as a result of subduction of continental crust at the continental margin during a collisional episode.

The main implication of the scenario depicted in Fig. 13 is that Famatinian magmas are derived primarily from the upper plate: the continental crust and the subcontinental mantle that was isolated from convection. A high-T/low-P hot regime prevailed during the stages of slab roll-back and break-off. A different and opposing interpretation of Famatinian magmatism, mainly based on observations in Sierra de Valle Fértil, considers that juvenile mantle additions of > 50% played a significant role in construction of the arc and that the evolved Hf composition and 'mixed' model ages resulted from contamination by upper crustal metasedimentary rocks (Otamendi et al., 2017). We believe that although major crustal contamination is evident in some metaluminous units, the complete Sr, Nd, Hf and O isotope data show that the mantle component was not juvenile, but mostly and old

subcontinental mantle accreted to Gondwana during an earlier episode (Fig. 12).

The inferred primary source of the mafic to felsic metaluminous series is the underlying lithospheric mantle (± mafic lower crust), while melting of mid-to-upper Cambrian (and older?) metasedimentary rocks formed the highly peraluminous granites. Subordinate less isotopically evolved rocks, such as some trondhjemite bodies in the **FFD** and the high silica rhyolites of the **CFD**, could be explained by partial melting of a primitive Late Mesoproterozoic ocean arc lithosphere, the upper crust of which crops out in the southern basement of the **WFD**. Even if the less isotopically evolved magmas are regarded as asthenospheric additions, the outcrop surface of these rocks is < 5% of the bulk basic to acid Famatinian magmatism with evolved isotopic compositions. This conclusion is coherent with geochemical and Nd isotope results in the volcano-intrusive Ordovician rocks in the northern Puna (Bierlein et al., 2006) and the Hf isotopic signature in detrital zircon of siliciclastic fills of Paleozoic basins in the central Andes (Bahlburg et al., 2009), both interpreted as indicating insignificant contribution of juvenile (asthenospheric) material. Similarly in West Antarctica, Hf isotope values have been taken to indicate reworking of an unexposed juvenile Mesoproterozoic source during the diachronous Ross–Delamerian orogeny (Yakymchuk et al., 2015). Such a Mesoproterozoic component was probably significant in the Early Paleozoic magma sources of the SW Gondwana margin.

8. Conclusions

In southern South America the Ordovician Famatinian belt is characterized by extensive metaluminous suites and peraluminous granites as well as wide ensialic marine basins. This contrasts with the typical N–S, relatively narrow, linear arrangement of the Mesozoic–Tertiary cordilleran Andean belt. At 27°–33°S, four margin-parallel geological domains, in some cases separated by large shear zones, were recognized in the type sector of the Famatinian belt in the Sierras Pampeanas: the western domain (**WFD**) intruded by minor leuco-monzogranites, the central (**CFD**) and eastern (**EFD**) domains dominated by extensive gabbro to monzogranite metaluminous sequences and peraluminous granites, and the foreland (**FFD**) domain intruded by adakitic trondhjemites and tonalite to granodiorite plutons.

The U—Pb ages of magmatic units in the type sector is mostly restricted to the interval 463 ± 4 to 486 ± 7 Ma, with the most intense period of emplacement between 468 Ma and 472 Ma being interpreted as a magmatic flare-up. Granitoid emplacement in northeastern Patagonia and the Cordon de Lila (Puna, northern Chile) was effectively synchronous with equivalent magmatic events in the type sector of the Sierras Pampeanas, apparently forming a continuous belt. As the initial (> 478 Ma) episode has not yet been identified in the **WFD** of the Sierras Pampeanas or NE Patagonia, a southwestward migration of the early arc is inferred.

We have not found isotopic evidence (Sr, Nd whole-rock; Hf, O zircon) for major asthenospheric addition to the crust during Famatinian magmatism. Despite the unavoidable need for the heat source provided by the asthenospheric mantle, its contribution to the growth of Early Paleozoic crust is apparently subordinate. This contrasts with the petrogenesis of Late Paleozoic and Mesozoic–Tertiary Andean-type cordilleran granites, where a significant asthenospheric contribution to the magmas is frequently recognized. Crustal recycling of a Mesoproterozoic lithosphere, mainly subcontinental mantle accreted during the early Cambrian, coupled with crustal melting of Early Paleozoic metasedimentary sequences formed most of the Famatinian crust.

A model of sequential tectonomagmatic evolution in two main stages at 485–468 Ma, attempts to explain the different characteristics in the four recognized domains.

(1) ca. 474–486 Ma, slab roll-back. This was a mostly extensional interval produced by asthenospheric upwelling and thinning of the subcontinental mantle. Full development of marine ensialic basins and emplacement of highly-peraluminous batholiths occurred during this stage. Early metaluminous sequences were emplaced in the **CFD**, coeval volcanic rocks were interbedded with marine sediments in the ensialic Puna–Famatina basin and trondhjemite plutons were emplaced in the **FFD**.

(2) 468–472 Ma, slab break-off. Steepening of the oceanic and arc migration to the southwest ended with slab break-off due to subduction of continental crust during continental collision with the Precordillera terrane. K-bentonites were deposited in the Precordillera during the initial collision stage. The magmatic flare-up episode was associated with slab break-off. Deformation along oblique thrusts and emplacement of leucogranites occurred in the **WFD**, coeval with shortening in the arc and ensialic back-arc. Voluminous metaluminous magmatism was conspicuous at the western edge of the **CFD,** and peraluminous and metaluminous bodies in this age interval are sparingly found in **EFD** and **FFD** domains. Roll-back and break-off stages developed during the high-T regime of a hot orogen.

Acknowledgements

Financial support for this paper was provided by Argentine public grants CONICET PIP0229, FONCYT PICT 2013-0472 and Spanish grants CGL2009-07984, GR58/08 UCM-Santander and CGL2016-76439-P. Ana M. Sato is thanked for zircon separation of three samples and Jorge Wlasiuk for handling and grinding all the samples analysed in this study. Two anonymous reviewers provided thoughtful reviews and numerous editorial comments.

Appendix A. Supplementary data

Supplementary data to this article can be found online at https://doi.org/10.1016/j.earscirev.2018.10.006.

References

Abruzzi, J.M., Kay, S.M., Bickford, M.E., 1993. Implications for the nature of the Precordilleran basement from the geochemistry and age of Precambrian xenoliths in Miocene volcanic rocks, San Juan province. In: 12 Cong. Geol. Arg. Mendoza, Actas 3, 331–339.

Aceñolaza, F.G., Toselli, A.J., 1976. Consideraciones estratigráficas y tectónicas sobre el Paleozoico inferior del Noroeste Argentino. Congreso Latinoamericano de Geología, Caracas, Actas 2, 755–764.

Aceñolaza, F.G., Toselli, A., 2000. Argentine Precordillera: allochthonous or autochthonous Gondwanic? Zbl. Geol. Paläontol. 7, 743–756.

Alasino, P.H., Casquet, C., Larrovere, M.A., Pankhurst, R.J., Galindo, C., Dahlquist, J.A., Baldo, E.G., Rapela, C.W., 2014. The evolution of a mid-crustal thermal aureole at Cerro Toro, Sierra de Famatina, NW Argentina. Lithos 190/191, 154–172.

Alasino, P.H., Casquet, C., Pankhurst, R.J., Rapela, C.W., Dahlquist, J.A., Galindo, C., Larrovere, M.A., Recio, C., Paterson, S.R., Colombo, F., Baldo, E.G., 2016. Mafic rocks of the Ordovician Famatinian magmatic arc (NW Argentina): new insights into the mantle contribution. Geol. Soc. Amer. Bull. 128, 1105–1120.

Albanesi, G.L., Esteban, S.B., Hünicken, M.A., Barnes, C.R., 2000. Las biozonas de conodontes de la Formación Volcancito (Cámbrico tardío–Ordovícico temprano), Sistema de Famatina, noroeste de Argentina. Ameghiniana 37 (4–sup), 5R.

Arndt, N.T., Goldstein, S.L., 1987. Use and abuse of crust-formation ages. Geology 15, 893–895.

Astini, R.A., 2003. The Ordovician Proto-Andean basins. In: Benedetto, J.L. (Ed.), Ordovician fossils of Argentina. Secretaría de Ciencias y Tecnología, Universidad Nacional de Córdoba, Córdoba, Argentina, pp. 1–74.

Astini, R.A., 2008. Sedimentación, facies, discordancias y evolución paleoambiental durante el Cambro-Ordovícico. In: Coira, B., Zappettini, E.O. (Eds.), Geología y recursos naturales de la provincia de Jujuy, Relatorio 17 Cong. Geol. Arg, pp. 50–73.

Astini, R.A., Dávila, F.M., 2004. Ordovician back arc foreland and Ocloyic thrust belt development on the western Gondwana margin as a response to Precordillera terrane accretion. Tectonics 23 (TC4008), 1–19.

Astini, R.A., Benedetto, J.L., Vaccari, N.E., 1995. The early Paleozoic evolution of the Argentine Precordillera as a Laurentian rifted, drifted, and collided terrane: a geodynamic model. Geol. Soc. Amer. Bull. 107, 3253–3273.

Astini, R.A., Collo, G., Martina, F., 2007. Ordovician K-bentonites in the upper-plate active margin of Western Gondwana, (Famatina ranges): Stratigraphic and palaeogeographic significance. Gond. Res. 11, 311–325.

Augustsson, C., Rüsing, T., Niemeyer, H., Kooijman, E., Berndt, J., Bahlburg, H., Zimmermann, U., 2015. 0.3 byr of drainage stability along the Palaeozoic palaeo-Pacific Gondwanamargin; a detrital zircon study. J. Geol. Soc. Lond. 172, 186–200. https://doi.org/10.1144/jgs2014-065.

Bahlburg, H., Vervoort, J.D., Du Frane, S.A., Bock, B., Augustsson, C., 2009. Timing of accretion and crustal recycling at accretionary orogens: insights learned from the western margin of South America. Earth-Sci. Rev. 97, 227–253.

Bahlburg, H., Berndt, J., Gerdes, A., 2016. The ages and tectonic setting of the Faja Eruptiva de la Puna Oriental, Ordovician, NW Argentina. Lithos 256-257, 41–54.

Baldo, E.G., Casquet, C., Galindo, C., 1998. Datos preliminares sobre el metamorfismo de la Sierra de Pie de Palo. Sierras Pampeanas Occidentales (Argentina). Geogaceta 24, 39–42.

Baldo, E.G., Dahlquist, J., Casquet, C., Rapela, C.W., Pankhurst, R.J., Galindo, C., Fanning, M., Ramacciotti, C., 2012. Ordovician peraluminous granites in the Sierra de Pie de Palo, Western Sierras Pampeanas of Argentina. Geotectonic implications. Congreso Geológico de España Oviedo. Geo-Temas 13, 569.

Baldo, E.G., Rapela, C.W., Pankhurst, R.J., Galindo, C., Casquet, C., Verdecchia, S.O., Murra, J.A., 2014. Geocronología de las Sierras de Córdoba: revisión y comentarios. In: Martino, R.D., Guereschi, A.B. (Eds.), Relatorio 18th. Cong. Geol. Arg. Geología y Recursos Naturales de la Provincia de Córdoba, pp. 845–868.

Basei, M.A.S., Costa Campos Neto, M., Pacheco Lopes, A., Nutman, A.P., Liu, D., Sato, K., 2013. Polycyclic evolution of Camboriú complex migmatites, Santa Catarina, Southern Brazil: integrated Hf isotopic and U–Pb age zircon evidence of episodic reworking of a Mesoarchean juvenile crust. Braz. J. Geol. 43, 427–443.

Bellos, L.I., Castro, A., Díaz-Alvarado, J., Toselli, A., 2015. Multi-pulse cotectic evolution and in-situ fractionation of calc-alkaline tonalite–granodiorite rocks, Sierra de Velasco batholith, Famatinian belt, Argentina. Gondwana Res. 27, 258–280.

Benedetto, J.L., 2004. The allochthony of the Precordillera ten years later (1993-2003): a new paleobiogeographic test of the microcontinental model. Gondwana Res. 7, 1027–1039.

Benedetto, J.L., Vaccari, N.E., Waisfeld, B.G., Sanchez, T.M., Foglia, R.D., 2009. Cambrian and Ordovician biogeography of the South American margin of Gondwana and accreted terranes. In: Bassett, M.G. (Ed.), Early Palaeozoic Peri-Gondwana Terranes: New Insights from Tectonics and Biogeography. Geol. Soc. Lond, pp. 201–232. https://doi.org/10.1144/SP325.11.

Bierlein, F.P., Stein, H.J., Coira, B., Reynolds, P., 2006. Timing of gold and crustal evolution of the Palaeozoic south Central Andes, NW Argentina—implications for the endowment of orogenic belts. Earth Planet. Sci. Let. 245, 702–721.

Black, L.P., Kamo, S.L., Allen, C.M., Aleinikoff, J.N., Davis, D.W., Korsch, R.J., Foudoulis, C., 2003. TEMORA 1: a new zircon standard for Phanerozoic U–Pb geochronology. Chem. Geol. 200, 155–170.

Booker, J.R., Favetto, A., Pomposiello, M.C., 2004. Low electrical resistivity associated with plunging of the Nazca flat slab beneath Argentina. Nature 429, 399–403.

Caminos, R., 1973. Some granites, gneisses and metamorphites of Argentina. In: Symposium on the Granites, Gneisses and Related Rocks of Rhodesia. Geol. Soc. South Africa, pp. 333–338.

Casquet, C., Baldo, E., Pankhurst, R.J., Rapela, C.W., Galindo, C., Fanning, C.M., Saavedra, J., 2001. Involvement of the Argentine Precordillera terrane in the Famatinian Mobile Belt: U–Pb SHRIMP and metamorphic evidence from the Sierra de Pie de Palo. Geology 29, 703–706.

Casquet, C., Pankhurst, R.J., Fanning, C.M., Baldo, E.G., Galindo, C., Rapela, C.W., González-Casado, J.M., Dahlquist, J.A., 2006. U-Pb SHRIMP zircon dating of Grenvillian metamorphism in Western Sierras Pampeanas (Argentina): correlation with the Arequipa Antofalla craton and constraints on the extent of the Precordillera Terrane. Gondwana Res. 9, 524–529.

Casquet, C., Pankhurst, R.J., Rapela, C.W., Galindo, C., Fanning, C.M., Chiaradia, M., Baldo, E., González-Casado, J.M., Dahlquist, J.A., 2008. The Mesoproterozoic Maz terrane in the Western Sierras Pampeanas, Argentina, equivalent to the Arequipa–Antofalla block of southern Peru? Implications for West Gondwana margin evolution. Gondwana Res. 13, 163–175.

Casquet, C., Rapela, C.W., Pankhurst, R.J., Baldo, E.G., Galindo, C., Fanning, C.M., Dahlquist, J.A., Saavedra, J., 2012a. A history of Proterozoic terranes in southern South America: from Rodinia to Gondwana. Geosci. Front. 3, 137–145. https://doi.org/10.1016/j.gsf.2011.11.004.

Casquet, C., Rapela, C.W., Pankhurst, R.J., Baldo, E., Galindo, C., Fanning, C.M., Dahlquist, J., 2012b. Fast sediment underplating and essentially coeval juvenile magmatism in the Ordovician margin of Gondwana, Western Sierras Pampeanas, Argentina. Gondwana Res. 22, 664–673.

Casquet, C., Dahlquist, J.A., Verdecchia, S.O., Baldo, E.G., Galindo, C., Rapela, C.W., Pankhurst, R.J., Morales, M.M., Murra, J.A., Fanning, C.M., 2018. Review of the Cambrian Pampean orogeny of Argentina; a displaced orogen formerly attached to the Saldania Belt of South Africa? Earth-Sci. Rev. 177, 209–225.

Castillo, P., Fanning, C.M., Pankhurst, R.J., Hervé, F., Rapela, C.W., 2017. Zircon O- and Hf-isotope constraints on the genesis and tectonic significance of Permian magmatism in Patagonia. J. Geol. Soc. Lond. 174, 803–816.

Cavosie, A.J., Valley, J.W., Wilde, S.A., 2005. Magmatic $\delta^{18}O$ in 4400-3900 Ma detrital zircons: a record of the alteration and recycling of crust in the early Archean. Earth Planet. Sci. Lett. 235, 663–681. https://doi.org/10.1016/j.epsl.2005.04.028.

Cawood, P.A., 2005. Terra Australis orogen: Rodinia breakup and development of the Pacific and Iapetus margins of Gondwana during the Neoproterozoic and Paleozoic. Earth-Sci. Rev. 69, 249–279.

Chapman, A.D., Ducea, M.N., Kidder, S., Petrescu, L., 2014. Geochemical constraints on the petrogenesis of the Salinian arc, Central California: Implications for the origin of intermediate magmas. Lithos 200 (201), 126–141.

Chappell, B.W., White, A.J.R., 1974. Two contrasting granite types. Pac. Geol. 8, 173–174.

Chernicoff, C.J., Zappettini, E.O., Santos, J.O.S., Allchurch, S., McNaughton, N.J., 2010. The southern segment of the Famatinian magmatic arc, La Pampa Province, Argentina. Gondwana Res. 17, 662–675.

Chew, D.M., Kirkland, C.L., Schalteger, U., Goodhue, R., 2007. Neoproterozoic glaciation in the Proto-Andes: tectonic implications and global correlation. Geology 35, 1095–1099.

Cingolani, C.A., Basei, M.A.S., Varela, R., Llambías, E.J., Chemale Jr., F., Abre, P., Uriz, N.J., Marques, J., 2017. The Mesoproterozoic basement of the San Rafael block, Mendoza province (Argentina): geochemical and isotopic age constraints. In: Cingolani, C.A. (Ed.), Precarboniferous evolution of the San Rafael block. Springer Earth System Science, pp. 19–58.

Cloos, M., Sapiie, B., van Ufford, A.Q., Weiland, R.J., Warren, P.Q., McMahon, T.-P., 2005. Collisional delamination in New Guinea: the geotectonics of subduction slab breakoff. Geol. Soc. Am. 51.

Cohen, K.M., Finney, S.C., Gibbard, P.L., Fan, J.-X., 2013. Updated. The ICS International Chronostratigraphic Chart. Episodes 36, 199–204.

Collins, W.J., 2002. Hot orogens, tectonic switching, and creation of continental crust. Geology 30, 535–538.

Collins, W.J., Richards, S.W., 2008. Geodynamic significance of S-type granites in circum-Pacific orogens. Geology 36, 559–662.

Collo, G., Astini, R., Cawood, P.A., Buchan, C., Pimentel, M., 2009. U-Pb detrital zircon ages and Sm-Nd isotopic features in low-grade metasedimentary rocks of the Famatina belt: implications for late Neoproterozoic eearly Palaeozoic evolution of the proto-Andean margin of Gondwana. J. Geol. Soc. Lond. 166, 303–319.

Cristofolini, E.A., Otamendi, J.E., Ducea, M.N., Peason, D., Tibaldi, A.M., Baliani, I., 2012. Detrital zircon U-Pb ages of metasedimentary rocks from the sierra de Valle Fértil: revealing entrapment of late Cambrian marine successions into the deep roots of the early Ordovician Famatinian arc. J. S. Am. Earth Sci. 37, 77–94.

Cristofolini, E.A., Otamendi, J.E., Walker Jr., B.A., Tibaldi, A.M., Armas, P., Bergantz, G.W., Martino, R.D., 2014. A Middle Paleozoic Shear Zone in the Sierra de Valle F_ertil, Argentina: Records of a Continent-Arc Collision in the Famatinian margin of Gondwana. J. South. Am. Earth Sci. 56, 170–185. https://doi.org/10.1016/j.jsames.2014.09.010.

Dahlquist, J.A., 2002. Mafic microgranular enclaves: early segregation from metaluminous magma (Sierra de Chepes), Pampean Ranges, NW Argentina. J. S. Am. Earth Sci. 15, 643–655.

Dahlquist, J.A., Rapela, C.W., Baldo, E.G., 2005. Cordierite-bearing S-type granitoids in the Sierra de Chepes (Sierras Pampeanas): petrogenetic implications. J. S. Am. Earth Sci. 20, 231–251.

Dahlquist, J.A., Galindo, C., Pankhurst, R.J., Rapela, C.W., Alasino, P.H., Saavedra, J., Fanning, C.M., 2007. Magmatic evolution of the Peñón Rosado granite: petrogenesis of garnet-bearing granitoids. Lithos 95, 177–207. https://doi.org/10.1016/j.lithos.2006.07.010.

Dahlquist, J.A., Pankhurst, R.J., Rapela, C.W., Galindo, C., Alasino, P., Fanning, C.M., Saavedra, J., Baldo, E., 2008. New SHRIMP U-Pb data from the Famatina complex: constraining Early–Mid Ordovician Famatinian magmatism in the Sierras Pampeanas, Argentina. Geologica Acta 6, 319–333.

Dahlquist, J.A., Rapela, C.W., Pankhurst, R.J., Fanning, C.M., Vervoort, J.D., Hart, G., Baldo, E.G., Murra, J.A., Alasino, P., Colombo, F., 2012. Age and magmatic evolution of the Famatinian granitic rocks of Sierra de Ancasti, Sierras Pampeanas, NW Argentina. J. S. Am. Earth Sci. 34, 10–25.

Dahlquist, J.A., Pankhurst, R.J., Gaschnig, R.M., Rapela, C.W., Casquet, C., Alasino, P.H., Galindo, C., Baldo, E., 2013. Hf and Nd isotopes in Early Ordovician to Early Carboniferous granites as monitors of crustal growth in the Proto-Andean margin of Gondwana. Gondwana Res. 23, 1617–1630.

Dahlquist, J.A., Pankhurst, R.J., Rapela, C.W., Basei, M.A.S., Alasino, P.H., Saavedra, J., Baldo, E.G., Murra, J.A., Campos Neto, M., 2016. The Capilla del Monte pluton, Sierras de Córdoba: the easternmost Early Carboniferous magmatism in the pre-Andean of SW Gondwana margin, Sierras Pampeanas, Argentina. Int. J. Earth Sci. 105, 1287–1305.

De los Hoyos, C.R., Willner, A.P., Larrovere, M.A., Rossi, J.N., Toselli, A.J., 2011. Tectonothermal evolution and exhumation history of the Paleozoic Proto-Andean Gondwana margin crust: the Famatinian belt in NW Argentina. Gondwana Res. 20, 309–324.

Delakowitz, B., Höll, R., Hack, M., Brodtkorb, M., Stärk, H., 1991. Geological and geochemical studies of the Sierra del Morro Oeste (San Luis Province, Argentina): metasediments and metavolcanics from a probable back-arc setting. J. S. Am. Earth Sci. 4, 189–200.

Demartis, M., Jung, S., Berndt, J., Aragón, E., Sato, A.M., Radice, S., Maffini, M.N., Coniglio, J.E., Pinotti, L.P., Eramo, F.J., Agulleiro Isúa, L.F., 2017. Famatinian inner arac: Petrographical observationsand geochronological constraints on pegmatites and leucogranites of the Comechingones pegmatitic field (Sierras de Córdoba, Argentina). J. S. Am. Earth Sci. 79, 239–253.

DePaolo, D.J., Linn, A.M., Schubert, G., 1991. The continental crustal age distribution: methods of determining mantle separation ages from Sm–Nd isotopic data and application to the southwestern U.S. J. Geophy. Res. 96B, 2071–2088.

D'Eramo, F., Tubía, J.M., Pinotti, L., Vegas, N., Coniglio, J., Demartis, M., Aranguren, A., Basei, M., 2013. Granite emplacement by crustal boudinage: example of the Calmayo and El Hongo plutons (Córdoba, Argentina). Terra Nova 25, 423–430.

D'Eramo, F., Pinotti, L., Bonalumi, A., Sfragulla, J., Demartis, M., Coniglio, J., Baldo, E.G., 2014. El magmatismo Ordovícico en las Sierras Pampeanas de Córdoba. In: Martino, R.D., Guereschi, A.B. (Eds.), Geología y Recursos Naturales de la provincia de Córdoba. 19° Cong. Geol. Argentino, Relatorio, pp. 233–254.

Drobe, M., López de Luchi, M., Steenken, A., Wemmer, K., Naumann, R., Frei, R., Siegesmund, S., 2011. Geodynamic evolution of the Eastern Sierras Pampeanas (Central Argentina) based on geochemical, Sm–Nd, Pb–Pb and SHRIMP data. Int. J.

Earth Sci. 100, 631–657.
Ducea, M.N., Otamendi, J.E., Bergantz, G., Stair, K.M., Valencia, V.A., Gehrels, G.E., 2010. Timing constraints on building an intermediate plutonic arc crustal section: U-Pb zircon geochronology of the Sierra Valle Fértil–La Huerta, Famatinian arc, Argentina. Tectonics 29, TC4002. https://doi.org/10.1029/2009TC002615.
Ducea, M.N., Bergantz, G.W., Crowley, J.L., Otamendi, J., 2017. Ultrafast magmatic buildup and diversification to produce continental crust during subduction. Geology. https://doi.org/10.1130/G38726.1.
Durand, F.R., Aceñolaza, F.G., 1990. Caracteres biofaunísticos, paleoecológicos y paleogeográficos de la Formación Puncoviscana (Precámbrico Superior-Cámbrico Inferior) del noroeste argentino. In: Aceñolaza, F.G., Miller, H., Toselli, A.J. (Eds.), El Ciclo Pampeano en el Noroeste Argentino, Serie Correlación Geológica N. 4. pp. 71–112.
Eggins, S.M., Grun, R., McCulloch, M.T., Pike, A.W.G., Chappell, J., Kinsley, L., Mortimer, G., Shelley, M., Murray-Wallace, C.V., Spotl, C., Taylor, L., 2005. In situ U-series dating by laser-ablation multi-collector ICPMS: new prospects for Quaternary geochronology. Quaternary Sci. Rev. 24, 2523–2538.
Escayola, M.P., van Staal, C.R., Davis, W.J., 2011. The age and tectonic setting of the Puncoviscana Formation in northwestern Argentina: an accretionary complex related to early Cambrian closure of the Puncoviscana Ocean and accretion of the Arequipa–Antofalla block. J. S. Am. Earth Sci. 32, 438–459. https://doi.org/10.1016/j.jsames.2011.04.013.
Fanning, C.M., Pankhurst, R.J., Rapela, C.W., Baldo, E.G., Casquet, C., Galindo, C., 2004. K-bentonites in the Argentine Precordillera contemporaneous with volcanism in the Famatinian arc. J. Geol. Soc. Lond. 161, 747–756.
Farina, F., Stevens, G., Gerdes, A., Frei, D., 2014. Small-scale Hf isotopic variability in the Peninsula pluton (South Africa): the processes that control inheritance of source $^{176}Hf/^{177}Hf$ diversity in S-type granites. Contrib. Mineral. Petrol. 168, 1–18.
Ferracutti, G., Bjerg, E., Mogessie, A., 2013. Petrology, geochemistry and mineralization of the Las Águilas and Virorco mafic–ultramafic bodies, San Luis Province, Argentina. Int. J. Earth Sci. 102, 701–720.
Finney, S.C., 2007. The parautochthonous Gondwanan origin of Cuyania (greater Precordillera) terrane of Argentina: a re-evaluation of evidence used to support an allochthonous Laurentian origin. Geol. Acta 5, 127–158.
Frost, B.R., Barnes, C.G., Collins, W.J., Arculus, R.J., Ellis, D.J., Frost, C.D., 2001. A geochemical classification for granitic rocks. J. Petrol. 42, 2033–2048.
Galindo, C., Casquet, C., Rapela, C.W., Pankhurst, R.J., Baldo, E.G., Saavedra, J., 2004. Sr, C and O isotope geochemistry and stratigraphy of Precambrian and lower Paleozoic carbonate sequences from the Western Sierras Pampeanas of Argentina: tectonic implications. Precambrian Res. 131, 55–71.
Galindo, C., Casquet, C., Baldo, E.G., Pankhurst, R., Rapela, C.W., Dahlquist, J.A., Fanning, C.M., 2017. Geocronología U-Pb SHRIMP y geoquímica de una adakita mesoproterozoica en el Bloque de San Rafael (Mendoza, Argentina): contexto geotectónico. Actas 20 Cong. Geol. Arg. Simposio 15, 25–27.
García-Ramírez, C.A., Rey-León, V., Valencia, V., 2017. Ortoneises en la Franja Silos-Babega, Macizo deSantander, Colombia: evidencias de la orogenia famatiniana en los Andes del norte. Andean Geol. 44, 307–327.
González, P.D., Tortello, M.F., Damborenea, S.E., 2011. Early Cambrian archeocyathan limestone blocks in low-grade meta-conglomerate from El Jaguelito Formation (Sierra Grande, Río Negro, Argentina). Geol. Acta 9, 159–173.
Goodge, J.W., Vervoort, J.D., 2006. Origin of Mesoproterozoic A-type granites in Laurentia: Hf isotope evidence. Earth Planet. Sci. Let. 243, 711–731. https://doi.org/10.1016/j.epsl.2006.01.040.
Grosse, P., Bellos, L.I., de los Hoyos, C.R., Larrovere, M.A., Rossi, J.N., Toselli, A.J., 2011. Across-arc variation of the Famatinian magmatic arc (NW Argentina) exemplified by I-, S- and transitional I/S-type Early Ordovician granitoids of the Sierra de Velasco. J. S. Am. Earth Sci. 32, 110–126.
Hauser, N., Matteini, M., Omarini, R.H., Pimentel, M.M., 2011. Combined U–Pb and Lu–Hf isotope data on turbidites of the Paleozoic basement of NW Argentina and petrology of associated igneous rocks: implications for the tectonic evolution of western Gondwana between 560 and 460 Ma. Gondwana Res. 19, 100–127.
Hervé, F., Pankhurst, R.J., Fanning, C.M., Calderón, M., Yaxley, G.M., 2007. The South Patagonian batholith: 150 my of granite magmatism on a plate margin. Lithos 97, 373–394. https://doi.org/10.1016/j.lithos.2007.01.007.
Hildebrand, R.S., Whalen, J.B., 2017. The tectonic setting and origin of Cretaceous batholiths within the North American Cordillera: the case for slab failure magmatism and its significance for crustal growth. Geol. Soc, Am. 532, 1–113. https://doi.org/10.1130/2017.2532.
Höckenreiner, M., Söllner, F., Miller, H., 2003. Dating the TIPA shear zone: an Early Devonian terrane boundary between the Famatinian and Pampean systems (NW Argentina). J. S. Am. Earth Sci. 16, 45–66.
Hongn, F., Vaccari, N.E., 2008. La discordancia tremadociano superior-arenigiana inferior en vega Pinato (Salta): Evidencia de deformación intraordovícica en el borde occidental de la Puna. 17° Congreso Geológico Argentino. pp. 1299–1300.
Huff, W.D., Davis, D., Bergström, S.M., Krekeler, M.P.S., Kolata, D.R., Cingolani, C., 1997. A biostratigraphic well-constrained K-bentonite U-Pb zircon age of the lowermost Darriwilian Stage (Middle Ordovician) from the Argentine Precordillera. Episodes 20, 29–33.
Huff, W.D., Bergstrom, S.M., Kolata, D.R., Cingolani, C.A., Astini, R.A., 1998. Ordovician K-Bentonites in the Argentine Precordillera: Relations to Gondwana Margin Evolution. In: Pankhurst, R.J., Rapela, C.W. (Eds.), The Proto-Andean Margin of Gondwana. Geol Soc.Lond., pp. 107–126.
Iannizzotto, N.F., Rapela, C.W., Baldo, E.G., Galindo, C., Fanning, C.M., Pankhurst, R.J., 2013. The Sierra Norte–Ambargasta batholith: late Ediacaran–early Cambrian magmatism associated with Pampean transpressional tectonics. J. S. Am. Earth Sci. 42, 127–143. https://doi.org/10.1016/j.jsames.2012.07.009.
Ickert, R.B., Hiess, J., Williams, I.S., Holden, P., Ireland, T.R., Lanc, P., Schram, N., Foster, J.J., Clement, S.W., 2008. Determining high precision, in situ, oxygen isotope ratios with a SHRIMP II: analyses of MPI-DING silicate-glass reference materials and zircon from contrasting granites. Chem. Geol. 257, 114–128.
Insel, N., Grove, M., Haschke, M., Barnes, J.B., Schmitt, A.K., Strecker, M.R., 2012. Paleozoic to early Cenozoic cooling and exhumation of the basement underlying the eastern Puna plateau margin prior to plateau growth. Tectonics 31. https://doi.org/10.1029/2012TC003168.
Kemp, A.I.S., Hawkesworth, C.J., 2014. Growth and Differentiation of the Continental Crust from Isotope Studies of Accessory Minerals. In: Treatise on Geochemistry, 2nd ed. Vol. 4. Elsevier, pp. 379–421.
Kemp, A.I.S., Hawkesworth, C.J., Paterson, B.A., Kinny, P.D., 2006. Episodic growth of the Gondwana supercontinent from hafnium and oxygen isotopes in zircon. Nature 439, 580–583.
Larrovere, M.A., Alasino, P.H., de los Hoyos, C.R., Willner, A.P., 2015. The Ordovician Las Chacritas pluton (Sierra de Humaya, NW Argentina): origin and emplacement triggered by lateral shortening and magmatic stoping at mid-crustal level. Int. J. Earth Sci. 104, 565–586. https://doi.org/10.1007/s00531-014-1112-8.
Larrovere, M.A., Alasino, P.H., Baldo, E.G., 2016. La faja de cizalla dúctil doble-vergente del noroeste de la Sierra de Velasco: deformación de la corteza media durante la orogenia famatiniana. Rev. Asoc. Geol. Arg. 73, 117–133.
Lork, A., Bahlburg, H., 1993. Precise U–Pb Ages of Monazites from the Faja Eruptiva de la Puna Oriental and the Cordillera Oriental, NW Argentina. XII Congreso Geológico Argentino y II Congreso de Exploración de Hidrocarburos, Actas, pp. 1–6.
Ludwig, K., 2009. SQUID 2: a User's Manual. Berkeley Geochron. Ctr. Spec, pp. 110.
Martino, R.D., Guereschi, A.B., Sfragulla, J.A., 2003. Petrografía, estructura y significado tectónico de la faja de deformación Los Túneles en las Sierras de Pocho y Guasapampa. Córdoba. Rev. Asoc. Geol. Arg. 58, 233–247.
Miller, C.F., McDowell, S.M., Mapes, R.W., 2003. Hot and cold granites? Implications of zircon saturation temperatures and preservation of inheritance. Geology 31, 529–532.
Morosini, A., Ortiz Suárez, A., Ramos, G., 2009. Los granitoides Famatinianos del sector suroccidental de la Sierra de San Luis: Clasificación y Geotermometría. Rev. Asoc. Geol. Arg. 64, 433–446.
Mulcahy, S.R., Roeske, S.M., McClelland, W.C., Nomade, S., Renne, P.R., 2007. Cambrian initiation of the Las Pirquitas thrust of the western Sierras Pampeanas, Argentina: Implications for the tectonic evolution of the proto-Andean margin of South America. Geology 35, 443–446. https://doi.org/10.1130/G23436A.1.
Mulcahy, S.R., Roeske, S.M., McClelland, W.C., Jourdan, F., Iriondo, A., Renne, P.R., Vervoort, J.D., Vujovich, G.I., 2011. Structural Evolution of a Composite Middle to Lower Crustal Section: The Sierra de Pie de Palo, Northwest Argentina. Tectonics 30.
Mulcahy, S.R., Roeske, S.M., McClelland, W.C., Ellis, J.R., Jourdan, F., Renne, P.R., Vervoort, J.D., Vujovich, G.I., 2014. Multiple migmatite events and cooling from granulite facies metamorphism within the Famatina arc margin of Northwest Argentina. Tectonics 33, 1–25. https://doi.org/10.1002/2013TC003398.
Murra, J.A., Casquet, C., Locati, F., Galindo, C., Baldo, E.G., Pankhurst, R.J., Rapela, C.W., 2016. Isotope (Sr, C) and U-Pb SHRIMP zircon geochronology of marble-bearing sedimentary series in the Eastern Sierras Pampeanas, Argentina. Constraining the SW Gondwana margin in Ediacaran to early Cambrian times. Precambrian Res. 281, 602–617.
Niemeyer, H., Meffre, S., Guerrero, R., 2014. Zircon U-Pb geochronology of granitic rocks of the Cordón de Lila and Sierra de Almeida ranges, northern Chile: 30 m.y. of Ordovician plutonism on the western border of Gondwana. J. S. Am. Earth Sci. 56, 228–241.
Otamendi, J.E., Ducea, M.N., Tibaldi, A.M., Bergantz, G., de la Rosa, J.D., Vujovich, G.I., 2009. Generation of tonalitic and dioritic magmas by coupled partial melting of gabbroic and metasedimentary rocks within the deep crust of the Famatinian magmatic arc, Argentina. J. Petrol. 50, 841–873.
Otamendi, J.E., Ducea, M.N., Bergantz, G.W., 2012. Geological, petrological and geochemical evidence for progressive construction of an arc crustal section, Sierra de Valle Fértil, Famatinian arc, Argentina. J. Petrol. 53, 761–800.
Otamendi, J.E., Ducea, M.N., Cristofolini, E.A., Tibaldi, A.M., Camilletti, G.C., Bergantz, G.W., 2017. U-Pb ages and Hf isotope compositions of zircons in plutonic rocks from the central Famatinian arc, Argentina. J. S. Am. Earth Sci. 76, 412–426.
Pankhurst, R.J., Rapela, C.W., 1998. The Proto-Andean margin of Gondwana: an introduction. In: Pankhurst, R.J., Rapela, C.W. (Eds.), The Proto-Andean Margin of Gondwana. Geol. Soc. Lond, pp. 1–9.
Pankhurst, R.J., Rapela, C.W., Saavedra, J., Baldo, E., Dahlquist, J., Pascua, I., Fanning, C.M., 1998. The Famatinian Magmatic Arc in the Central Sierras Pampeanas: an Early to Mid-Ordovician Continental Arc on the Gondwana Margin. In: Pankhurst, R.J., Rapela, C.W. (Eds.), The Proto-Andean Margin of Gondwana. Geol. Soc. Lond, pp. 343–367.
Pankhurst, R.J., Rapela, C.W., Fanning, C.M., 2000. Age and origin of coeval TTG, I- and S-type granites in the Famatinian belt of NW Argentina. Trans. Roy. Soc. Edinb. Earth Sci. 91, 151–168. https://doi.org/10.1017/S0263593300007343.
Pankhurst, R.J., Rapela, C.W., Fanning, C.M., Márquez, M., 2006. Gondwanide continental collision and the origin of Patagonia. Earth Sci. Rev. 76, 235–257.
Pankhurst, R.J., Rapela, C.W., Lopez De Luchi, M.G., Rapalini, A.E., Fanning, C.M., Galindo, C., 2014. The Gondwana connections of northern Patagonia. J. Geol. Soc. Lond. 171, 313–328. https://doi.org/10.1144/jgs2013-081.
Pankhurst, R.J., Hervé, F., Fanning, C.M., Calderón, M., Niemeyer, H., Griem-Klee, S., Soto, F., 2016. The pre-Mesozoic rocks of northern Chile: U-Pb ages, and Hf and O isotopes. Earth-Sci. Rev. 152, 88–105. https://doi.org/10.1016/j.earscirev.2015.11.009.
Petford, N., Atherton, M., 1996. Na-rich partial melts from newly underplated basaltic crust: the Cordillera Blanca Batholith, Peru. J. Petrol. 37, 1491–1521. https://doi.

org/10.1093/petrology/37.6.1491.
Ramacciotti, C.D., Baldo, E.G., Casquet, C., 2015. U-Pb SHRIMP detrital zircon ages from the Neoproterozoic Difunta Correa Metasedimentary Sequence (Western Sierras Pampeanas, Argentina): provenance and paleogeographic implications. Precambrian Res. 270, 39–49.
Ramacciotti, C.D., Casquet, C., Baldo, E.G., Galindo, C., Pankhurst, R.J., Verdecchia, S.O., Rapela, C.W., Fanning, C.M., 2013. A Cambrian mixed carbonate–siliciclastic platform in SW Gondwana:evidence from the Western Sierras Pampeanas (Argentina) and implications for the early Paleozoic paleogeography of the proto-Andean margin. Int. J. Earth Sci. 107 (7), 2605–2625.
Ramos, V.A., 2004. Cuyania, an exotic block to Gondwana: review of a historical success and the present problems. Gondwana Res. 7, 1009–1026. https://doi.org/10.1016/S1342-937X(05)71081-9.
Rapalini, A.E., López de Luchi, M., Tohver, E., Cawood, P.A., 2013. The South American ancestry of the North Patagonian Massif: geochronological evidence for an autochthonous origin? Terra Nova 25, 337–342. https://doi.org/10.1111/ter. 12043.
Rapela, C.W., Toselli, A., Heaman, L., Saavedra, J., 1990. Granite Plutonism of the Sierras Pampeanas: an Inner Cordilleran Paleozoic Arc in the Southern Andes. In: Kay, S.M., Rapela, C.W. (Eds.), Plutonism from Antarctica to Alaska. Geol. Soc. Amer, pp. 77–90.
Rapela, C.W., Pankhurst, R.J., Casquet, C., Baldo, E., Saavedra, J., Galindo, C., Fanning, C.M., 1998. The Pampean orogeny of the southern proto-Andes: evidence for Cambrian continental collision in the Sierras de Córdoba. In: Pankhurst, R.J., Rapela, C.W. (Eds.), The Proto-Andean Margin of Gondwana. Geol. Soc. Lond, pp. 181–217.
Rapela, C.W., Casquet, C., Baldo, E.G., Dahlquist, J.A., Pankhurst, R.J., Galindo, C., Saavedra, J., 2001. Las orogenesis del paleozoico inferior en el margen proto-andino de América del Sur, Sierras Pampeanas Argentina. J. Iber. Geol. 27, 23–41.
Rapela, C.W., Pankhurst, R.J., Casquet, C., Fanning, C.M., Baldo, E.G., González-Casado, J.M., Galindo, C., Dahquist, J., 2007. The Río de la Plata craton and the assembly of SW Gondwana. Earth-Sci. Rev. 83, 49–82.
Rapela, C.W., Pankhurst, R.J., Casquet, C., Baldo, E., Galindo, C., Fanning, C.M., Dahlquist, J., 2010. The Western Sierras Pampeanas: protracted Grenville-age history (1330–1030 Ma) of intra-oceanic arcs, subduction–accretion at continental-edge and AMCG intraplate magmatism. J. S. Am. Earth Sci. 29, 105–127.
Rapela, C.W., Verdecchia, S.O., Casquet, C., Pankhurst, R.J., Baldo, E.G., Galindo, C., Murra, J.A., Dahlquist, J.A., Fanning, C.M., 2016. Identifying Laurentian and SW Gondwana sources in the Neoproterozoic to early Paleozoic metasedimentary rocks of the Sierras Pampeanas: Paleogeographic and tectonic implications. Gondwana Res. 32, 193–201.
Reissinger, M., 1983. Evolución geoquímica de la Sierra de Ancasti. In: Aceñolaza, F.F., Miller, H., Toselli, A.J. (Eds.), Geología de la Sierra de Ancasti. Münstersche Forschungen zur Geologie und Paläontologie, pp. 101–112.
Rubiolo, D., Cisterna, C., Villeneuve, M., Hickson, C., 2002. Edad U/Pb del Granito de Las Angosturas en la Sierra de Narváez (Sistema de Famatina, provincia de Catamarca). Actas 15 Cong. Geol. Arg. T1, 359–368.
Sato, A.M., Tickyj, H., Llambías, E.J., Sato, K., 2000. The Las Matras tonalitic–-trondhjemitic pluton, Central Argentina: Grenvillian-age constraints, geochemical characteristics, and regional implications. J. S. Am. Earth Sci. 13, 587–610.
Sato, K., Basei, M.A.S., Ferreira, C.M., Vlach, S.R.F., Ivanuch, W., Siga Jr., O., Onoi, A.T., 2010. In situ U–Th–Pb isotopic analyses by Excimer laser ablation/ICP–MS on Brazilian xenotime megacrystal: first U–Pb results at CPGeo-IG-USP. In: VII South American Symposium on Isotope Geology, Brasília, DF, CDROM.
Schröter, F.C., Stevenson, J.A., Dackzo, N.R., Clarke, G.L., Pearson, N.J., Klepeis, K.A., 2004. Trace element partitioning during high-P partial melting and melt–rock interaction; an example from northern Fiordland, New Zealand. J. Met. Geol. 22, 443–457.
Semenov, I., Weimberg, R.F., 2017. A major mid-crustal decollement of the Paleozoic convergent margin of western Gondwana: the Guacha Corral shear zone, Argentina. J. Str. Geol. 103, 75–99.
Sendek, C., 2016. Zircon geochemical and isotopic constraints on the evolution of the Mount Givens pluton, central Sierra Nevada batholith. San José State University, Department of Geology, pp. 165.
Shaw, S.E., Todd, V.R., Kimbrough, D.L., Pearson, N.J., 2014. A West-to-East Geologic Transect across the Peninsular Ranges Batholith, San Diego County, California: Zircon $^{176}Hf/^{177}Hf$ Evidence for the Mixing of Crustal- and Mantle-Derived Magmas, and Comparisons with the Sierra Nevada Batholiths. In: Morton, D.M., Miller, F.K. (Eds.), Peninsular Ranges Batholith, Baja California and Southern California. Geol. Soc. Amer.
Simpson, C., Law, R.D., Gromet, P., Miró, R., Northrup, C.J., 2003. Paleozoic deformation in the Sierras de Córdoba and Sierra de Las Minas, Eastern Sierras Pampeanas, Argentina. J. S. Am. Earth Sci. 15, 749–764.
Sims, J.P., Ireland, T.R., Camacho, A., Lyons, P., Pieters, P.E., Skirrow, R.G., Stuart-Smith, P.G., Miró, R., 1998. U-Pb, The Pb and Ar-Ar geochronology from the southern Sierras Pampeanas, Argentina: implications for the Palaeozoic tectonic evolution of the western Gondwana margin. In: Pankhurst, R.J., Rapela, C.W. (Eds.), The Proto-Andean Margin of Gondwana. Soc. Lond, pp. 259–281.
Steenken, A., Siegesmund, S., López De Luchi, M.G., Frei, R., Wemmer, K., 2006. Neoproterozoic to early Palaeozoic events in the Sierra de San Luis: implications for the Famatinian geodynamics in the Eastern Sierras Pampeanas (Argentina). J. Geol. Soc. Lond. 163, 965–982. https://doi.org/10.1144/0016-76492005-064.
Thomas, W.A., Astini, R.A., 1996. The Argentine Precordillera: a traveler from the Ouachitan embayment of North American Laurentia. Science 273, 752–757. https://doi.org/10.1126/science.273.5276.752.
Toselli, A.J., Rossi, J.N., Miller, H., Báez, M.A., Grosse, P., López, J.P., Bellos, L.I., 2005. Las rocas graníticas y metamórficas de la sierra de Velasco. San Miguel de Tucumán, pp. 211–220.
Toselli, A.J., Miller, H., Aceñolaza, F.G., Rossi, J.N., Söllner, F., 2007. The Sierra de Velasco (northwestern Argentina) - an example for polyphase magmatism at the margin of Gondwana. N. Jahr. Geol. Paläont. 246, 325–345.
Toselli, A.J., Rossi, J.N., Basei, M.A.S., 2014. Geología e interpretación petrológica de los granitos y pegmatitas de la Sierra de Mazán, La Rioja, Argentina. Serie Correlación Geológica 30, 35–73.
Turner, J.C.M., 1964. Descripcion geologica de la hoja 7c, Nevado de Cachi. Dir. Nac. Geol. Min. Bol. 99, 75.
Valley, J.W., Lackey, J.S., Cavosie, A.J., 2005. 4.4 billion years of crustal maturation: oxygen isotope ratios of magmatic zircon. Contrib. Mineral. Petrol. 150, 561–580.
Van der Lelij, R., Spikins, R., Ulianov, A., Chiaradia, M., Mora, A., 2016. Palaeozoic to Early Jurassic history of the northwestern corner of Gondwana, and implications for the evolution of the Iapetus, Rheic and Pacific Oceans. Gondwana Res. 31, 271–294.
van Staal, C.R., Vujovich, G.I., Currie, K.L., 2011. An Alpine-style Ordovician collision complex in the Sierra de Pie de Palo, Argentina: Record of subduction of Cuyania beneath the Famatina arc. J. Struct. Geol. 33, 343–361. https://doi.org/10.1016/j.jsg.2010.10.011.
Varela, R., Basei, M.A.S., Sato, A.M., Cingolani, C.A., Siga Jnr., O., Sato, K., 1998. Edades isotópicas Rb/Sr y U/Pb en rocas de Mina Gonzalito y Arroyo Salado, Macizo Norpatagónico Atlántico, Río Negro, Argentina. X Cong. Latinoamer. Geol. y VI Cong. Nac. Geol. Economica 1, 71–76.
Varela, R., Basei, M.A.S., González, P.D., Sato, A.M., Naipauer, M., Campos Neto, M., Cingolani, C.A., Meira, V.T., 2011. Accretion of Grenvillian terranes to the southwestern border of the Río de la Plata craton, western Argentina. Int. J. Earth Sci. 100, 243–272.
Verdecchia, S.O., Baldo, E.G., Benedetto, J.L., Borghi, P.A., 2007. The first shelly faunas from metamorphic rocks of the Sierras Pampeanas (La Cébila Formation, Sierra de Ambato, Argentina): age and paleogeographic implications. Ameghiniana 44, 493–498.
Verdecchia, S.O., Casquet, C., Baldo, E.G., Pankhurst, R.J., Rapela, C.W., Fanning, C.M., Galindo, C., 2011. Mid- to late Cambrian docking of the Río de la Plata craton to southwestern Gondwana: age constraints from U-Pb SHRIMP detrital zircon ages from Sierra de Ambato and Velasco (Sierras Pampeanas, Argentina). J. Geol. Soc. Lond. 168, 1061–1071. https://doi.org/10.1144/0016-76492010-143.
Vervoort, J.D., Blichert-Toft, J., 1999. Evolution of the depleted mantle: Hf isotope evidence from juvenile rocks through time. Geochim. Cosmochim. Acta 63, 533–556.
Vervoort, J.D., Patchett, P.J., Blichert-Toft, J., Albarède, F., 1999. Relationships between Lu–Hf and Sm–Nd isotopic systems in theglobal sedimentary system. Earth Planet. Sci. Lett. 168, 79–99.
Villaros, A., Buick, I.S., Stevens, G., 2012. Isotopic variations in S-type granites: an inheritance from a heterogeneous source? Contrib. Mineral. Petrol. 163, 243–257.
Viramonte, J.M., Becchio, R.A., Viramonte, J.G., Pimentel, M.M., Martino, R.D., 2007. Ordovician igneous and metamorphic units in southeastern Puna: new U–Pb and Sm–Nd data and implications for the evolution of northwestern Argentina. J. S. Am. Earth Sci. 24, 167–183.
von Gosen, W., Prozzi, C., 2010. Pampean deformation in the Sierra Norte de Córdoba, Argentina: implications for the collisional history at the western pre-Andean Gondwana margin. Tectonics 29, 1–33.
Vujovich, G., Kay, S., 1998. A Laurentian? Grenville-age oceanic arc/back-arc terrane in the Sierra de Pie de Palo, western Sierras Pampeanas, Argentina. In: Pankhurst, R.J., Rapela, C.W. (Eds.), The Proto-Andean Margin of Gondwana. Geol. Soc. Lond, pp. 159–180.
Vujovich, G.I., van Staal, C.R., Davis, W., 2004. Age constraints on the tectonic evolution and provenance of the Pie de Palo complex, Cuyania composite terrane, and the Famatinian orogeny in the Sierra de Pie de Palo, San Juan, Argentina. Gondwana Res. 7, 1041–1056. https://doi.org/10.1016/S1342-937X(05)71083-2.
Walker Jr., B.A., Bergantz, G.W., Otamendi, J.E., Ducea, M.N., Cristofolini, E.A., 2015. A MASH zone revealed: the mafic complex of the sierra Valle Fértil. J. Petrol. 56, 1863–1896.
Wen, D.R., Liu, D., Chung, S.L., Chu, M.F., Ji, J., Zhang, O., Song, B., Lee, T.Y., Yeh, M.W., Lo, C.H., 2008. Zircon SHRIMP U–Pb ages of the Gangdese Batholith and implications for Neotethyan subduction in southern Tibet. Chem. Geol. 252, 191–201. https://doi.org/10.1016/j.chemgeo.2008.03.003.
Willner, A., 1983. Evolución metamórfica. In: Aceñolaza, F.F., Miller, H., Toselli, A.J. (Eds.), Geología de la Sierra de Ancasti. Münstersche Forschungen zur Geologie und Paläontologie, pp. 157–187.
Yakymchuk, C., Brown, C.R., Brown, M., Siddoway, C.S., Fanning, C.M., Korhonen, F.J., 2015. Paleozoic evolution of western Marie Byrd Land, Antarctica. Geol. Soc. Amer. Bul. 127, 1464–1484.
Zen, E., 1986. Aluminum enrichment in silicate melts by fractional crystallization: some mineralogic and petrographic constraints. J. Petrol. 27, 1095–1117.
Zhang, K.J., Zhang, Y.X., Tang, X.C., Xia, B., 2012. Late Mesozoic tectonic evolution and growth of the Tibetan plateau prior to the Indo-Asian collision. Earth Sci. Rev. 114, 236–249.